N-ACYLETHANOLAMINE METABOLISM DURING SEED GERMINATION: MOLECULAR IDENTIFICATION OF A FUNCTIONAL *N*-ACYLETHANOLAMINE AMIDOHYDROLASE

Rhidaya Shrestha

Dissertation Prepared for the Degree of

DOCTOR OF PHILOSOPHY

UNIVERSITY OF NORTH TEXAS

August 2004

APPROVED:

Kent D. Chapman, Major Professor
Robert M. Pirtle, Committee Member
John Knesek, Committee Member
Rebecca Dickstein, Committee Member
Douglas D. Root, Committee Member
Art Goven, Chair of the Department of Biological Sciences
Sandra L. Terrell, Dean of the Robert B. Toulouse School of Graduate Studies

Shrestha, Rhidaya, *N*-Acylethanolamine metabolism during seed germination: Molecular identification of a functional *N*-acylethanolamine amidohydrolase. Doctor of Philosophy (Biochemistry), August 2004, 191 pp., 6 tables, 27 figures, 101 references.

N-Acylethanolamines (NAEs) are endogenous lipid metabolites that occur in a variety of dry seeds, and their levels decline rapidly during the first few hours of imbibition (Chapman et al., 1999, Plant Physiol., 120:1157-1164). Biochemical studies supported the existence of an NAE amidohydrolase activity in seeds and seedlings, and efforts were directed toward identification of DNA sequences encoding this enzyme. Mammalian tissues metabolize NAEs *via* an amidase enzyme designated fatty acid amide hydrolase (FAAH). Based on the characteristic amidase signature sequence in mammalian FAAH, a candidate *Arabidopsis* cDNA was identified and isolated by reverse transcriptase-PCR. The *Arabidopsis* cDNA was expressed in *E. coli* and the recombinant protein indeed hydrolyzed a range of NAEs to free fatty acids and ethanolamine. Kinetic parameters for the recombinant protein were consistent with those properties of the rat FAAH, supporting identification of this *Arabidopsis* cDNA as a FAAH homologue. Two T-DNA insertional mutant lines with disruptions in the *Arabidopsis* NAE amidohydrolase gene (At5g64440) were identified. The homozygous mutant seedlings were more sensitive than the wild type to exogenously applied NAE 12:0. Transgenic seedlings overexpressing the NAE amidohydrolase enzyme showed noticeably greater tolerance to NAE 12:0 than wild type seedlings. These results together provide evidence *in vitro* and *in vivo* for the molecular identification of *Arabidopsis* NAE amidohydrolase. Moreover, the plants with altered NAE amidohydrolase expression may provide new tools for improved understanding of the role of NAEs in germination and seedling growth.

ACKNOWLEDGMENTS

I would like to thank Dr. Kent D. Chapman for his kind supervision as my major professor throughout this study, and for his continued encouragement. My sincere gratitude also goes to my graduate committee, Dr. Robert M. Pirtle, Dr. John Knesek, Dr. Rebecca Dickstein and Douglas D. Root for their guidance and support during my project.

I am indebted to my colleagues in the lab for their help and friendship: Mrs. Luna Joseph, Ms. Jane Hodson, Dr. Kathryn Kleppinger-Sparace, Dr. Swati Tripathy, Dr. Chau Hoang, Dr. Tu Huynh, Ms. Sylvia Wanji, Mr. John McHugh, Ms. Amy Rommel, Ms. Agnes Stawaska, Mr. Will Wiant, Ms. Cheryl Waggoner, Mr. Gabriel Gonzalez, Mr. Neal Teaster and Mr. Matthew Cotter.

Finally, I would like to offer my sincere appreciation to my parents back home, my wife Gita and sons Saurav and Summit for their patience and inspiration.

TABLE OF CONTENTS

LIST OF TABLES

LIST OF FIGURES

CHAPTER II

CHAPTER III

COMPREHENSIVE LIST OF ABBREVIATIONS

AHase, amidohydrolase

AOS, 13-allene oxide synthase

AS, amidase signature

ATMK, arachidonyl trifluoromethyl ketone

Bis-Tris, 2-[bis(2-hydroxyethyl)amino]-2-(hydroxymethyl)propane-1,3-diol

BSTFA, bis(trimethylsilyl)trifluoroacetamide

CHAPS (3-[(-cholamidopropyl)-dimethylammonia]-1-propanesulfonate)

C_T, threshold cycle

DMSO, dimethyl sulfoxide

DDM, n-dodecyl-β-D-maltoside

dpm, disintegrations per minute

EC_{50}, half-maximal effective concentration

EDTA, ethylenediamine tetraacetic acid

EGTA, ethylene glycol-bis(β-amino ethylether) tetraacetic acid

ETYA, 5,8,11,14-eicosatetraynoic acid

FAAH, fatty acid amide hydrolase

FFA, free fatty acid

GC-MS, gas chromatography-mass spectrometry

GFP, green fluorescent protein

HPLC, high performance liquid chromatography

IPTG, isopropyl β-D-thiogalactopyranoside

LOX, lipoxygenase

MAFP, methyl arachidonyl fluorophosphonate

MS, Murashige and Skoog

NAE 12:0, *N*-lauroylethanolamine

NAE 14:0, *N*-myristoylethanolamine

NAE 16:0, *N*-palmitoylethanolamine

NAE 18:2, *N*-linoleoylethanolamine

NAE 20:4, *N*-arachidonoylethanolamine (anandamide)

NAE, *N*-acylethanolamine

NAE, *N*-acylethanolamine

NAPE, *N*-acylphosphatidylethanolamine

NDGA, nordihydroguaiaretic acid

PLD, phospholipase D

PMSF, phenylmethylsulfonyl fluoride

PVDF, polyvinylidene fluoride

RT-PCR, reverse transcriptase- polymerase chain reaction

SDS, sodium dodecyl sulfate

smGFP, soluble modified green fluorescent protein

T-DNA, transfer DNA

WT, wild type

GENERAL INTRODUCTION

N-Acylphosphatidylethanolamines (NAPEs), a minor lipid constituent of cellular membranes, are formed by transfer of an acyl chain from a glycerophospholipid to the primary amine of the ethanolamine moiety of phosphatidylethanolamine (PE) by *N*-acyltransferase in animals (Di Marzo, 1998). In plants NAPEs are formed by direct *N*-acylation of PE with unesterfied free fatty acid (FFA) to PE by the catalytic action of NAPE synthase (Chapman and Moore, 1993). These NAPEs, upon hydrolysis by a phosphodiesterase of the phospholipase D type, produce *N*-acylethanolamines (NAEs) in animals and plants (Schmid et al., 1996; Chapman, 2000). There are several NAE types and *N*-arachidonoylethanolamine (anandamide) is the most widely studied lipid mediator among NAEs in animal system (Ueda et al., 1995). Anandamide exhibits a variety of cannabimimetic activities such as inhibition of adenylyl cyclase activity, inhibition of calcium channels, sedation, catalepsy, analgesia and hypothermia (review; Ueda, 2002). Other NAEs, even though they are more prevalent than anandamide in most tissues, are less characterized than anandamide in terms of physiological roles (Schmid, 2000; Hansen et al., 2000). *N*-Linoleoylethanolamine (NAE 18:2) and *N*-oleoylethanolamine (NAE 18:1) play indirect roles as “endocannabinoids” by competing with anandamide for degradation by fatty acid amide hydrolase, FAAH (Di Tomaso et al., 1996) and these were termed “entourage” lipids (Ben-Shabat, 1998).

In plants, NAEs were first reported as constituents of soy lecithin and peanut meal in the 1950s (Kuehl et al., 1957). Several NAE types have been identified in varieties of desiccated seeds including monocots and dicots (Chapman et al., 1999; Chapman, 2004). The NAE types in seeds contain acyl length from 12C to 18C with up to three double bonds. Anandamide was not reported in plants and roles of NAEs in plant systems are only beginning to be investigated and are not as clear as in animal system (Chapman, 2004). NAEs are produced in plant cell suspensions (Chapman et al., 1998) and leaves (Tripathy et al., 1999) in minutes following pathogen elicitor perception, raising the possibility that these molecules function in plant defense signaling. When exogenous *N*-myristoylethanolamine (NAE 14:0) is administered to cell suspensions or leaves of tobacco plants at submicromolar concentrations, there is activation of phenylalanine ammonia-lyase (PAL) expression (Tripathy et al., 1999). The occurrence of NAEs in seeds with substantially different structural properties from those found in elicitor-treated leaves and their rapid depletion during seed imbibition (Chapman, 2000), suggests that these fatty acid amides may have a role in the regulation of seed germination. NAEs also were found selectively inhibit the activity of phospholipase Dα *in vitro* and application of NAEs to leaf epidermal sections abolished abscisic acid (ABA)-induced causing stomatal closure in tobacco and *Commelina communis* (Austin-Brown and Chapman, 2002). In other work, elevated level of exogenous *N*-lauroylethanolamine (NAE 12:0) altered drastically seedling growth and

development (Blancaflor et al., 2003) suggesting a possible lipid mediator role of NAE 12:0.

The occurrence of substantial amounts of NAEs in desiccated seeds and their depletion in the first few hours of imbibition raises the question of metabolic fate of those NAEs (Chapman et al., 1999). Literature in animal systems indicate two enzymatic activities metabolize NAEs - one that hydrolyzes NAEs and the other that oxidizes them to form novel oxylipins. The enzyme responsible for hydrolyzing NAEs, designated fatty acid amide hydrolase, has been characterized at the biochemical and molecular levels in animal system (Schmid et al., 1985; Cravatt et al., 1996). Molecular genetic results from FAAH gene knockout mice revealed a 15 fold increase of anadamide levels and these mutant mice were supersensitive to endogenous cannabinoid lipid mediators (Cravatt et al., 2001).

In addition to FAAH, lipoxygenase also can act on NAEs with two or more double bonds. Recent studies showed that NAE 18:2 and *N*-linolenoylethanolamine (NAE 18:3) could be converted to hydroperoxy NAEs by purified soybean lipoxygenase-1 (Van der Stelt et al., 1997; Van der Stelt et al., 2000). Subsequently, the hydroperoxides of NAE 18:2 and NAE 18:3 could be converted by alfalfa hydroperoxide (HPO) lyase and flax seed allene oxide synthase (AOS) into novel oxylipins (Van der Stelt et al., 2000). Anandamide could be converted into hydroperoxy NAE by purified 5-lipoxygenase from barley and tomato (Van Zadelhoff et al., 1998). Also, anandamide was found acted by cyclooxygenase-2 generating prostaglandin ethanolamide in animal cellular and

subcellular systems (Kozak et al., 2002). Thus, there are two possible enzymatic pathways (lipoxygenase, LOX and NAE amidohydrolase), which might be responsible for the observed decline in NAEs during seed imbibition and germination.

I proposed to explore the physiological significance of NAE metabolism in seed germination and early seedling growth, a period previously noted to be active in NAPE/NAE metabolism (Chapman, 2000). One hypothesis was that NAEs were negative regulators of seed germination and seedling growth, and their levels must be depleted during imbibition for the synchronized progression of physiological processes associated with seed germination and seedling growth. I planned to identify the endogenous pathway(s) in seeds and seedlings for NAE metabolism, to characterize the enzyme(s) responsible for NAE metabolism, and to manipulate the expression of NAE amidohydrolase(s) *in vivo* to assess the role of this pathway during normal seed germination. The specific objectives were: (1) to evaluate the metabolic fate of *N*-acylethanolamines during germination to identify enzymatic pathways; (2) to identify functional NAE amidohydrolase(s) by expressing candidate plant FAAH ortholog(s) in *Escherichia coli* and/or *Saccharomyces cerevisiae* and compare the biochemical properties of the recombinant enzyme(s) with cotton microsomal enzyme activity and rat FAAH, and (3) to analyze functional role of NAE amidohydrolase *in planta* by determining endogenous expression patterns and by manipulating expression (over/under) in transgenic *Arabidopsis thaliana*.

In chapter I, I describe the existence of two pathways for NAE metabolism during seed imbibition – one to hydrolyze NAEs in manner similar to the inactivation of endocannabinoid mediators in animal systems, and the other to form novel NAE-derived oxylipins. The rapid metabolism of NAEs by these pathways continues to point to a role for NAE metabolites in seed germination. In chapter II, I report the identification, the heterologous expression (in *E. coli*) and the biochemical characterization of an *Arabidopsis thaliana* FAAH. Collectively these molecular data presented in this chapter provided support at the molecular level for a conserved mechanism between plants and animals for the metabolism of NAEs. In chapter III, I describe several experiments to determine the role of the enzyme FAAH *in planta* by characterizing transgenic (overexpressor and antisense) plants and mutant plants with T-DNA insertion in the FAAH gene disrupting the function of the gene. Taken together, the results are consistent with a metabolic role *in vivo* for the *Arabidopsis* NAE amidohydrolase gene, At5g64440, in the catabolism of NAEs, and suggest that this lipid hydrolytic pathway may be important for normal seed germination and seedling growth.

Here my results are presented in three chapters: Chapter-I, *N*-acylethanolamines are metabolized by lipoxygenase and amidohydrolase in competing pathways during cotton (*Gossypium hirsutum* L.) seed imbibition; Chapter-II, molecular identification of a functional homologue of the mammalian fatty acid amide hydrolase in *Arabidopsis thaliana*; and Chapter-III, altered *N*-

acylethanolamine (NAE) amidohydrolase expression in *Arabidopsis thaliana* alters the sensitivity of seedlings toward exogenous NAE lipid mediators.

CHAPTER I

N-ACYLETHANOLAMINES ARE METABOLIZED BY LIPOXYGENASE AND AMIDOHYDROLASE IN COMPETING PATHWAYS DURING COTTON (*Gossypium hirsutum* L.) SEED IMBIBITION

[This chapter was published: Shrestha et al., (2002) Plant Physiol 130: 391-401, used with permission]

Abstract

Saturated and unsaturated *N*-acylethanolamines (NAEs) occur in desiccated seeds primarily as 16C and 18C species with *N*-palmitoylethanolamine (NAE 16:0) and *N*-linoleoylethanolamine (NAE 18:2) being most abundant. Here, we examined the metabolic fate of NAEs *in vitro* and *in vivo* in imbibed cottonseeds. When synthetic [1-^{14}C]16:0 NAE was utilized as a substrate, free fatty acids (FFA) were produced by extracts of imbibed cottonseeds. When synthetic [1-^{14}C]18:2 NAE was utilized as a substrate, FFA as well as an additional lipid product(s), were formed. Based on polarity, we presumed the unidentified lipid was a product of the lipoxygenase (LOX) pathway and inclusion of the characteristic LOX inhibitors, nordihydroguaiaretic acid (NDGA) and eicosatetraynoic acid (ETYA) reduced its formation in *in vitro* and *in vivo*. The conversion of NAE 18:2 in imbibed cottonseed extracts to 12-oxo-13-hydroxy-*N*-(9Z)-octadecanoylethanolamine was confirmed by GC/MS indicating

the presence of 13-LOX and 13-allene oxide synthase (AOS) which metabolized NAE 18:2. Cell fractionation studies showed that the NAE amidohydrolase, responsible for FFA production, was associated mostly with microsomes while LOX, responsible for NAE 18:2-oxylipin production, was distributed in cytosol-enriched fractions and microsomes. The highest activity toward NAE by amidohydrolase was observed 4 to 8 h after imbibition and by LOX 8 h after imbibition. Collectively our results indicate that two pathways exist for NAE metabolism during seed imbibition-one to hydrolyze NAEs in manner similar to the inactivation of endocannabinoid mediators in animal systems, and the other to form novel NAE-derived oxylipins. The rapid depletion of NAEs by these pathways continues to point to a role for NAE metabolites in seed germination.

Abbreviations

AHase, amidohydrolase

AOS, 13-allene oxide synthase

ATMK, arachidonyl trifluoromethyl ketone

dpm, disintegrations per minute

EDTA, ethylenediamine tetraacetic acid

EGTA, ethylene glycol-bis(β-amino ethylether) tetraacetic acid

ETYA, 5,8,11,14-eicosatetraynoic acid

FAAH, fatty acid amide hydrolase

FFA, free fatty acid

GC-MS, gas chromatography-mass spectrometry

LOX, lipoxygenase

NAE, *N*-acylethanolamine

NAE 16:0, *N*-palmitoylethanolamine

NAE 18:2, *N*-linoleoylethanolamine

NAE 20:4, *N*-arachidonoylethanolamine (anandamide)

NAPE, *N*-acylphosphatidylethanolamine

NDGA, nordihydroguaiaretic acid; PLD, phospholipase D

PMSF, phenylmethylsulfonyl fluoride

Introduction

In mammalian cells, *N*-acylethanolamines (NAEs) have varied physiological roles. *N*-Arachidonylethanolamine (anandamide), a type of NAE in mammalian brain tissue is an endogenous ligand for the cannabinoid receptor and modulates neurotransmission. Anandamide also can activate vanilloid (capsaicin) receptors and function as an endogenous analgesic (Pertwee, 2001), and appears to be involved in neuroprotection (Hansen et al., 2000; Van der Stelt et al., 2001). In other animal tissues NAEs have been implicated in immunomodulation (Buckley et al., 2000), synchronization of embryo development (Paria and Dey, 2000) and induction of apoptosis (Sarker et al., 2000). These endogenous bioactive molecules termed “endocannabinoids” are hydrolyzed by fatty acid amidohydrolase to terminate their signaling functions.

In plants, NAEs are present in substantial amounts in desiccated cottonseeds (1.6 μg^{-1} g fresh wt) and their levels decline after a few hours of imbibition (Chapman et al., 1999). Individual NAEs were identified predominantly as 16C and 18C species with *N*-palmitoylethanolamine (NAE 16:0) and *N*-linoleoylethanolamine (NAE 18:2) being the most abundant. NAEs in both plant and animal cells are derived from *N*-acylphosphatidylethanolamines (NAPEs), a minor membrane lipid constituent of cellular membranes (Schmid et al., 1990; Chapman, 2000). NAEs are produced by the action of a phospholipase D (PLD). In plants NAEs were produced in cell suspensions (Chapman et al., 1998) and

leaves (Tripathy et al., 1999) in minutes following pathogen elicitor perception, raising the possibility that these molecules function in plant defense signaling. Indeed, exogenous NAE 14:0 at submicromolar concentrations, was sufficient to activate phenylalanine ammonia-lyase (PAL) expression in cell suspensions and leaves of tobacco (Tripathy et al., 1999). The occurrence of NAEs in seeds with substantially different structural properties than those found in elicitor treated leaves and their rapid depletion during seed imbibition (Chapman, 2000), suggests that these lipids may have a role in the regulation of seed germination.

Recent studies showed that NAE 18:2 and NAE 18:3 could be converted into hydroperoxy NAE by purified soybean lipoxygenase-1 (Van der Stelt et al., 1997; Van der Stelt et al., 2000). Subsequently, the hydroperoxides of NAE 18:2 and NAE 18:3 could be converted by alfalfa hydroperoxide (HPO) lyase and flax seed allene oxide synthase (AOS) into novel oxylipins (Van der Stelt et al., 2000). NAE 20:4 (anandamide), the mammalian neurotransmitter, could be converted into hydroperoxy NAE by purified 5-lipoxygenase from barley and tomato (Van Zadelhoff et al., 1998). Alternatively, NAE amidohydrolase, also designated fatty acid amide hydrolase (FAAH, Cravatt et al., 2001) acts upon NAE to produce free fatty acid and ethanolamine, and in mammalian cells this pathway is responsible for inactivation of endocannabinoid lipid mediators (Schmid, 2000). Thus, there are two possible enzymatic pathways (lipoxygenase, LOX and NAE amidohydrolase), which might be responsible for the observed decline in NAEs during seed imbibition.

To begin to understand the role of NAEs in seeds, we investigated the metabolic fate of NAEs in cottonseeds upon imbibition, germination and during post-germinative growth, a period previously noted to be active in NAPE/NAE metabolism (Chapman, 2000). Our results indicate that, indeed, there are two pathways capable of metabolizing NAEs in seeds – a LOX-mediated pathway selective for unsaturated NAEs (e.g. NAE 18:2), and a NAE amidohydrolase activity, which utilizes both unsaturated and saturated NAEs. Both enzymatic pathways were most active in imbibed seeds consistent with depletion of NAEs *in vivo*, and at a time period just preceding or coincident with radicle emergence, suggesting NAE metabolism may play a role in the regulation of seed germination. These results will provide the basis for future studies aimed at understanding the functional role of NAE metabolism in seed germination and seedling growth.

Results

Identification of NAE Metabolites and Subcellular Distribution of the Enzymes

Several types of *N*-acylethanolamines (NAEs) are prevalent in the desiccated seeds of plants (Chapman et al., 1999). For example, the total NAE content in desiccated cottonseeds was approximately 1600 ng g^{-1} fresh weight, of which NAE 18:2 comprised of approximately 940 ng and NAE 16:0 was about 380 ng g^{-1} fresh weight, respectively. The levels of these NAEs declined sharply within few hours of seed imbibition to 200 ng for NAE 18:2 and about 160 ng for NAE 16:0. Here, these two most abundant NAEs in desiccated seeds, NAE 16:0 and NAE 18:2, were used to evaluate the metabolic fate of NAE in imbibing seeds. When [1-^{14}C]16:0 NAE was utilized as substrate there was only one product (comigrating with palmitic acid, $R_f \cong 0.48$) formed by extracts of imbibed cottonseeds (Fig.1A). When [1-^{14}C]18:2 NAE was utilized as a substrate there were two apparent products formed (Fig.1B) one comigrating with linoleic acid ($R_f \cong 0.46$) and the other more polar, near the origin ($R_f \cong 0.12$), was tentatively identified as NAE oxylipin. These data suggested that endogenous NAEs in desiccated seeds were metabolized by two pathways – one producing free fatty acids and other likely producing NAE-derived oxylipins.

The subcellular distribution of NAE-LOX (NAE oxylipin formation) and NAE amidohydrolase (FFA formation) differed in cell fractions prepared from 4 h imbibed cottonseeds (Tables I and II). The presumed NAE-oxylipin formation

was distributed both in membrane and cytosol-enriched fractions, whereas the enzyme responsible for FFA formation was localized almost exclusively to microsomes (Tables I and II). AHase activity toward NAE 18:2 was higher than AHase activity toward NAE 16:0; while formation of NAE oxylipin from NAE 18:2 was considerably higher than the corresponding amidohydrolase activity. These relative activities toward the different NAEs are consistent with the more rapid consumption of NAE 18:2 *in vivo* during seed imbibition.

To test if the oxylipins were formed by the LOX pathway, the influence of two widely used LOX inhibitors on their formation was determined (Fig. 2). Both 5,8,11,14-eicosatetraynoic acid (ETYA) and nordihydroguaiaretic acid (NDGA) reduced NAE-oxylipin formation in a concentration dependent manner. NDGA appeared to be a more potent inhibitor of NAE 18:2-LOX than ETYA, particularly at higher concentrations. Alternatively, NAE 18:2-dependent lipid peroxide formation was estimated spectrophotometrically (Fig. 3). And consistent with the above results, inclusion of both inhibitors reduced the formation of NAE 18:2 lipid hydroperoxide. The small amount of lipid peroxide detected in the absence of enzyme (control-enzyme) was likely due to the spontaneous oxidation of NAE 18:2 during assay reactions, because no lipid peroxide was detected when NAE 18:2 was omitted from reactions (not shown). These data indicate that the polar product in the incubation is formed by the lipoxygenase pathway.

To elucidate the structure of the polar compound, GC/MS analysis was performed (Fig. 4). Selective ion monitoring at m/z 116 (diagnostic of ethanolamine containing lipids) revealed the presence of two oxygenated NAE

18:2 metabolites in incubations of cottonseed extracts incubated with NAE 18:2, with retention times of 18.22 and 18.29 min (Fig. 4A). These compounds were identified as trimethylsilylated, reduced alfa-ketols (diastereomers) 12-oxo-13-hydroxy-*N*-(9Z)-octadecenoylethanolamine by their EIMS (Fig. 4C). Predictable fragmentation ions including the molecular ion [M^+] (m/z 573) were clearly identifiable and spectra were comparable to those recorded in previous studies (Van der Stelt et al., 2000). Only α-ketols originating from 13-hydroperoxy NAE (18:2) were detected indicating that imbibed cottonseeds contained both a 13-LOX and 13-AOS that metabolized NAE 18:2. Of interest also was the identification of the α-ketols 12-oxo-13-hydroxy-(9Z)-octadecenoic acid in the TIC at retention times 14.85 and 14.94 (Fig. 4B, diastereomers), which can be explained by the subsequent actions of NAE amidohydrolase, LOX and AOS. Most importantly these results demonstrate unequivocally that NAE 18:2 was metabolized by 13-LOX (and 13-AOS) in extracts of imbibed cottonseeds raising the possibility that a new class of oxylipins may be involved in seed germination.

Inclusion of FAAH inhibitors to study sensitivity of the cottonseed FFA producing enzyme showed a concentration-dependent effect (Table III). There was approximately a 40 percent inhibition of FFA production with 10 mM phenylmethylsulfonyl fluoride (PMSF), a potent inhibitor of FAAH activity consistent with the catalytic mechanism of a serine hydrolase (Wiley et al., 2000). By contrast there was only 10 percent inhibition by 10 μM arachidonyl trifluoromethyl ketone (ATMK), an analog of anandamide. ATMK is a potent inhibitor of mammalian anandamide hydrolysis showing complete inhibition at 7.5

μM (Koutek et al., 1994). The difference in sensitivity to ATMK may indicate a different property of cottonseed NAE amidohydrolase or may simply be a reflection of the lack of arachidonyl fatty acid derivatives in higher plant tissues.

Developmental Changes in NAE Metabolism

The capacity for NAE oxylipin formation by cytosol-enriched fractions increased during seed imbibition to the highest levels (7 nmol h^{-1} mg^{-1} protein) by 8 h after commencing imbibition (Fig. 5). Activity remained at this level throughout the first 24 h of post germinative growth. Under these conditions, cottonseeds germinate at 12 to 18 h after commencing imbibition, and lipid mobilization (marked by glyoxylate cycle enzymes) is most active in 24 to 48-h-old seedlings (summarized in Chapman and Sprinkle, 1996). As before, inclusion of NDGA helped to confirm that the activity was due to LOX-like enzyme.

The developmental change in cytosolic NAE oxylipin formation was somewhat different from that associated with microsomes (Fig. 6). Microsomal NAE oxylipin formation, like that associated with the cytosol-enriched fractions, increased during imbibition to its highest levels by 8 h after commencing imbibition; however, the membrane associated activity dropped substantially by 16 h (Fig. 6) and was undetectable by 24 h (not shown). The developmental change in membrane associated NAE oxylipin formation paralleled that of NAE amidohydrolase (Fig. 6). In the case of microsomes, NDGA had a profound effect on NAE oxylipin formation (indicative of a LOX-mediated pathway), but had only a modest effect on amidohydrolase activity. Overall these results indicate

that metabolism of NAEs is most active during seed imbibition, just prior to seed germination, and well before the period of lipid mobilization for post germinative seedling growth. This conclusion is consistent with the time period of NAE depletion *in vivo* (Chapman et al., 1999).

Enzymatic Properties of Amidohydrolase and NAE Oxylipin Formation

We compared the enzymatic properties of the NAE AHase pathway and NAE-LOX mediated pathway in cottonseed microsomes to estimate the relative capacity of each pathway to contribute to the metabolism of the predominant seed NAEs (Fig. 7, Table IV). Both pathways exhibited typical Michaelis Menten kinetics when initial velocity measurements were made at increasing NAE concentrations (Fig. 7). For the NAE AHase, the apparent K_m values were similar for NAE 16:0 and NAE 18:2 (K_m values for NAE 16:0 and NAE 18:2 are 83 μM and 74 μM, respectively), although the apparent V_{max} values estimated for NAE 18:2 were nearly twice that as for NAE 16:0 (V_{max} values for NAE 16:0 and NAE 18:2 are 1.6 nmol h^{-1} mg^{-1} protein and 3.0 nmol h^{-1} mg^{-1} protein, respectively). NAE oxylipin formation from NAE 18:2 also exhibited typical saturation kinetics at increasing NAE concentrations (Fig. 7B). The apparent K_m value (70 μM) was similar to that estimated for the NAE AHase, indicating similar substrate affinities for both pathways. On the other hand, the apparent V_{max} (12 nmol h^{-1} mg^{-1} protein) was 4 times that of the NAE AHase-mediated pathway, indicating a greater capacity for NAE oxylipin formation than for NAE hydrolysis. While comparisons of kinetic parameters cannot be interpreted to indicate

relative metabolic flux, these data do indicate that the capacity for NAE consumption by these two pathways estimated *in vitro* exceeds that required for NAE depletion *in vivo*. The degradation rates for NAE 18:2 and NAE 16:0 were calculated to be 15 ng h^{-1} $seed^{-1}$ and 4.5 ng h^{-1} $seed^{-1}$, respectively *in vivo* (Chapman et al., 1999). While the rates were 160 ng h^{-1} $seed^{-1}$ and 80 ng h^{-1} $seed^{-1}$ for NAE 18:2 and NAE 16:0, respectively *in vitro* through NAE amidohydrolase pathway, based on data presented in Table IV. The conversion rate for NAE 18:2 through NAE-LOX pathway was 20 μg h^{-1} $seed^{-1}$ *in vitro* (Table IV) indicating this pathway was relatively more capable of contributing to the metabolism of polyunsaturated NAE (18:2) than was AHase.

NAE Metabolism in vivo

NAE was metabolized *in vivo* by both the NAE-LOX pathway and NAE amidohydrolase pathway during seed imbibition (Fig. 8). Radiotracer experiments with imbibing seeds showed that [1-^{14}C]18:2 NAE was converted to NAE oxylipin and FFA in a time dependent manner. In the presence of the LOX inhibitor, nordihydroguaiaretic acid (NDGA) there was reduction of NAE-oxylipin formation, which was particularly evident after 4 h. Production of FFA from NAE 18:2 also was reduced in the presence of the LOX inhibitor, which may suggest these two pathways are somewhat interdependent. Application of NAE 18:2 or NDGA under these conditions did not influence seed germination. The metabolic results *in vivo* are consistent with those obtained *in vitro* and confirm that NAE 18:2 is metabolized by LOX and AHase pathways, which together likely account

for the *in vivo* depletion of NAE 18:2 during seed imbibition (Chapman et al., 1999).

Discussion

The recent identification and quantification of NAEs in desiccated seeds and their disappearance after 4 h imbibition (Chapman et al., 1999) raised the question as to the metabolic fate of these compounds. Preliminary evidence suggested that these NAEs could be hydrolyzed in imbibed seeds by an NAE amidohydroase activity (Chapman et al., 1999), similar to the fatty acid amide hydrolase (FAAH) found in some animal systems. However, here a detailed evaluation now indicates a more complicated scheme for NAE metabolism in seeds than originally anticipated (Fig. 9). NAEs with saturated fatty acid constituents, like the endogenous NAE 16:0, are indeed hydrolyzed by an amidohydrolase activity. Whereas polyunsaturated NAEs (NAE 18:2) appear to be metabolized by two pathways, the NAE amidohydrolase pathway and a LOX-mediated pathway. The amidohydrolase pathway leads to the formation of free fatty acids, which could be reincorporated, into NAPE, the precursor for NAEs (see Fig. 9). In fact NAPE biosynthesis was shown to be increased during seed imbibition, germination and early post-germinative growth (Sandoval et al., 1995; Chapman and Sprinkle, 1996) as judged by increases in lipid levels and enzyme activity.

Metabolism of NAEs during seed imbibition by a membrane-associated amidohydrolase activity is reminiscent of the mechanism for NAE activation in animal systems. The fatty acid amide hydrolase (FAAH) has been cloned from a

number of mammalian tissues and shown to encode an enzyme with amidase and esterase activities of broad substrate specificity including several fatty acid amides and acylglycerols (Cravatt et al., 1996). Recently, more extensive studies of substrate specificity for the purified recombinant rat enzyme showed that it was capable of hydrolyzing a wide array of unsaturated, and to a less extent saturated, fatty acid primary amides (Boger et al., 2000). As the chain length of fatty acid (saturated) constituents decreased, the rate of hydrolysis increased (Ueda et al., 2000). Mammalian FAAH inhibitors had a relatively modest effect on cottonseed NAE amidohydrolase enzyme(s) (Table III). This may indicate that plant NAE AHases are diverged from the mammalian counterparts to reflect a specificity for NAEs abundant in plant tissues. Although recently, Ueda et al. (2001) reported a new enzyme from lung tissues, designated *N*-palmitoylethanolamine hydrolase that was much less sensitive to inhibition of FAAH suggesting that animal systems may contain more than one NAE amidohydrolase. Additional work will be required at the biochemical and molecular levels to more fully understand the nature of NAE AHase activity(ies) in plant systems, and to define specific what role this pathway plays in seed germination.

Recent evidence demonstrated that purified plant LOX, AOS and HPO lyase could metabolize synthetic NAEs to generate novel oxylipins (Van der Stelt et al., 2000), raising the possibility that plants might catalyze these reactions *in vivo*. Here we provide several lines of evidence that support this concept and highlight seed imbibition and germination as a period intensely involved in

formation of these metabolites. The time course of NAE 18:2 metabolism in cytosol-enriched fractions isolated at various times of seed imbibition, germination and post germinative growth showed the maximum specific activity of LOX (7 nmol h^{-1} mg^{-1} protein) at 8 h after imbibition which is just prior to seed germination (Fig. 5). Similarly, microsomes isolated at the same developmental stages showed the same time period for the highest specific activity of LOX (8 nmol h^{-1} mg^{-1} protein) and NAE amidohydrolase (2 nmol h^{-1} mg^{-1} protein) (Fig. 6) consistent with results *in vivo* (Chapman et al., 1999).

The fate of NAE derived oxylipins is unclear at this point, but it is tempting to speculate these NAE oxylipins may have a role of their own during seed germination. For example, Feussner and coworkers (2001), recently proposed that 13-LOX mediated pathway is associated with a “priming” function in oilseeds for post-germinative triacylglycerol mobilization. It should be emphasized, however, that here the timing of the most intensive NAE metabolism of cottonseed NAEs preceded radicle emergence and lipid mobilization (Figs. 5,6; also see Chapman and Sprinkle, 1996), so these NAE derived oxylipins may play other roles perhaps as lipid mediators involved in the regulation of seed germination. In any case, the role of NAE metabolism in imbibing seeds is not specific to oilseeds since a similar depletion of seed NAEs was observed in non-oilseeds (e.g. pea, Chapman et al., 1999).

Materials and Methods

Chemicals

[1-^{14}C]Palmitic acid (53 mCi^{-1}mmol in ethanol) and [1-^{14}C]linoleic acid (53 mCi mmol^{-1} in ethanol) were from NEN, Life Science Products, Inc., Boston, MA 02118.

Chemical Synthesis of NAEs

Specific NAE types were synthesized from respective radiolabeled FFA by first producing the fatty acyl chloride (Hillard et al., 1995). The FFA was dissolved in dichloromethane then mixed with dimethylformamide (1 mole equivalent) and oxalyl chloride (1.2 mole equivalent). The fatty acyl chloride was mixed with a ten-fold excess of ethanolamine to convert the acyl chloride to the corresponding *N*-acylethanolamine. Products were extracted in dichloromethane and purified by TLC. Yield and purity of NAEs were estimated by radiometric scanning (Bioscan system 200 image scanner). The yield was routinely 65-70% (starting from FFA) and purity after TLC was >99%. Radiospecific activity was calculated from the original [^{14}C]-labeled free fatty acid and adjusted accordingly with non-radiolabeled synthetic NAE produced by the same method.

Plant Material

Cottonseeds (*Gossypium hirsutum* L., Stoneville 7A glandless) were provided by Dr. R.B. Turley (USDA-ARS Cotton Physiology and Genetics

Laboratory, Stoneville, MS). For all the experiments, seeds were surface-sterilized with 20% (v/v) commercial bleach (sodium hypochlorite) solution for 5 min. Seeds were rinsed several times and imbibed in distilled water (in the dark) for 4 h at 30 °C with aeration. For time course experiments, imbibed seeds were placed in filter paper scrolls as previously described (Chapman and Trelease, 1991a) and germinated and grown in the dark (30 °C).

Preparation of Cellular Fractions

Cell fractions were prepared by differential centrifugation as described (Chapman and Trelease, 1991b) with some modifications. Briefly, seeds imbibed for 4 h were chopped with a steel blade on ice in homogenization medium containing 100 mM potassium-phosphate (pH 7.2), 10 mM KCl, 1 mM EDTA, 1 mM EGTA and 400 mM sucrose. The homogenates were filtered through four layers of cheesecloth and centrifuged at 650 x g_{max} (4 °C) for 10 min in a Sorvall RC 5C centrifuge (SS 34 rotor). The 650 x g_{max} supernatant was centrifuged at 10,000 x g_{max} (4 °C) for 30 min in the same centrifuge. The resulting supernatant was centrifuged at 150,000 x g_{max} (4 °C) for 60 min in Sorvall Discovery 90 model ultracentrifuge centrifuge (Beckman Ti45 rotor). Microsomes (150,000 x g_{max} pellet) were resuspended in homogenization medium (0.3 mL per original g.f.w.). Protein concentration was estimated according to Bradford (1976) using bovine serum albumin as the standard.

Lipid Extractions and Analysis

For enzymatic assays *in vitro*, 100 μM (20,000 dpm) of [^{14}C]NAE substrate (combined with non-radioactive NAE and radiolabeled on the carbonyl carbon) was suspended by sonication in 50 mM MES buffer (pH 6.5). Reactions were initiated by adding 400 μL cell fractions. Reactions were terminated and lipids were extracted into chloroform according Bligh and Dyer (1959) modified to eliminate endogenous phospholipase D activity (Chapman and Moore, 1993). Briefly, reactions were stopped by adding 2 mL of hot 2-propanol (70 °C) to 800 μL of the aqueous assay reaction mixture and heated at 70 °C for 30 min. One mL of chloroform was added to the mixtures, and lipids were extracted at 4 °C overnight. One mL of chloroform and 2 mL of KCl (1M) were added to induce phase separation. The aqueous layer was aspirated off and the organic layer was washed two times with 2 mL of KCl (1M) and once with deionized H_2O (MilliQ UF plus). The organic phase was collected and dried under nitrogen. Lipid classes were separated by TLC (Hexane:Ethyl acetate:Methanol; 60:40:5; v/v/v). Identification and quantification of radiolabeled lipids were performed by radiometric scanning (Bioscan system 200 image scanner) and comigration with known standards.

NAE Metabolism in vivo

For radiolabeling experiments *in vivo*, seed coats were removed from imbibed (4h) seeds, which were then preincubated for 30 min with (or without, DMSO only control) LOX inhibitor (5 μL of 16 mM NDGA per seed) before

application of radiolabeled NAE 18:2. Synthetic NAE 18:2 (0.1 μCi, 2.04 mCi^{-1} mmol) was applied in a small volume to each seed. Imbibed seeds were incubated for various time periods in the dark on moistened filter paper in 100x15 mm covered Petri dishes. Radiolabeled lipids were extracted and analyzed as described above.

Spectrophotometric Assay of Lipid Hydroperoxide Formation

Determination of LOX activity also was performed with a commercially available Lipid Hydroperoxide (LPO) assay kit (Cayman chemical; Cat # 705002). For each assay 80 nmol of NAE 18:2 was utilized as substrate and incubated with crude extract for 1 h at 30 °C with shaking (110 rpm). The lipid peroxides that were formed were extracted from the samples into chloroform and quantified by measuring absorbance at 500 nm compared with the standard lipid hydroperoxide (13-hydroperoxy octadecadienoic acid). Lipid peroxide formation in imbibed cottonseed extracts was protein, temperature and NAE 18:2 dependent.

Identification of NAE Oxylipins by GC/MS

NAE-derived oxylipins were evaluated by GC/MS as previously described (Van der Stelt et al., 2000) except lipids were reduced with $NaBH_4$ instead of $NaBD_4$. Briefly, imbibed cottonseed cell fractions, prepared as described above, were diluted 1:1 in 50 mM potassium phosphate buffer, pH 6, and incubated with 100 μM NAE 18:2 for 2 hours at room temperature. Lipid products were

extracted, reduced with $NaBH_4$, methylated, and trimethylsilylated before identification by GC/MS using the conditions described previously (Van der Stelt et al., 2000).

Table I. *Subcellular distribution of NAE-LOX (NAE oxylipin formation) and NAE amidohydrolase (FFA formation) activities in 4 h imbibed cottonseed cell fractions utilizing NAE 16:0 as substrate*

Cell fractions were prepared in (and pellets resuspended in) 100 mM potassium-phosphate (pH 7.2), 10 mM KCl, 1 mM EDTA, 1 mM EGTA and 400 mM sucrose. For assays, 100 μM of [^{14}C]NAE 16:0 (20,000 dpm) in 50 mM MES buffer (pH 6.5) was used. Reactions were initiated by adding 400 μL of respective cell fraction in a total volume of 800 μL. The data are means and SD of three replicates and are representative of three experiments.

	FFA		Oxylipin	
	Total Activity	Specific Activity	Total Activity	Specific Activity
	nmol h^{-1}	*nmol h^{-1} mg^{-1}*	*nmol h^{-1}*	*nmol h^{-1} mg^{-1}*
Cell Fraction		*Protein*		*Protein*
10,000*g* supernatant	51.04±1.42	0.53±0.01	0	0
10,000*g* pellet	0	0	0	0
150,000*g* supernatant	0	0	0	0
150,000*g* pellet	10.68±0.51	0.63±0.03	0	0

Table II. *Subcellular distribution of NAE-LOX (NAE oxylipin formation) and NAE amidohydrolase (FFA formation) activities in 4 h imbibed cottonseed cell fractions utilizing NAE 18:2 as substrate*

Cell fractions were prepared in (and pellets resuspended in) 100 mM potassium-phosphate (pH 7.2), 10 mM KCl, 1 mM EDTA, 1 mM EGTA and 400 mM sucrose. For assays, 100 μM of [^{14}C]NAE 18:2 (20,000 dpm) in 50 mM MES buffer (pH 6.5) was used. Reactions were initiated by adding 400 μL of respective cell fraction in a total volume of 800 μL. The data are means and SD of three replicates and are representative of three experiments.

	FFA		Oxylipin	
	Total Activity	Specific Activity	Total Activity	Specific Activity
	nmol h^{-1}	*nmol h^{-1} mg^{-1}*	*nmol h^{-1}*	*nmol h^{-1} mg^{-1}*
Cell Fraction		*Protein*		*Protein*
10,000*g* supernatant	33.06±2.37	0.35±0.02	780.97±3.08	8.16±0.03
10,000*g* pellet	0	0	18.09±1.67	0.46±0.04
150,000*g* supernatant	0	0	435.49±2.87	7.01±0.05
150,000*g* pellet	19.46±2.27	1.15±0.13	126.16±1.56	7.44±0.08

Table III. *The effects of FAAH inhibitors on metabolism of NAE 18:2* in vitro

The amounts of FFA formation was determined by incubating (1h) synthetic NAE 18:2 with 150,000 x g_{max} (60 min) microsomes from 10,000 x g_{max} (30 min) supernatant. The radiometric analysis showed arachidonyl trifluoromethyl ketone (ATMK) was more potent than phenylmethylsulfonyl fluoride (PMSF). Both inhibitors had similar effect when NAE 16:0 was utilized as substrate. The data are means and SD of three replicates and are representative of two experiments.

Concentrations	Specific Activity *nmol h^{-1} mg^{-1} Protein*	*Relative Inhibition (%)*
Phenylmethylsulfonyl fluoride (PMSF)		
0 mM	1.88±0.20	0.0
0.01 mM	1.90±0.42	-1.1
0.1 mM	1.68±0.32	10.6
1 mM	1.62±0.12	13.8
10 mM	1.14±0.11	39.4
Arachidonyl trifluoromethyl ketone (ATMK)		
0 μM	1.79±0.30	0.0
0.01 μM	1.71±0.35	4.5
0.1 μM	1.60±0.26	10.6
1 μM	1.64±0.28	8.4
10 μM	1.63±0.10	8.9

Table IV. *Summary of kinetic parameters of NAE utilizing enzymes in cottonseed microsomes.*

Parameters were estimated by fitting the data in Fig. 7 to the Michaelis-Menten equation (GraphPad Prism software, version 3.0).

Substrate	Pathway	K_m (μM)	V_{max} (nmol h^{-1} mg^{-1} protein)
NAE 16:0	AHase	83.43	1.62
NAE 18:2	AHase	73.65	2.97
NAE 18:2	NAE-LOX	69.91	11.82

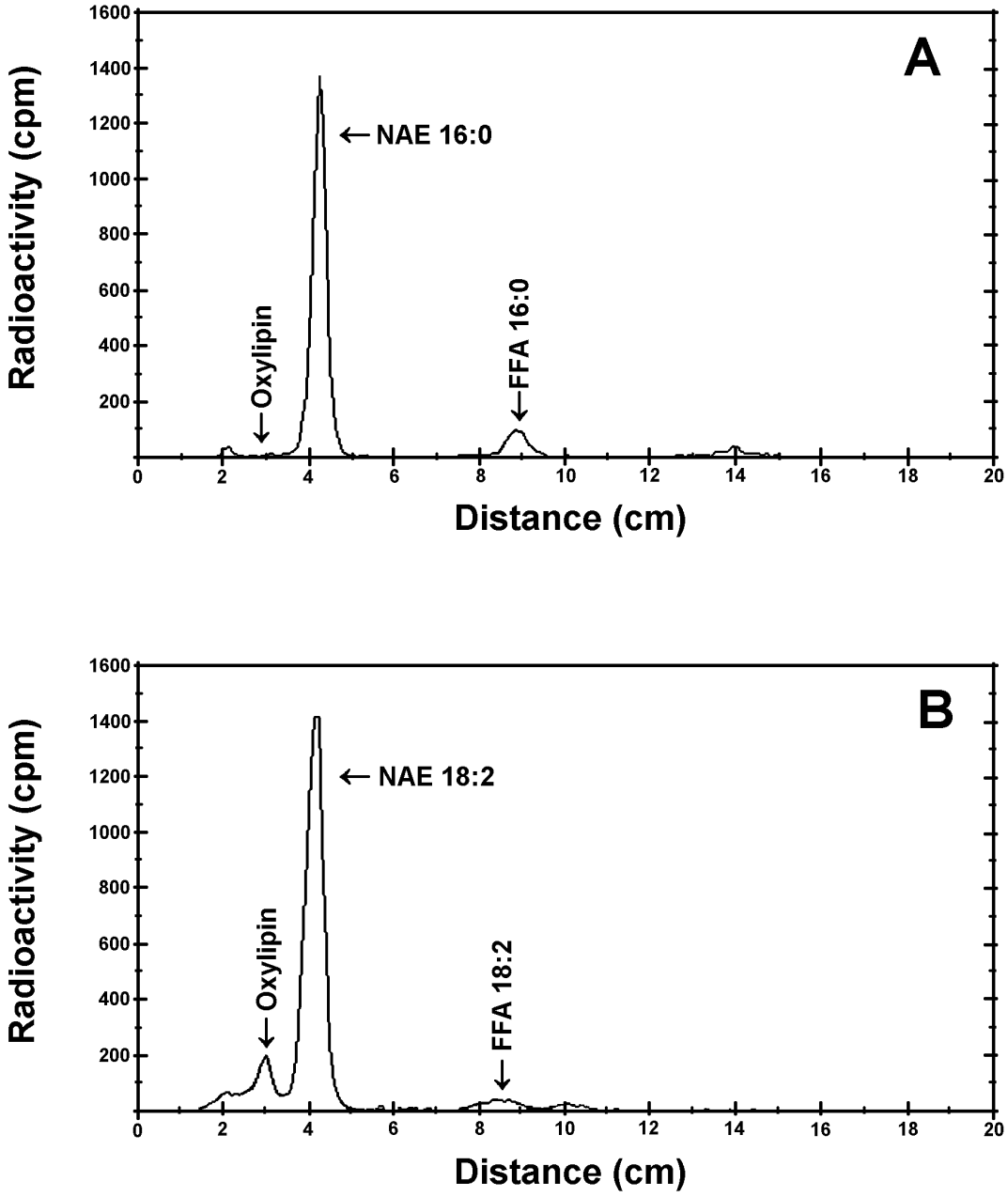

Figure 1. Representative chromatograms of radioactive lipids separated on TLC plates. For the assay 100 μM of [^{14}C]NAE (*N*-[1-^{14}C]acylethanolamine) with 20,000 dpm in 50 mM MES buffer (pH 6.5) was used. Reactions were initiated by adding 400 μL microsomes and incubated at 30 °C for 1 h with shaking.

Lipids are extracted as described in “Materials and Methods” and distribution of radioactivity on TLC plates was evaluated by radiometric scanning (Bioscan system 200 image scanner). When synthetic NAE 16:0 was utilized as a substrate, FFA was produced (A) and when synthetic NAE 18:2 was utilized as a substrate, FFA as well as an additional lipid product(s) were formed (B).

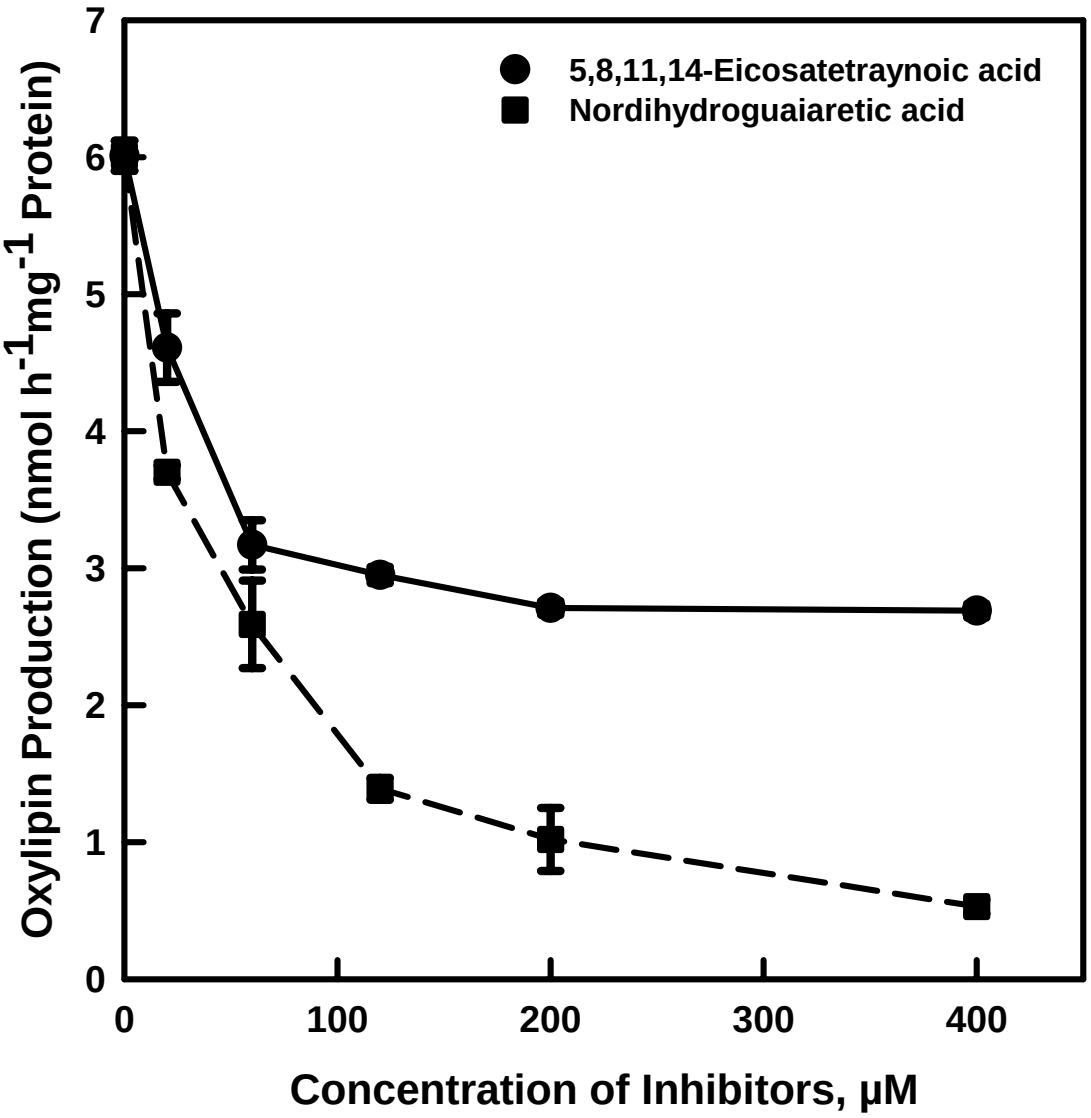

Figure 2. The effects of LOX inhibitors on the metabolism of NAE 18:2 *in vitro*. The amount of NAE-oxylipin was determined by incubating (1 h) synthetic NAE 18:2 with a 150,000 x g_{max} (60 min) supernatant of imbibed cottonseeds. Total lipids were extracted from the reaction mixture and were separated by TLC (Hexane:Ethyl acetate:Methanol; 60:40:5; v/v/v). Identification and quantification

of radiolabeled lipids were performed by radiometric scanning. 5,8,11,14-Eicosatetraynoic acid (ETYA) is a dual-specific inhibitor, affecting both lipoxygenase and cyclooxygenases and is irreversible (Grullich et al., 2000). Nordihydroguaiaretic acid (NDGA) is a classical inhibitor of different lipoxygenases (Kulkarni and Sajan, 1999). There was almost complete inhibition of oxylipin production at 400 μM NDGA and 50% inhibition at 400 μM ETYA. The data points are means and SD of three replicates of one experiment.

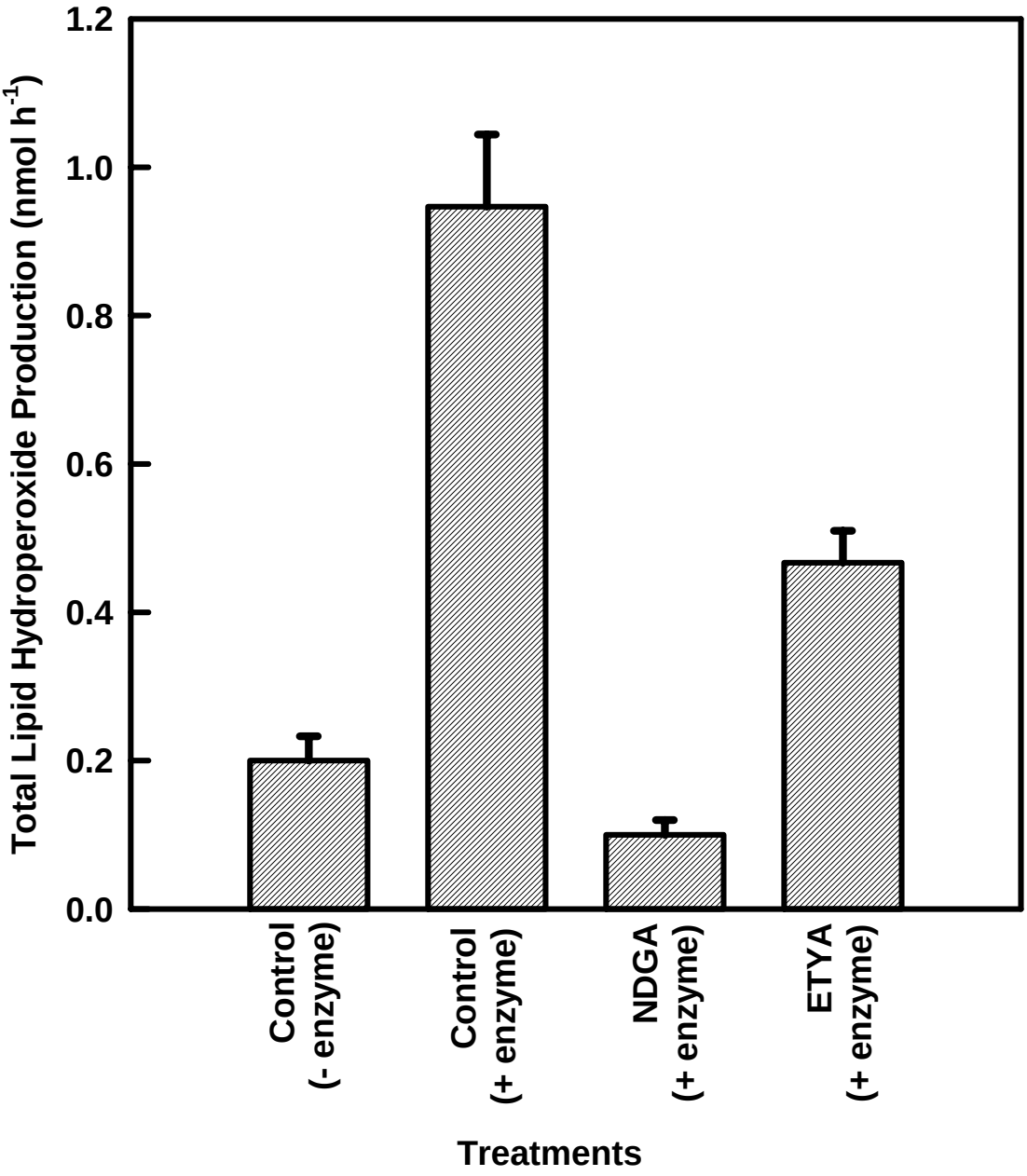
Total Lipid Hydroperoxide Production (nmol h-1)
1.2
1.0
0.8
0.6
0.4
0.2
0.0
Control (- enzyme)
Control (+ enzyme)
NDGA (+ enzyme)
ETYA (+ enzyme)
Treatments

Figure 3. Determination of LOX activity was performed with a Lipid Hydroperoxide assay kit. (a) Control: 80 nmol of NAE without enzyme showed the natural hydroperoxidation, which is 0.200 nmol h^{-1}; (b) control with enzyme (3.33 mg protein per assay): the total activity was 0.947 nmol h^{-1}; (c) NDGA (100 μM) with enzyme showed the effect of a classical LOX inhibitor. This inhibitor inhibited the effect of natural peroxidation as well which was also observed in other radiolabeled experiments; and (d) ETYA (100 μM) with enzyme showed the expected effect of LOX inhibitor. There was 50% inhibition, which was also observed in radiolabeled NAE 18:2 substrate metabolism experiments. Experiments without synthetic substrate was also carried out in order to confirm the absence of lipid hydroperoxide in the cell extract itself. Also, an experiment without EDTA was carried out to investigate any possible role of EDTA. All those experiments were negative. Determination of LOX activity was performed with a commercially available Lipid Hydroperoxide (LPO) assay kit (Cayman chemical; Cat # 705002). For each assay 80 nmol of NAE 18:2 was utilized as substrate and incubated with crude extract for 1 h at 30 °C with shaking (110 rpm). The lipid peroxides that were formed were extracted from the samples into chloroform and quantified by measuring absorbance at 500 nm compared with the standard lipid hydroperoxide (13-hydroperoxy octadecadienoic acid). The data points are means and SD of three replicates of one experiment.

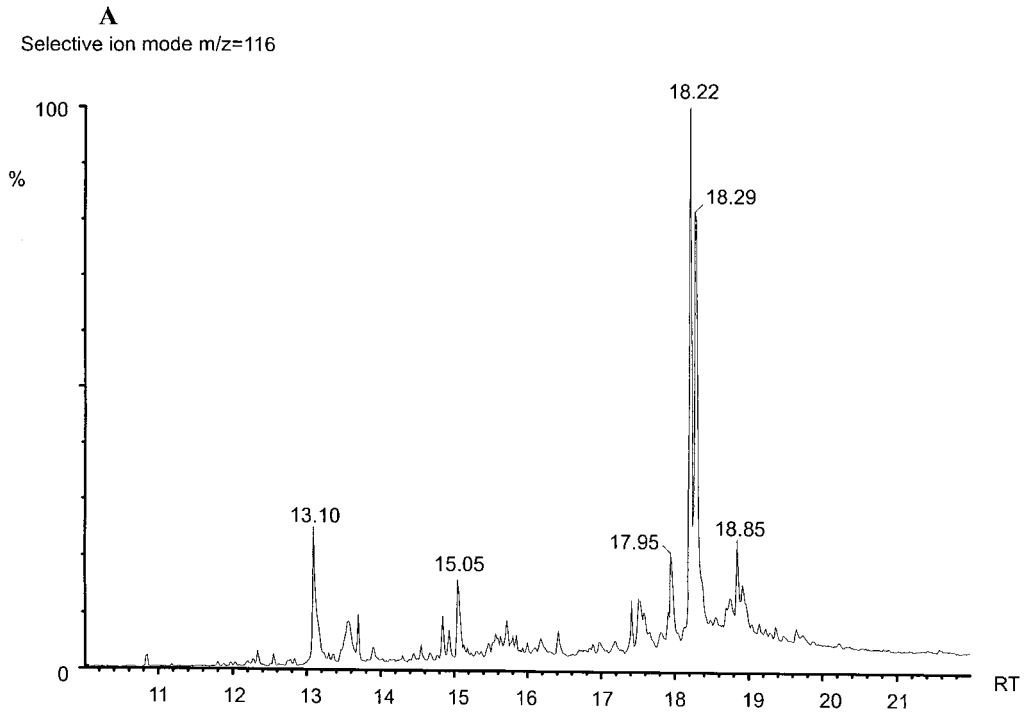
A
Selective ion mode m/z=116
100
%
0
18.22
18.29
13.10
15.05
17.95
18.85
11
12
13
14
15
16
17
18
19
20
21
RT

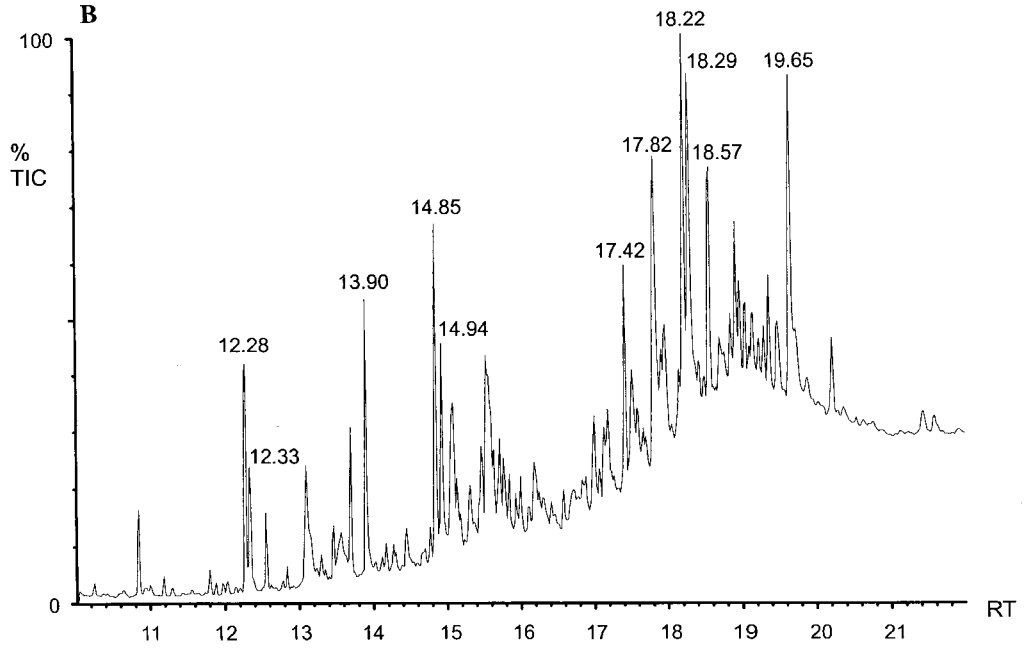
B
100
%
TIC
0
18.22
18.29
19.65
17.82
18.57
14.85
17.42
13.90
14.94
12.28
12.33
11
12
13
14
15
16
17
18
19
20
21
RT

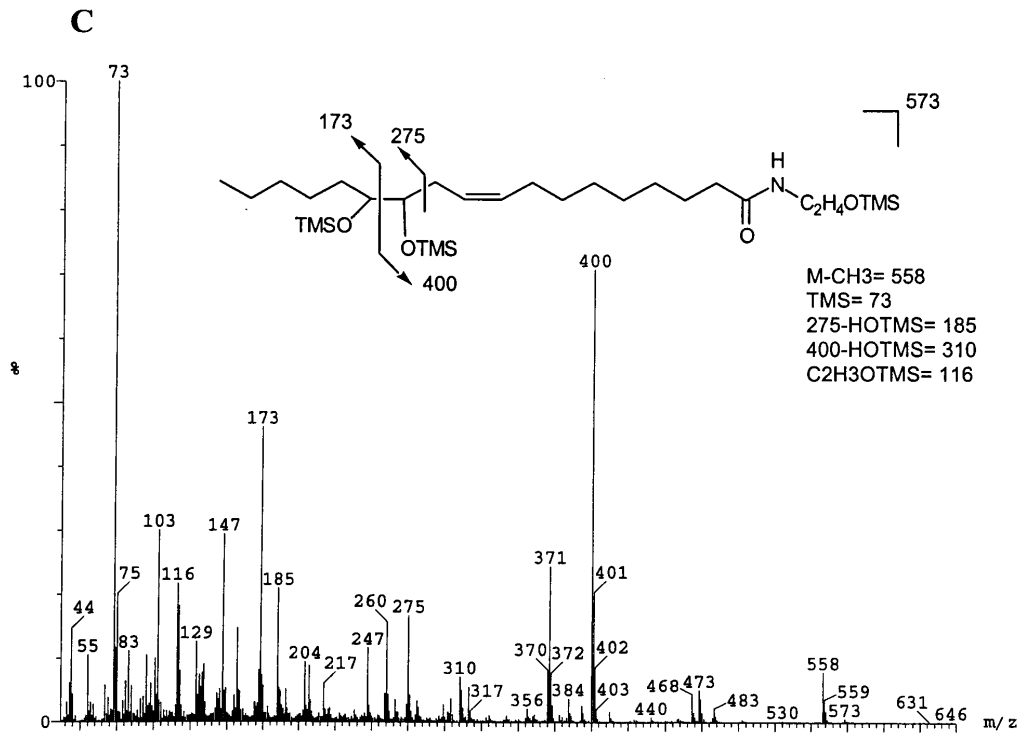

Figure 4. A, Single-ion chromatogram at m/z 116 (characteristic fragment for the ethanolamine group) of NAE metabolites after incubating with 150,000 x *g* supernatant of cottonseeds. The peaks with RT=18.22 and 18.29 are alfa-ketols of 13-hydroperoxy NAE (two diastereomers) = 12-oxo-13-hydroxy-*N*-(9Z)-octadecenoylethanolamine.

B, Total ion chromatogram (TIC) of derivatized lipid products after incubating NAE 18:2 with the 150,000 x *g* supernatant of imbibed cottonseeds. Several peaks were identified by MS: 12.28 min: C18:2 linoleic acid; 12.33 min: C18:1 oleic acid; 12.55 min: C18:0 stearic acid; 13.90 min: 13-HPOD (13-hydroperoxy octadecadienoic acid); 14.85 and 14.94 min: alfa-ketols of 13-HPOD; 18.22 and

18.29 min: alfa-ketols of 13-hydroperoxy NAE = 12-oxo-13-hydroxy-*N*-(9Z)-octadecenoylethanolamine.

C, Electron impact mass spectrum (EIMS) of fully reduced TMS-ethers of 12-oxo-13-hydroxy-*N*-(9Z)-octadecenoylethanolamine, the compound eluting with retention time of 18.22 min (above A,B).

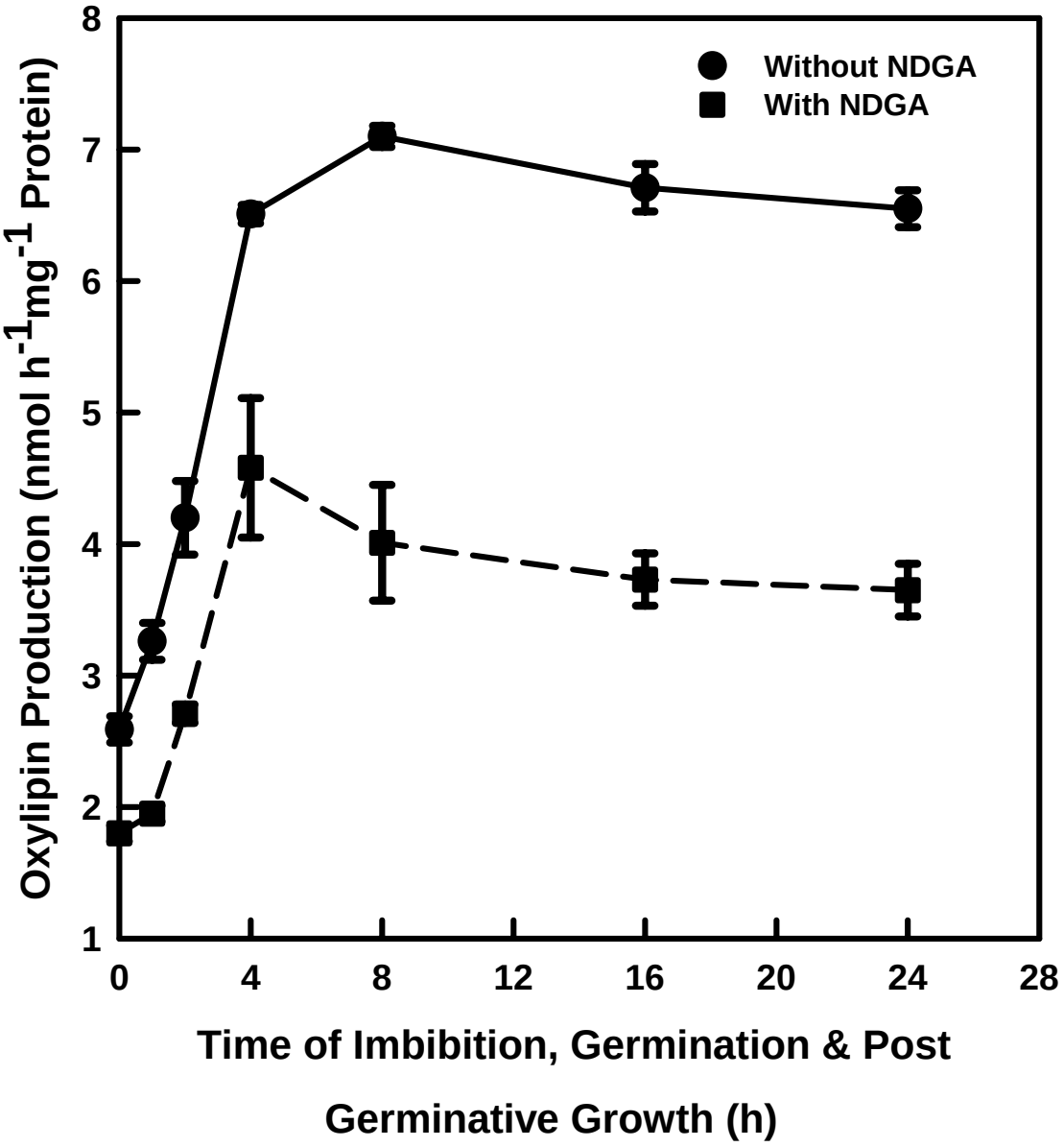

Figure 5. Time course of NAE 18:2 metabolisms in cytosol-enriched fractions isolated at various times of seed imbibition (up to 4 h), germination (at about 12 h) and post germinative growth. The amount of oxylipin production was determined by incubating 100 μM synthetic NAE 18:2 (20,000 dpm) with 400 μL of the supernantant (150,00 x g_{max} supernatant of 10,000 x g_{max} supernatant) in a

final volume of 800 μL with shaking for 1 h at 30 °C. Lipids were extracted as described in “Materials and Methods”. Identification and quantification of radiolabeled NAE-lipids were performed by radiometric scanning. The maximum specific activity of “LOX” was at 8 h (just prior to seed germination). When 100 μM NDGA was used there was almost 50% inhibition of oxylipin production. It indicates that the product of NAE 18:2 was most likely due to enzymatic action of LOX. The data points are means and SD of three replicates of one representative experiment repeated for three times.

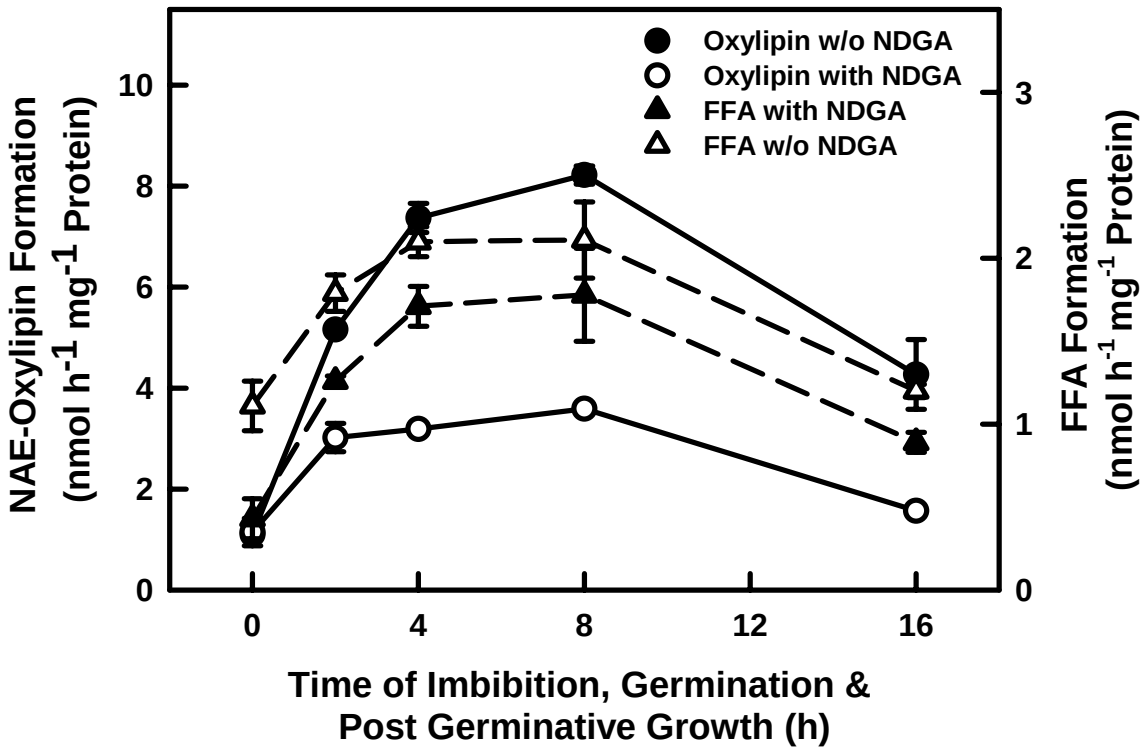

Figure 6. Time course of NAE 18:2 metabolism in microsomes isolated at various stages of cottonseed imbibition, germination, and post germinative seedling growth. Both amidohydrolase and "LOX" activities were detected in microsomes (see also Tables I, II). Both activities increased prior to and decreased after seed germination. NDGA reduced substantial oxylipin formation, whereas, there was minimal effect on FFA production *in vitro*. The highest specific activities of "LOX" and NAE amidohydrolase were at 8 h and 4 - 8 h, respectively after commencing imbibition (just prior to seed germination, 12 to 18 h). The data points are means and SD of three replicates within a given experiment and are representative of three experiments.

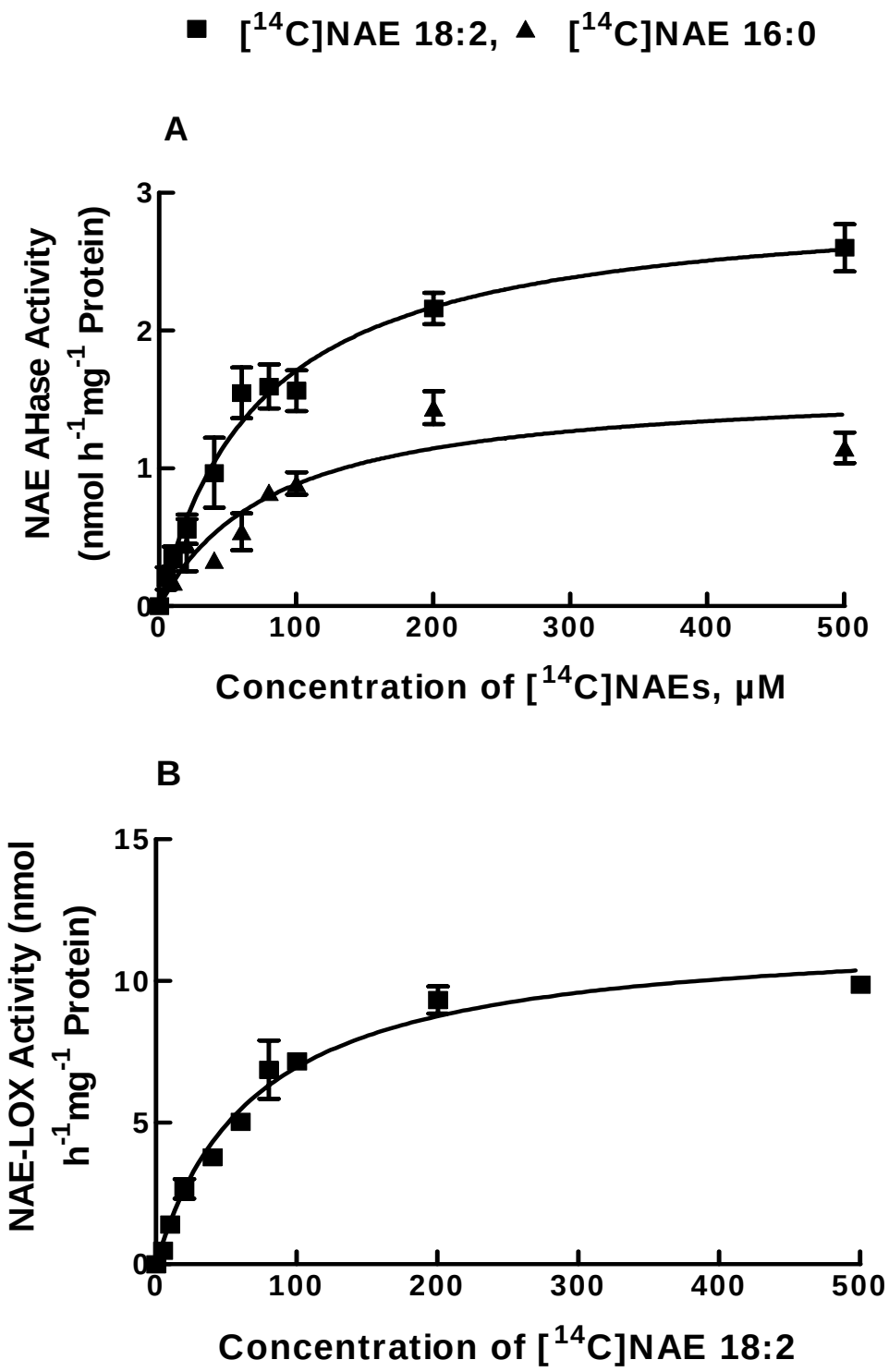
■ [14C]NAE 18:2, ▲ [14C]NAE 16:0
A
NAE AHase Activity (nmol h-1mg-1 Protein)
0
1
2
3
0
100
200
300
400
500
Concentration of [14C]NAEs, μM
B
NAE-LOX Activity (nmol h-1mg-1 Protein)
0
5
10
15
0
100
200
300
400
500
Concentration of [14C]NAE 18:2

Figure 7. Concentration dependent formation of FFA from NAE substrate in cottonseed microsomes under initial velocity conditions. The apparent K_m and V_{max} for NAE 16:0 were estimated to be 83 μM and 1.6 nmol h^{-1} mg^{-1} protein, respectively. The apparent K_m and V_{max} for NAE 18:2 were estimated to be 74 μM and 3.0 nmol h^{-1} mg^{-1} protein, respectively. Concentration dependent formation of oxylipin from NAE 18:2 incubating the same cell fraction showed the apparent K_m and V_{max} to be 70 μM and 12 nmol h^{-1} mg^{-1} protein, respectively. In panel A, NAE 16:0 and NAE 18:2 were the substrates and in panel B, NAE 18:2 was the substrate. Lines represent non-linear regression fits of the data using Michaelis-Menten equation (GraphPad Prism software, version 3.0). Kinetic parameters were estimated from regression analyses. While the microsomal NAE amidohydrolase appears to have similar affinities for saturated and polyunsaturated NAE species, the maximum rate of product formation from NAE 18:2 is about 2 times that for NAE 16:0. Similarly in panel B, the enzyme has similar affinity of 70 μM with 4 times more production rate of conversion of NAE 18:2 into NAE-LOX product. Data points are averages of triplicate samples within a representative experiment.

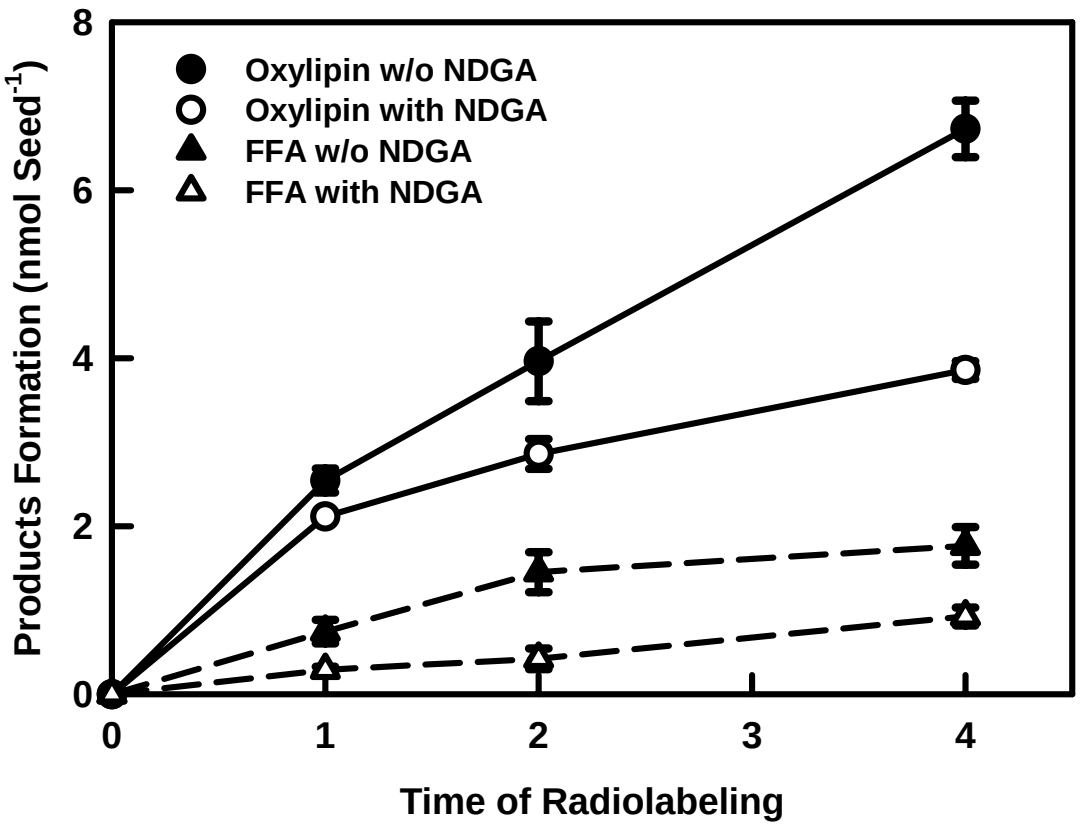

Figure 8. Metabolism of [^{14}C]-labeled NAE 18:2 *in vivo* by imbibing cottonseeds. Seed coats were removed from imbibing (4h) seeds, which were then incubated 30 min with (or without, DMSO-only control) LOX inhibitor (5 μL of 16 mM NDGA per seed) before application of radiolabeled NAE 18:2 (0.1 μCi seed^{-1}, 2.04 mCi^{-1} mmol per seed). Imbibed seeds were incubated on moist filter paper in covered Petri dishes for additional 1, 2 and 4 h in the dark. Lipids were extracted, separated by TLC as described in "Materials and Methods" and distribution of radioactivity was evaluated by radiometric scanning (Bioscan system 200 image scanner). The data points are means and SD of four replicates within a single

experiment. Additional experiments showed identical trends, although the efficiency of incorporation of radiolabel varied somewhat from experiment to experiment. Both oxylipin and FFA production increased with time. The conversion of NAE 18:2 to NAE-oxylipin was reduced by application of a classical LOX inhibitor, NDGA (see Fig. 2). NDGA had some effect on production of FFA, as well. For clarity, the amount of radioactivity in NAE 18:2 is not included but represented nearly all of the remaining proportion of radioactive lipid.

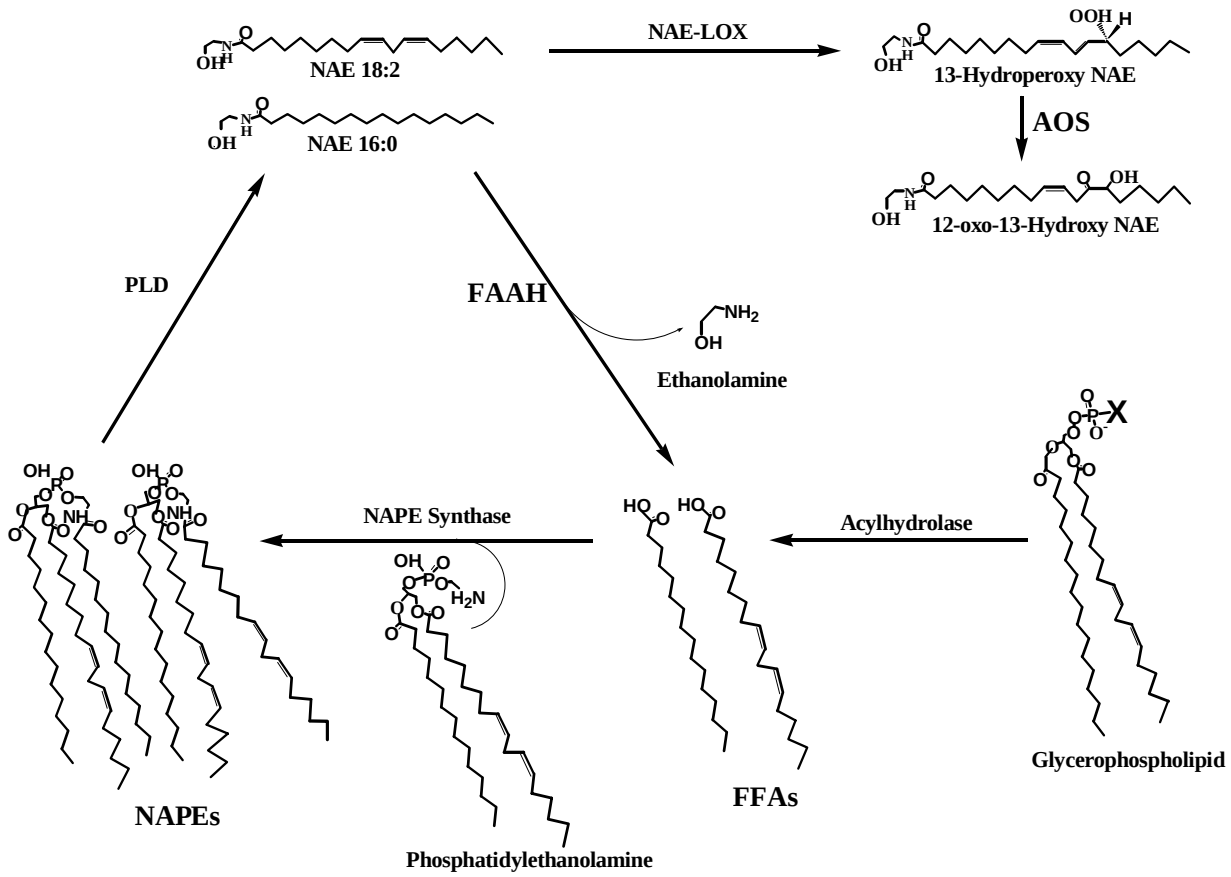

Figure 9. Proposed scheme for the metabolism of *N*-acylethanolamines (NAEs) in seeds and seedlings. NAPEs are hydrolyzed by PLD to yield saturated and unsaturated species of NAE. FAAH hydrolyzes NAEs to free fatty acids and ethanolamine. Alternatively, some polyunsaturated NAEs are metabolized by 13-LOX and 13-AOS to yield NAE oxylipins (13-hydroperoxy NAE, 13-hydroperoxy octadecadienoylethanolamine and 12-oxo-13-hydroxy NAE, 12-oxo-13-hydroxy octadecenoylethanolamine). Free fatty acids formed from hydrolysis of NAE or glycerophospholipids can be incorporated directly into the *N*-position of NAPE (Chapman, 2000; Rawyler and Braendle, 2001) by NAPE synthase. This overall cycle could be used for signal transduction (formation of NAE lipid mediators) or

to scavenge free fatty acids (for membrane protection) depending upon cellular demands. The “X” in the glycerophospholipid molecule represents the head group of any phospholipid class (e.g. serine, choline, ethanolamine etc.).

Acknowledgments

I thank Dr. Swati Tripathy, University of North Texas, Dr. Ivo Feussner, Institute of Crop Genetics, Gatersleben, Germany for helpful advice regarding NAEs and LOX, respectively, and Dr. Gerrit A. Veldink's lab, Bijvoet Center for Biomolecular Research, Utrecht University, the Netherlands for molecular identification of NAE lipoxygenase products.

Literature Cited

Bligh EG, Dyer WG (1959) A rapid method of total lipid extraction and purification. Can J Biochem Physiol 37: 911-917

Boger DL, Fecik RA, Patterson JE, Miyauchi H, Patricelli MP, Cravatt BF (2000) Fatty acid amide hydrolase substrate specificity. Bioorg Med Chem Lett 10: 2613-2616

Bradford MM (1976) A rapid and sensitive method for quantification of microgram quantities of protein utilizing the principle of protein-dye bind. Anal Biochem 72: 248-254

Buckley NE, McCoy KL, Mezey E, Bonner T, Zimmer A, Felder CC, Glass M, Zimmer A (2000) Immunomodulation by cannabinoids is absent in mice deficient for cannabinoid CB2 receptor. Eur J Pharmacol 396: 141-149

Chapman KD (2000) Emerging physiological roles for *N*-acylphosphatidylethanolamine metabolism in plants: signal transduction and membrane protection. Chem Phys Lipids 108: 221-230

Chapman KD, Moore TS, Jr (1993) *N*-Acylphosphatidylethanolamine synthesis in plants: occurrence, molecular composition, and phospholipid origin. Arch Biochem Biophys 301: 21-33

Chapman KD, Sprinkle WB (1996) Developmental, tissue-specific and environmental factors regulate the biosynthesis of *N*-

Acylphosphatidylethanolamine in cotton (*Gossypium hirsutum* L.). Plant Physiol 149: 277-284

Chapman KD, Trelease RN (1991a) Acquisition of membrane lipids by differentiating glyoxysomes: role of lipid bodies. J Cell Biol 115: 995-1007

Chapman KD, Trelease RN (1991b) Intracellular localization of phosphotidylcholine and phosphotidylethanolamine synthesis in cotyledons of cotton seedlings. Plant Physiol 95: 69-76

Chapman KD, Tripathy S, Venables BJ, Desouza AD (1998) *N*-Acylethanolamines: formation and molecular composition of a new class of plant lipids. Plant Physiol 116: 1163-1168

Chapman KD, Venables BJ, Markovic R, Blair RW, Bettinger C (1999) *N*-Acylethanolamines in seeds: quantification of molecular species and their degradation upon imbibition. Plant Physiol 120: 1157-1164

Cravatt BF, Demarest K, Patricelli MP, Bracey MH, Giang DK, Martin BR, Lichtman AH (2001) Supersensitivity to anandamide and enhanced endogenous cannabinoid signaling in mice lacking fatty acid amide hydrolase. Proc Natl Acad Sci 98: 9371-9376

Cravatt BF, Giang DK, Mayfield SP, Boger DL, Lerner RA, Gilula NB (1996) Molecular characterization of an enzyme that degrades neuromodulatory fatty-acid amides. Nature 84: 83-87

Feussner I, Kuhn H, Wasternack C (2001) Lipoxygenase-dependent degradation of storage lipids. Trends Plant Sci 6: 268-273

Grullich C, Duvoisin RM, Wiedmann M, Leyen K (2001) Inhibition of 15-lipoxygenase leads to delayed organelle degradation in the reticulocyte. FEBS Lett 489: 51-54

Hansen HS, Moesgaard B, Hansen HH, Petersen G (2000) *N*-Acylethanolamines and precursor phospholipids – relation to cell injury. Chem Phys Lipids 108: 135-150

Hillard CJ, Edgemond WS, Campbell WB (1995) Characterization of ligand binding to the cannabinoid receptor of rat brain membranes using a novel method: application to anandamide. J Neurochem 64: 677-683

Koutek B, Prestwick GD, Howlett AC, Chin SA, Salehani D, Akhavan N, Deutsch DG (1994) Inhibitors of arachidonoyl ethanolamide hydrolysis. J Biol Chem 269(37): 22937-22940

Kulkarni AP, Sajan M (1999) Lipoxygenase – another pathway for glutathione conjugation of xenobiotics: A study with human term placental lipoxygenase and ethacrynic acid. Arch Biochem Biophys 371: 220-227

Paria BC, Dey SK (2000) Ligand-receptor signaling with endocannabinoids in preimplantation embryo development and implantation. Chem Phys Lipids 108: 211-220

Pertwee RG (2001) Cannabinoid receptors and pain. Prog Neurobiol 63:569-611

Rawyler AJ, Braendle RA (2001) *N*-Acylphosphatidylethanolamine accumulation in potato cells upon energy shortage caused by anoxia or respiratory inhibitors. Plant Physiol 127: 240-251

Sandoval JA, Huang Z-H, Garrett DC, Gage DA and Chapman KD (1995) *N*-Acylphosphatidylethanolamine in dry and imbibing cotton (*Gossypium hirsutum* L.) seeds: amounts, molecular species and enzymatic synthesis. Plant Physiol 109: 269-275

Sarker KP, Obara S, Nakata M, Kitajima I, Maruyama I (2000) Anandamide induces apoptosis of PC-12 cells: involvement of superoxide and caspase-3. FEBS Lett 472: 39-44

Schmid HHO (2000) Pathways and mechanisms of *N*-acylethanolamine biosynthesis: can anandamide be generated selectively? Chem Phys Lipids 108: 71-87

Schmid HHO, Schmid PC, Nataranjan V (1990) *N*-Acylated glycerophospholipids and their derivatives. Prog Lipid Res 29: 1-43

Tripathy S, Venables BJ, Chapman KD (1999) *N*-Acylethanolamines in signal transduction of elicitor perception: attenuation of alkalinization response and activation of defense gene expression. Plant Physiol 121: 1299-1308

Ueda N, Puffenbarger RA, Yamamoto S, Deutsch DG (2000) The fatty acid amide hydrolase (FAAH). Chem Phys Lipids 108: 107-121

Ueda N, Yamanaka K, Yamamoto S (2001) Purification and characterization of an acid amidase selective for *N*-palmitoylethanolamine, a putative endogenous anti-inflammatory substance. J Biol Chem 276(38): 35552-35557

Van der Stelt M, Nieuwenhuizen WF, Veldink GA, Vliegenthart JFG (1997) Dioxygenation of *N*-linoleoyl amides by soybean lipoxygenase-1. FEBS Lett 411: 287-290

Van der Stelt M, Noordermeer MA, Kiss T, Van Zadelhoff G, Merghart B, Veldink GA, Vliegenthart JFG (2000) Formation of a new class of oxylipins from *N*-acyl(ethanol)amines by the lipoxygenase pathway. Eur J Biochem 267: 2000-2007

Van der Stelt M, Veldhuis WB, Van Haaften GW, Fezza F, Bisogno T, Bar PR, Veldink GA, Vliegenthart JFG, Di Marzo V, Nicolay K (2001) Exogenous anandamide protects rat brain against acute neuronal injury in vivo. J Neurosci 21: 8765-8771

Van Zadelhoff G, Veldink GA, Vliegenthart JFG (1998) With anandamide as substrate Plant 5-lipoxygenases behave like 11-lipoxygenase. Biochem Biophy Res Comm 248: 33-38

Wiley JL, Dewey MA, Jefferson RG, Winckler RL, Bridgen DT, Willoughby KA, Martin BR (2000) Influence of phenylmethylsulfonyl fluoride on anandamide brain levels and pharmacological effects. Life Sci 67: 1573-1583

CHAPTER II

MOLECULAR IDENTIFICATION OF A FUNCTIONAL HOMOLOGUE OF THE MAMMALIAN FATTY ACID AMIDE HYDROLASE IN *Arabidopsis thaliana*

[This chapter was published: Shrestha et al., (2003) J Biol Chem 278: 34990-34997, used with the permission]

Abstract

N-Acylethanolamines (NAEs) are endogenous constituents of plant and animal tissues, and in vertebrates their hydrolysis terminates their participation as lipid mediators in the endocannabinoid signaling system. The membrane-bound enzyme responsible for NAE hydrolysis in mammals has been identified at the molecular level (designated fatty acid amide hydrolase, FAAH), and although an analogous enzyme activity was identified in microsomes of cotton seedlings, no molecular information is available for this enzyme in plants. Here we report the identification, the heterologous expression (in *E. coli*) and the biochemical characterization of an *Arabidopsis thaliana* FAAH homologue. Candidate *Arabidopsis* DNA sequences containing a characteristic amidase signature sequence (PS00571) were identified in plant genome databases and a cDNA was isolated by RT-PCR using *Arabidopsis* genome sequences to develop appropriate oligonucleotide primers. The cDNA was sequenced and predicted to encode a protein of 607 amino acids with 37% identity to rat FAAH within the

amidase signature domain (18% over the entire length). Residues determined to be important for FAAH catalysis were conserved between the *Arabidopsis* and rat protein sequences. In addition, a single transmembrane domain near the N-terminus was predicted in the *Arabidopsis* protein sequence, similar to that of the rat FAAH protein. The putative plant FAAH cDNA was expressed as an epitope/His-tagged fusion protein in *E. coli*, and solubilized from cell lysates in the nonionic detergent, dodecylmaltoside. Affinity-purified recombinant protein was indeed active in hydrolyzing a variety of naturally-occurring *N*-acylethanolamine types. Kinetic parameters and inhibition data for the recombinant *Arabidopsis* protein were consistent with these properties of the enzyme activity characterized previously in plant and animal systems. Collectively these data now provide support at the molecular level for a conserved mechanism between plants and animals for the metabolism of NAEs.

Abbreviations

AHase, amidohydrolase

AS, amidase signature

Bis-Tris, 2-[bis(2-hydroxyethyl)amino]-2-(hydroxymethyl)propane-1,3-diol

CHAPS (3-[(-cholamidopropyl)dimethylammonia]-1-propanesulfonate)

DDM, n-dodecyl-β-D-maltoside

EDTA, ethylenediamine tetraacetic acid

EGTA, ethylene glycol-bis(β-amino ethylether) tetraacetic acid

FAAH, fatty acid amide hydrolase

FFA, free fatty acid

IPTG, isopropyl β-D-thiogalactopyranoside

LOX, lipoxygenase

MAFP, methyl arachidonyl fluorophosphonate

NAE 12:0, *N*-lauroylethanolamine

NAE 14:0, *N*-myristoylethanolamine

NAE 16:0, *N*-palmitoylethanolamine

NAE 18:2, *N*-linoleoylethanolamine

NAE 20:4, *N*-arachidonoylethanolamine (anandamide)

NAE, *N*-acylethanolamine

NAPE, *N*-acylphosphatidylethanolamine

PLD, phospholipase D

PMSF, phenylmethylsulfonyl fluoride

PVDF, polyvinylidene fluoride

SDS, sodium dodecyl sulfate

WT, wild type

Introduction

N-Acylethanolamines (NAEs) are lipid mediators, which are produced from the PLD-mediated hydrolysis of *N*-acylphosphatidylethanolamines (NAPEs), a minor membrane lipid constituent of cellular membranes (Schmid et al., 1996). In animal systems, anandamide (NAE 20:4) acts as an endogenous ligand for cannabinoid receptors and has varied physiological roles, such as the modulation of neurotransmission in the central nervous system (Wilson and Nicoll, 2002). Anandamide also activates vanilloid receptors and functions as an endogenous analgesic (Pertwee, 2001) and appears to be involved in neuroprotection (Hansen et al., 2000; Van der Stelt et al., 2001). In other tissues, NAEs have been implicated in immunomodulation (Buckley et al., 2000), synchronization of embryo development (Paria and Dey, 2000), and induction of apoptosis (Sarker et al., 2000). These endogenous bioactive molecules lose their signaling activity upon hydrolysis by fatty acid amide hydrolase (FAAH; Cravatt and Lichtman, 2002).

In plants NAEs are present in substantial amounts in desiccated seeds (~1 $\mu g\, g^{-1}$ fresh wt) and their levels decline after a few hours of imbibition (Chapman et al., 1999). Individual NAEs were identified predominantly as 12C, 16C and 18C species with *N*-linoleoylethanolamine (NAE 18:2) generally being the most abundant. Like in animal cells, NAEs are derived from NAPEs (Schmid et al., 1990; Chapman, 2000) by the action of a PLD (Chapman et al., 1998; Pappan et

al., 1998). The occurrence of NAEs in seeds and their rapid depletion during seed imbibition to barely detectable levels in seedlings (Chapman, 2000), suggests that these lipids may have a role in the regulation of seed germination and normal seedling development. In fact, recent experiments with *Arabidopsis thaliana* seedlings showed that when seeds were germinated and maintained on elevated levels (micromolar concentrations) of the naturally-occurring NAE12:0, seedling roots developed abnormally in a manner consistent with a disruption of both normal cell division and cellular expansion (Blancaflor et al., 2003), signifying the importance of regulating NAE levels for normal plant growth and development.

The concept of NAEs acting as lipid mediators in plant systems is supported by an increasing amount of experimental evidence in vegetative tissues where normal levels of NAEs are quite low (low nanomolar concentrations). For example, NAE14:0 appears to function as an endogenous modulator of pathogen elicitor signaling by plant cells (Chapman, 2000; Tripathy et al., 2003). NAE14:0 levels, quantified by GC-MS, increased 10 to 50 fold in leaves of tobacco plants that were treated for a few minutes with either xylanase or cryptogein elicitor proteins (Tripathy et al., 1999). These “elicitor-activated” levels of NAE14:0 (submicromolar concentrations) were sufficient to induce defense gene expression (*e.g.*, phenylalanine-ammonia lyase, PAL2 transcript abundance) in tobacco plants within hours of treatment in a manner similar to but independent of elicitor proteins (Tripathy et al., 1999). Mammalian cannabinoid receptor antagonists at concentrations equimolar to NAE blocked the activation

of defense gene expression induced by either NAEs or by fungal elicitor proteins (Tripathy et al., 2003). A membrane-associated protein was identified in leaves of tobacco (and other plant species) which specifically bound to ^{3}H-NAE14:0 with high affinity (K_d in the low nanomolar range). This NAE14:0 binding protein was proposed to mediate the NAE activation of PAL2 expression in tobacco leaves, a conclusion that was based on the similarities between NAE binding properties *in vitro* and NAE-induced physiological responses *in vivo*, including experiments with cannabinoid receptor antagonists (Tripathy et al., 2003). Although some clear differences are evident between the emerging NAE signaling pathway in plants and the better characterized endocannabinoid signal pathway of animals, there appear to be some remarkable similarities in the formation and perception of bioactive acylethanolamides by these two diverse groups of multicellular organisms. Likewise, we propose that a FAAH-like mechanism operates in plants for NAE signal termination and overall regulation of NAE levels under various physiological conditions.

Recently, depletion of NAEs during seed imbibiton/germination was determined to occur via two metabolic pathways – one LOX-mediated, for the formation of NAE oxylipins from NAE 18:2, and one amidase-mediated for hydrolysis of saturated and unsaturated NAEs (Shrestha et al., 2002). Hydrolysis of NAEs was reconstituted and characterized in microsomes of cottonseeds, and appeared to be catalyzed by an enzyme similar to the FAAH of mammalian species (Shrestha et al., 2002). Here we report the identification of a plant ortholog of mammalian FAAH by bioinformatic approaches, isolation of its cDNA

sequence, expression of this cDNA in *E. coli*, and identification of the protein product as an NAE amidohydrolase. These results support our previous studies on the metabolism of NAEs in plant tissues, and for the first time provide molecular evidence for a conserved pathway in both plants and animals for the hydrolysis of NAEs. Moreover, the results of this research now provide a means to manipulate the levels of endogenous NAEs in plants to evaluate the physiological role(s) of these bioactive lipids.

Results

Tentative Identification of Arabidopsis *NAE Amidohydrolase*

In animal tissues, fatty acid amide hydrolase (E.C. 3.5.1.4), a member of the amidase signature (AS) family (Cravatt et al., 1996; Ueda, 2002), hydrolyzes NAEs to produce FFA and ethanolamine (Ueda et al., 2000). A similar enzymatic activity was characterized previously in cottonseed microsomes (Shrestha et al., 2002). Mammalian FAAH enzymes have a conserved stretch of approximately 130 amino acids (Patricelli and Cravatt, 2000) containing a Ser/Ser/Lys catalytic triad (McKinney and Cravatt, 2003). The predicted amidase structure has a central conserved motif of G-G-S-S-(G/A/S)-G (Chebrou et al., 1996) and a somewhat longer stretch of amino acids G-[GA]-S-[GS]-[GS]-G-x-[GSA]-[GSAVY]-x-[LIVM]-[GSA]-x(6)-[GSAT]-x-[GA]-x-[DE]-x-[GA]-x-S-[LIVM]-R-x-P-GSAC] is present in all enzymes of the amidase class (PS00457). Two serine residues at 217 and 241, highly conserved in the AS sequence were found essential for enzymatic activity of recombinant rat FAAH (Omeir et al., 1999). Mutation of either one of the residues into alanine caused complete loss of activity of the enzyme (Omeir et al., 1999; Patricelli et al., 1999). Also, mutation of serine 218 into alanine caused marked loss of activity (Patricelli et al., 1999). Taking these conserved residues in the AS consensus sequence into consideration, several putative plant orthologs were identified computationally. BLAST searches (Gish W, 1996-2003, http://blast.wustl.edu) in various

databases using the AS consensus block embedded in rat FAAH (http://blocks.fhcrc.org) identified one *Arabidopsis thaliana* gene (At5g64440) that was selected for further characterization (Fig. 1).

The structure and organization of the At5g64440 gene is relatively complex with 21 exons including 5' utr (untranslated region) and 3' utr (Fig. 1A). The predicted gene is 4689 nucleotides in length and encodes a predicted protein of 607 amino acids with a molecular weight of 66.1 kDa. Based on the presence of the conserved residues characteristic of the canonical AS sequence, this gene seemed likely to encode an *Arabidopsis* NAE amidohydrolase. To assess if this gene was expressed and to isolate a full length cDNA for functional studies, oligonucleotide primers were designed within the 5' and 3' utr, and a cDNA fragment was amplified by RT-PCR from *Arabidopsis* leaf RNA (Fig. 1B). The RT-PCR product was sequenced and found to be 99.9% identical with the corresponding TC139316 annotated at TIGR. The protein domain prediction tools, ProDom (Servant et al., 2002), identified six domain families in the *Arabidopsis* protein, five of which were also found in rat FAAH (Fig. 1C). A single putative transmembrane segment was identified near the N-terminus (TMHMM, Krogh et al., 2001; Sonnhammer et al., 1998) similar to the predicted topological organization in rat FAAH.

Alignment of the deduced amino acid sequences from the *Arabidopsis* NAE amidohydrolase cDNA and the rat FAAH (Cravatt et al., 1996) showed only 18.5% identity over the entire length. Alignment within the AS sequence of 125 amino acids showed 37% identity with five residues determined to be important

for catalysis (Lys-142, Ser-217, Ser-218, Ser-241 and Arg-243; Patricelli and Cravatt, 2000) absolutely conserved (denoted by arrows; Fig. 2A). Comparison of a 47 amino acid motif within the AS showed the *Arabidopsis* protein had close to 60% identity with FAAHs from several mammalian species (Fig. 2B). Organization of predicted secondary structure within this *Arabidopsis* and rat FAAH AS motif were similar (Fig. 2C) and the structure of the rat enzyme has been confirmed by X-ray crystallography (Bracey et al, 2002). In addition, this putative *Arabidopsis thaliana* NAE amidohydrolase and rat FAAH have similar predicted molecular weights (~66 kDa), similar predicted topologies (single transmembrane segment near the N-terminus with C-terminus facing the cytosol, via TMHMM transmembrane and topology predictor, Krogh et al., 2001; Sonnhammer et al., 1998) and similar predicted subcellular locations (secretory pathway, pSORT, Nakai and Kanehisa, 1992).

Functional Identification of Arabidopsis *NAE Amidohydrolase*

The *Arabidopsis* putative NAE amidohydrolase was subcloned into pTrcHis and pTrcHis2 for expression in *E. coli* of N-terminal and C-terminal epitope- and polyhistidine-tagged fusion proteins, respectively. *E. coli* lysates were surveyed for expression of enzyme activity using [^{14}C]NAE 18:2 (radiolabeled on the carbonyl carbon) as substrate. Representative chromatograms shown in Figure 3 indicate that, like the recombinant rat FAAH (expressed in the same vector), the recombinant *Arabidopsis* protein effectively hydrolyzed [1-^{14}C]NAE 18:2 to [1-^{14}C]FFA 18:2. As a control, *E. coli* expressing

the *Arabidopsis* cDNA in reverse orientation showed no hydrolytic activity (Fig. 3). In these preliminary experiments with crude *E. coli* lysates, the *Arabidopsis* NAE amidohydrolase activity was determined to be time-, temperature-, pH-, and protein concentration-dependent. The *Arabidopsis* NAE amidohydrolase showed hydrolytic activity on 2-arachidonoylglycerol (2AG) when non-labeled 2-AG was employed as the substrate for qualitative purpose and a robust enzymatic reaction was observed (Fig. 4) The *Arabidopsis* NAE amidohydrolase did not hydrolyze ceramide, nor did ceramide influence NAE hydrolysis (not shown). The *Arabidopsis* NAE amidohydrolase did not catalyze the reverse reaction of NAE hydrolysis (formation of NAE) under any conditions tested (not shown). Higher activity was reproducibly recovered in cells expressing C-terminal fusions, compared with cells expressing N-terminal fusions. Similar to reports for the rat protein (Patricelli et al., 1998), the recombinant *Arabidopsis* NAE amidohydrolase was mostly associated with *E. coli* membranes.

Affinity-Purification of Recombinant Enzyme

The *Arabidopsis* NAE amidohydrolase, expressed as a C-terminal fusion protein, was solubilized in DDM, and subjected to native Ni^{2+}-affinity purification, SDS-PAGE, western blot analyses, and enzyme activity assays (Fig. 5). A protein of approximately 70 kDa was enriched under native conditions by Ni^{2+}-affinity purification and was detected by the c-myc antibody (Fig. 5A, B arrows, recombinant protein lanes). Likewise, NAE amidohydrolase activity was enriched in this native affinity-purified protein fraction (Fig. 5C) by approximately 375 fold,

relative to the DDM-solubilized supernatant (supt) fraction. More stringent denaturing conditions led to purification of the recombinant protein to homogeneity (single 70 kDa band on gel), but also inactivated the enzyme irreversibly (not shown).

Biochemical Characterization

Recombinant NAE amidohydrolase activity was evaluated by incubating affinity-purified NAE amidohydrolase with [1-^{14}C]NAE 20:4, [1-^{14}C]NAE 18:2, [1-^{14}C]NAE 16:0, [1-^{14}C]NAE 14:0 or [1-^{14}C]NAE 12:0 and measuring the rate of conversion to their respective [1-^{14}C]FFA products. NAE amidohydrolase exhibited saturation kinetics with respect to all NAE substrates tested including those identified in plant tissues and those not found in plant tissues. The enzyme exhibited typical Michaelis-Menten kinetics when initial velocity measurements were made at increasing substrate concentrations (Fig. 6) and parameters calculated from these plots are summarized in Table I. The relative apparent K_m of the *Arabidopsis* enzyme varied by a factor of about four depending upon NAE type. Surprisingly, the *Arabidopsis* enzyme had a higher affinity toward the non-plant NAE 20:4, than toward the more abundant endogenous plant NAE 16:0 and NAE18:2. The highest maximum rate of NAE hydrolysis also was estimated for NAE 20:4 compared to the endogenous plant NAEs, although the range of the difference was not as great. The specificity constant (k_{cat}/K_m) was calculated for the *Arabidopsis* enzyme toward all NAE substrates and supported the conclusion that NAE 20:4 appeared to be the best substrate for the plant enzyme *in vitro*.

Similar published data for the rat FAAH indicated this enzyme showed a 10-fold preference for NAE 20:4 over NAE 16:0 (Katayama et al., 1999). With respect to NAE 20:4, the best substrate for both the plant and animal FAAH, the catalytic efficiency for the *Arabidopsis* NAE amidohydrolase reported here ($2.4 \times 10^4\ M^{-1}\ s^{-1}$), is about 10 times less than that reported for the rat FAAH ($2.2 \times 10^5\ M^{-1}\ s^{-1}$). This may be due to different assay conditions, different detergents, or a difference in relative enzyme purity. In any case the same trend was noted for both enzymes in terms of the lower k_{cat}/K_m for NAE 16:0 than for NAE 20:4, despite the much higher levels of endogenous NAE 16:0 content in both systems. These parameters together suggest that the *Arabidopsis* recombinant enzyme recognizes a wide range of NAE types, similar to the situation with mammalian FAAH, and highlights the caution of over interpreting *in vitro* kinetics data since the best substrate in these studies, NAE20:4, has not been detected in plants (Chapman, 2000).

Two different mechanism-based inhibitors of mammalian FAAH were tested for potency on the hydrolysis of [1-^{14}C]NAE 18:2 by this novel plant NAE amidohydrolase (Table II). Phenylmethylsulfonyl fluoride (PMSF), a non-specific irreversible serine hydrolase inhibitor that inhibits NAE hydrolysis by mammalian FAAH at low mM concentrations (Desarnaud et al., 1995) was only modestly effective on the *Arabidopsis* enzyme (inhibited by 44% at 10 mM). However, methyl arachidonyl fluorophosphonate (MAFP), the irreversible, active-site targeted inhibitor of rat FAAH (Bracey et al., 2002) completely eliminated NAE hydrolysis by the *Arabidopsis* enzyme at 10 nM. Overall, our biochemical results

strongly support the identification of At5g64440 as a functional homologue of the mammalian FAAH.

Discussion

The results presented here predict and functionally confirm that the *Arabidopsis* gene AT5g64440 (Fig. 1) encodes a homologue of the mammalian FAAH. Although there was limited primary amino acid sequence identity over the length of the *Arabidopsis* protein compared with the rat protein (18%), there was substantially higher similarity within the amidase catalytic domain both at the primary (37-60% depending on the lengths compared) and secondary structural levels (Fig. 2). Expression of the *Arabidopsis* cDNA in *E. coli* indicated that the *Arabidopsis* protein product was capable of hydrolyzing a wide range of NAE substrates to free fatty acids (Figs. 3-5, Table I), a feature also of the mammalian enzyme (Ueda et al., 2000; Borger et al., 2000). Kinetic parameters summarized in Table I indicated that the plant enzyme has similar affinities for NAE substrates as the FAAH from several mammalian species (Bisogno et al., 1997; Boger et al., 2000; Cravatt et al., 1996; Fowler et al., 2001; Pertwee et al., 1995; Tiger et al., 2000). Anandamide and 2-arachidonoylglycerol were thought to act as endogenous ligands of cannabinoid receptor (Di Marzo et al., 1998; Schmid et al., 1996) and lose their biological activities by enzymatic hydrolysis (Goparaju et al., 1998). Hydrolysis of 2-AG proceeded about 4 fold faster than anandamide hydrolysis with K_m value as low as 6 μM (Goparaju et al., 1998). Here, non-labeled 2-AG was employed as the substrate for qualitative purpose and a robust enzymatic reaction was observed (Fig. 4). Moreover, the inhibition of the

Arabidopsis NAE amidohydrolase by MAFP (Table II), the active-site directed irreversible inhibitor of rat FAAH (Bracey et al., 2002; Deutsch et al., 1997), strongly suggests a conserved enzyme mechanism between the plant and animal NAE amidases supporting the predictions from sequence/domain comparisons. We suggested the annotation of "glutamyl-tRNA amidotransferase similarity" now accompanying this *At5g64440* gene be modified to include the new functional information herein regarding NAE hydrolysis. Most amidases, including the mammalian FAAHs, carry the glutamyl-tRNA amidotransferase similarity annotation due to the presence of sequence similarity within the amidase signature domain, often as the only identifiable domain within this family of proteins. Based on our functional studies, it is unlikely that this At5g64440 gene product functions as a glutamyl-tRNA amidotransferase, and this activity has not been attributed to membrane-bound mammalian FAAH enzyme. Additionally, in plants these glutamyl-tRNA amidotransferases are localized in the stroma of chloroplast as soluble, oligomeric complexes of multiple subunits (Becker et al., 2000; Schon et al., 1988). In fact, nuclear-encoded, chloroplast-localized orthologues of the glutamyl-tRNA amidotransferase subunits have been cloned from *Arabidopsis* and expressed/characterized by the Soll group (GenBank™ accession numbers, AF241841, AF240465, AF239836, and AF224745), and these proteins share less than 24% amino acid sequence identity with the At5g64440 NAE amidohydrolase. Thus there is a need to clarify the descriptive annotation within these amidase protein subfamilies.

The signal-mediated activation of NAE metabolism constitutes a major regulatory feature of the endocannabinoid signaling system in animal systems through the rapid generation and timely degradation of bioactive acylethanolamides (Hillard, 2000; Cravatt et al., 1996; Bisogno et al., 2002; Hansen et al. 2000; Cravatt and Lichtman, 2002). While a principal role for NAE 20:4 as an endogenous ligand for cannabinoid receptors has emerged as a paradigm for endocannabinoid signaling (Desarnaud et al., 1995; Wilson and Nicoll, 2002), other types of NAEs as well as other fatty acid derivatives likely interact with this pathway directly or indirectly to modulate a variety of physiological functions in vertebrates (Lambert and Di Marzo, 1999; Lambert et al., 2002; Schmid and Berdyshev, 2002; Schmid et al., 2002). An increasingly detailed understanding of the degradation of these bioactive NAEs by fatty acid amide hydrolase (FAAH) has pointed to this metabolic step as a key regulator of NAE levels, and hence NAE function, *in vivo* (Cravatt and Lichtman, 2002; Ueda, 2002; Ueda et al., 2000). Recent, major advances in the understanding of FAAH function in mammals at the structural level (Bracey et al., 2002), mechanistic level (McKinney and Cravatt, 2003), and the physiological level (Cravatt and Lichtman, 2002), have been made possible only through the cloning, expression and manipulation of the cDNA/gene encoding FAAH (Giang and Cravatt, 1997). We anticipate the identification of this plant cDNA will facilitate a similar increased appreciation for this lipid pathway in plant physiology.

Research in the last decade has made it apparent that NAE metabolism occurs in plants by pathways analogous to those in vertebrates and invertebrates

(Chapman, 2000, Shrestha et al., 2002), pointing to the possibility that these lipids may be part of an evolutionarily conserved mechanism for the regulation of physiology in multicellular organisms. Two physiological situations in plant systems have been identified in which the endogenous levels of NAEs are transiently modulated. The first is in the perception of fungal elicitors by plant cells, wherein the levels of endogenous NAE 14:0 were elevated 10-50 fold in leaves of tobacco plants following elicitation (Tripathy et al., 1999). In other work, NAEs (mostly C12, C16 and C18 types) were quantified in desiccated seeds of higher plants, but were metabolized rapidly during the first few hours of seed imbibition/germination (Chapman et al., 1999), in part by an amidohydrolase-mediated pathway (Shrestha et al., 2002), suggesting that the transient changes in NAE content may play a role in seed germination. In fact, *Arabidopsis* seedlings germinated and grown in the presence of exogenous NAE exhibited dramatically altered developmental organization of root tissues (Blancaflor et al., 2003). With evidence of conserved enzymatic machinery in plants for the formation and degradation of NAEs, and the potent biological effects caused by altered exogenous NAE levels, it is now important to begin to address NAE function in plants by forward and reverse genetics approaches. The identification of an *Arabidopsis* cDNA clone encoding a functional NAE amidohydrolase re-enforces the similarity between plants and animals in terms of NAE metabolism, but more importantly, provides a tool for the future manipulation of NAE levels in plants as a means to understand the physiological role(s) of these bioactive lipids in the plant kingdom.

Materials and Methods

Materials

[1-^{14}C]Arachidonic acid was purchased from PerkinElmer Life Sciences and [1-^{14}C]lauric acid was from Amersham Biosciences. [1-^{14}C]Myristic acid, arachidonic acid, lauric acid, linoleic acid, myritstic acid, anandamide, ethanolamine, phenylmethylsulfonyl fluoride (PMSF), and isopropyl β-D-thiogalactopyranoside (IPTG) were from Sigma Chemical Co (St Louis). [1-^{14}C]Linoleic, [1-^{14}C]palmitic acids, and [1,2-^{14}C]ethanolamine were purchased from NEN (Boston, MA). Ceramide was from Avanti Polar Lipids (Alabaster, AL), and 2-arachidonoylglycerol (2-AG) was from Cayman Chemical (Ann Arbor, MI). Methyl arachidonyl fluorophosphonate (MAFP) was from TOCRIS (Ellisville, MO), n-dodecyl-β-D-maltoside (DDM) was from Calbiochem (La Jolla, CA), and silica gel G (60 Å)-coated glass plates for thin-layer chromatography (20 cm x 20 cm, 0.25 mm thickness) were from Whatman (Clifton, NJ). Specific types of *N*-[1-^{14}C] acylethanolamines (and non-radiolabeled NAEs) were synthesized from ethanolamine and the respective [1-^{14}C]fatty acids (and non-radiolabeled FFAs) by first producing the fatty acid chloride (Hillard et al., 1995) and purified by TLC as described elsewhere (Shrestha et al., 2002).

Bioinformatics and cDNA Isolation

BLAST searches (http://blast.wustl.edu) in various databases were done using the amidase signature (AS) consensus block embedded in rat FAAH (http://blocks.fhcrc.org). DNA sequences containing a characteristic AS sequence (PS00571) were identified in the *Arabidopsis thaliana* genome database annotated by the Institute for Genomic Research (TIGR) and available at www.tigr.org, and one candidate *Arabidopsis* FAAH ortholog, At5g64440, was selected for further analyses. This selection was based largely on results from sequence analysis tools and database comparisons including BLAST and cDART (www.ncbi.nlm.nih.gov), ProDom (Servant et al., 2002), Prosite (Sigrist et al., 2002), TMHMM transmembrane and topology predictor (Krogh et al., 2001; Sonnhammer et al., 1998) and pSORT (Nakai and Kanehisa, 1992). Sequence alignments and some sequence analyses were made with DNASIS software (Hitachi).

Sequence-specific primers were designed within the 5' and 3' utr regions of At5g64440 based on predicted exon sequences and were used for reverse transcriptase (RT)-PCR (forward, 5'- CATTCAAGTTCCCAACAACTTCACCGC – 3' and reverse, 5'- GTCGACGTAAGAAATTCCAACACGG – 3'). The template for RT-PCR was total RNA extracted from the leaves of mature *Arabidopsis* plants using Trizol reagent (Invitrogen). Fresh leaf tissue (100 mg) was harvested, ground to a fine powder in liquid nitrogen, and combined with 2 mL of Trizol reagent for RNA isolation according to the manufacturer's instructions. For RT-PCR, the first-strand cDNA synthesis from total RNA was carried out at 50 °C for

30 min and incubated for 4 min at 94 °C before the targeted amplification of the At5g64440 mRNA by Platinum Taq (RT-PCR mixture; Invitrogen) was achieved through 25 cycles of 94 °C for 1 min, 45 °C for 1 min, 72 °C for 2 min followed by a final polymerization step at 72 °C for 7 min. The RT-PCR product was gel-purified and ligated into pTrcHis for nucleotide sequencing. Commercial DNA sequencing of both strands (complete 2X each strand) verified the identity of the cDNA as the AT5g64440 gene product, and the complete cDNA sequence was deposited in GenBank.

Protein Expression

For protein expression, oligonucleotide primers (forward, 5'-ATGGGTAAGTATCAGGTCATGAAACG – 3' and reverse, 5'-GTTTGTATTGAGAATATCATAAAAGATTGC – 3') were designed to amplify only the open reading frame (ORF) of the above At5g64440 cDNA, and PCR conditions were as above, except that a 10-to-1 ratio of polymerases (Taq-to-Pfu; Invitrogen) was used for amplification and the template was the RT-PCR product (GenBank # AY308736) in pTrcHis. The open reading frame-PCR product was gel purified as above and subcloned into expression vectors, pTrcHis and pTrcHis2, and the constructs were introduced into chemically-competent *E. coli*TOP10 cells as host. Transformed colonies were selected with correct inframe fusions and cDNA sequence by sequencing of plasmid DNA over the vector insert junctions and by sequencing the inserts completely on both strands.

Selected transformed cell lines were grown in LB medium without glucose to an OD_{600} of 0.6 to 0.7 and induced with 1 mM IPTG for 4 h. Pelleted cells

were resuspended in lysis buffer (50 mM Tri-HCl, pH 8.0, 100 mM NaCl and 0.2 mM DDM) at a ratio of 1-to-10^8 (*E. coli* cells-to-DDM molecules; 0.1 OD_{600} = 10^8 cells/mL, Elbing and Brent, 2002). After incubation on ice for 30 min resuspended cells were sonicated on ice with six 10 s bursts at high intensity with a 10 s cooling (ice bath) period between each burst. The selection of DDM as the detergent, and determination of optimal DDM concentration and content ratio was based on empirical comparisons for recovery of solubilized active enzyme with the highest specific activity. By the same criteria, DDM was determined to be better for solubilizing active enzyme than either Titron X-100 or CHAPS (3-[(-cholamidopropyl)dimethylammonia]-1-propanesulfonate).

Solubilization and Ni^{2+} Affinity Purification

Routinely, cultured cells (50 mL) were pelleted, resuspended in 8 mL of native binding buffer (50 mM $NaP0_4$ buffer, pH 8.0, and 0.5 M NaCl) with 8 mg of lysozyme (Sigma) and 0.2 mM DDM (final), incubated on ice for 30 min, and disrupted by sonication as above. The crude lysate was centrifuged at 105,000 x*g* for 1 h in a Sorvall Discovery 90 model ultracentrifuge (Beckman Ti45 rotor). The supernatant was combined with ProBond resin, precharged with Ni^{2+} and gently agitated for 60 min to keep the resin suspended in the lysate supernatant. The resin with adsorbed protein was settled and the supernatant was aspirated off. The resin was washed 4 times to remove non-specific proteins, and the adsorbed proteins were eluted with imidazole-containing buffer. Eluted proteins were concentrated and imidazole was removed with 50 mM Tris-HCl, pH 8.0, 100 mM NaCl and 0.2 mM DDM by filtration-centrifugation using Centricon YM-30

(Millipore, Bedford, MA) devices. Affinity-purified proteins were stored at –80 °C in 10% glycerol and were stable for more than two months.

Gel Electrophoresis and Western Blotting

Protein samples were diluted in 60 mM Tris-HCl, pH 6.8, 2% SDS, 10% glycerol, 0.025% bromophenol blue in 1:1 ratio and separated on 8 cm, precast 10% polyacrylamide/SDS gels (Bio-Rad) at 35 mA for 30 min and 60 mA for 60 min. For western blot analysis, separated proteins were electrophoretically transferred to PVDF (polyvinylidene fluoride, 0.2 μm, Bio-Rad) membrane in a Semidry Trans-Blot apparatus (Bio-Rad) for 30 min at constant 14 volts. Recombinant proteins expressed as c-myc-epitope fusions were localized with 1-to-5000 dilution of anti-c-myc antibodies (mouse monoclonal, Invitrogen) and detected by chemiluminescence (Bio-Rad substrate solutions) following incubation with 1-to-2500 goat antimouse IgG conjugated to horseradish peroxidase (Bio-Rad).

NAE Amidohydrolase Assays

NAE substrates were synthesized and purified, and enzyme assays were conducted as previously described (Shrestha et al., 2002) with a few modifications. Generally the enzyme source was incubated with 100 μM [^{14}C]NAE (20,000 dpm) in 50 mM Bis-Tris buffer (pH 9.0) for 30 min to survey for NAE amidohydrolase activity (Shrestha et al., 2002). Enzyme activity was examined for time, temperature, protein- and substrate-concentration

dependence. For enzyme characterization, reactions were initiated with 1 μg of affinity-purified protein and incubated at 30 °C with shaking for 30 min. Assays of lysates of *E. coli* cells expressing rat FAAH (WT-FAAH; Patricelli et al., 1998) served as a comparison of NAE amidohydrolase activity, whereas non-transformed cell lysates or cell lysates with the *Arabidopsis* cDNA cloned in reverse orientation with respect to the lacZ promoter served as negative controls for activity assays. Enzyme assays were terminated by the addition of boiling isopropanol (70 °C) and lipids were extracted into chloroform. Lipid products were separated by TLC and the distribution of radioactivity was evaluated by radiometric scanning (Shrestha et al., 2002). Activity was calculated based on the radiospecific activity of [^{14}C]-labeled substrate. A general serine hydrolase inhibitor, phenylmethylsulfonyl fluoride (PMSF), and an irreversible active-site-directed FAAH inhibitor, methyl arachidonyl fluorophosphonate (MAFP), were used to probe the sensitivity of recombinant *Arabidopsis* NAE amidohydrolase activity. Inhibitors were added from stock solutions dissolved in isopropanol for PMSF or DMSO for MAFP, and activity was adjusted for minimal solvent effects where necessary based on assays in the presence of the appropriate amount of solvent alone. Protein content was determined by Coomassie blue-dye binding using bovine serum albumin as the protein standard (Bradford, 1976).

Table I. *Summary of apparent kinetic parameters of the affinity-purified recombinant* Arabidopsis thaliana *NAE amidohydrolase*.

Parameters were estimated by fitting the data in Fig. 6 to the Michaelis-Menten equation (Prism software, version 3.0, GraphPad).

Substrate	K_m (M)	V_{max} (μmol h^{-1} mg^{-1} protein)	k_{cat} (s^{-1})	k_{cat}/K_m (M^{-1} s^{-1})
NAE 20:4	13.6 X 10^{-6}	17.9	0.33	2.4 X 10^4
NAE 18:2	26.2 X 10^{-6}	14.1	0.26	9.9 X 10^3
NAE 16:0	50.8 X 10^{-6}	12.1	0.22	4.3 X 10^3
NAE 14:0	37.0 X 10^{-6}	9.1	0.17	4.6 X 10^3
NAE 12:0	17.6 X 10^{-6}	13.9	0.26	1.5 X 10^4

Table II. *The effects of two mechanism-based inhibitors of mammalian FAAH on the hydrolysis of [1-^{14}C]NAE 18:2 by the affinity-purified recombinant* Arabidopsis *enzyme*.

Assays were conducted for 30 min at 30 °C in the absence or presence of increasing concentrations of phenylmethylsulfonyl fluoride (PMSF) or methyl arachidonyl fluorophosphonate (MAFP). The amount of [1-^{14}C]FFA 18:2 formed was quantified by radiometric scanning following TLC separation of reactions products. The data are means and SD of three replicates and are representative of two experiments.

Concentrations	Specific Activity ($\mu mol\ h^{-1}\ mg^{-1}$ protein)	Relative Inhibition (%)
Phenylmethylsulfonyl fluoride (PMSF)		
0 mM	10.56±0.29	0
0.01 mM	11.34±0.55	-7
0.1 mM	9.06±1.86	14
1 mM	7.89±0.37	25
2.5 mM	6.72±0.70	36
10 mM	5.96±0.43	44
Methyl arachidonyl fluorophosphonate (MAFP)		
0 nM	10.46±0.32	0
0.1 nM	9.69±0.89	7
1 nM	5.62±0.56	46
10 nM	0.00±0.00	100

A

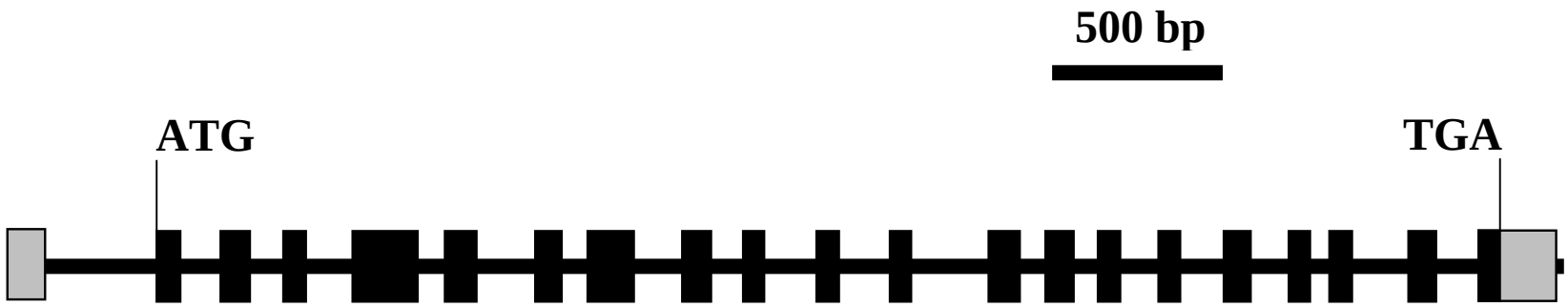

B

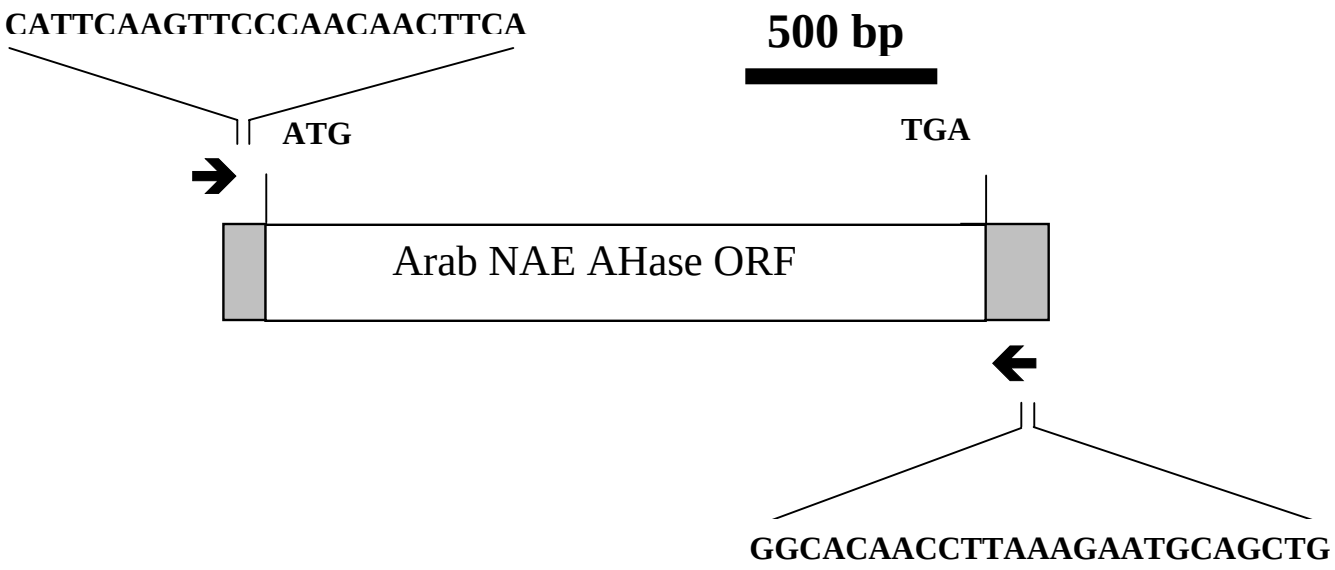
CATTCAAGTTCCCAACAACTTCA
500 bp
ATG
TGA
Arab NAE AHase ORF
GGCACAACCTTAAAGAATGCAGCTG

C

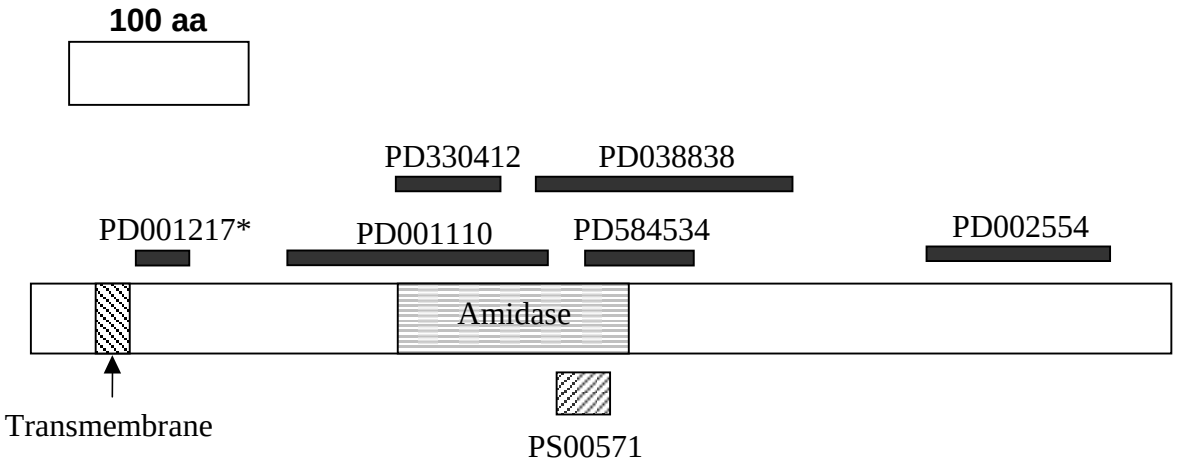
100 aa
PD330412
PD038838
PD001217*
PD001110
PD584534
PD002554
Amidase
Transmembrane
PS00571

Figure 1. A, The structure and organization of the *Arabidopsis* NAE amidohydrolase genomic sequence (TIGR/TAIR ID At5g64440). This gene is 4689 bp in length and the predicted protein is 607 amino acids in length with a molecular weight of 66.1 kDa and pI of 6.44. There are 21 exons including 5' utr (untranslated region) and 3' utr (www.tigr.org). The boxes represent exons and bars between exons represents introns. The light shaded boxes are utrs.

B, Schematic Structure of the cDNA corresponding to At5g64440. Sequence-specific reverse transcriptase (RT) PCR primers were designed based on the genomic sequence *Arabidopsis thaliana* annotated at the Institute for Genomic Research (TIGR). The arrows denote the position of primers in the 5' and 3' utr. RT-PCR was performed with total RNA extracted from the *Arabidopsis* leaves and the nucleotide sequence of the isolated cDNA was deposited in GenBank (AY308736) and was 99.9% identical to coding region of TC139316 (arabidopsis.org).

C, Schematic of domain organization of predicted *Arabidopsis* NAE amidohydrolase protein. Various domains identified in other proteins with ProDom are depicted above the diagram of the polypeptide. These domains are also found in rat FAAH except the one denoted by an asterisk. Domains are organized to scale and domain family identifiers (ProDom) are provided. PD038838, from amino acid 271-407, is found in 167 other proteins including a glutamyl-tRNA amidotransferase subunit A from *Methanococcus jannaschii* (swiss-prot Q58560). PD001110, from amino acid 138-276, is found in 121 other

proteins including a predicted glutamyl-tRNA amidotransferase subunit A from *Aeropyrum pernix* (swiss-prot Q9YB80). PD002554, from amino acid 477-575, is found in 173 other proteins including an unknown, predicted amidase from *Homo sapiens* (swiss-prot Q9NV19). PD330412, from amino acid 197-253, is found in 64 other proteins including a predicted glutamyl-tRNA amidotransferase subunit A from *Mesorhizobium loti* (swiss-prot Q987F8). PD584534, from amino acid 298-358, is found in 36 other proteins including a FAAH from *Rattus norvegicus* (swiss-prot P97612). PD001217, from amino acid 60-88, is found in 234 other proteins including a predicted dipeptide binding/transporter protein from *Yersinia pestis* (swiss-prot Q8ZA19). PS00571 (PROSITE dictionary) denotes the amidase consensus sequence motif of G-[GA]-S-[GS]-[GS]-G-x-[GSA]-[GSAVY]-x-[LIVM]-[GSA]-x(6)-[GSAT]-x-[GA]-x-[DE]-x-[GA]-x-S-[LIVM]-R-x-P-[GSAC] present in all proteins of the amidase class (Chang and Abelson, 1990; Cravatt et al., 1996; Curnow et al., 1997; Hashimoto et al., 1991; Mayaux et al., 1990; Tsuchiya et al., 1989). A single predicted transmembrane spanning region shaded near the N-terminus (TMHMM, refs. Krogh et al., 2001; Sonnhammer et al., 1998), and the amidase signature sequence (ref. Patricelli and Cravatt, 2000; see Fig 2A) used to conduct the original search for homologues, are also diagrammed.

A

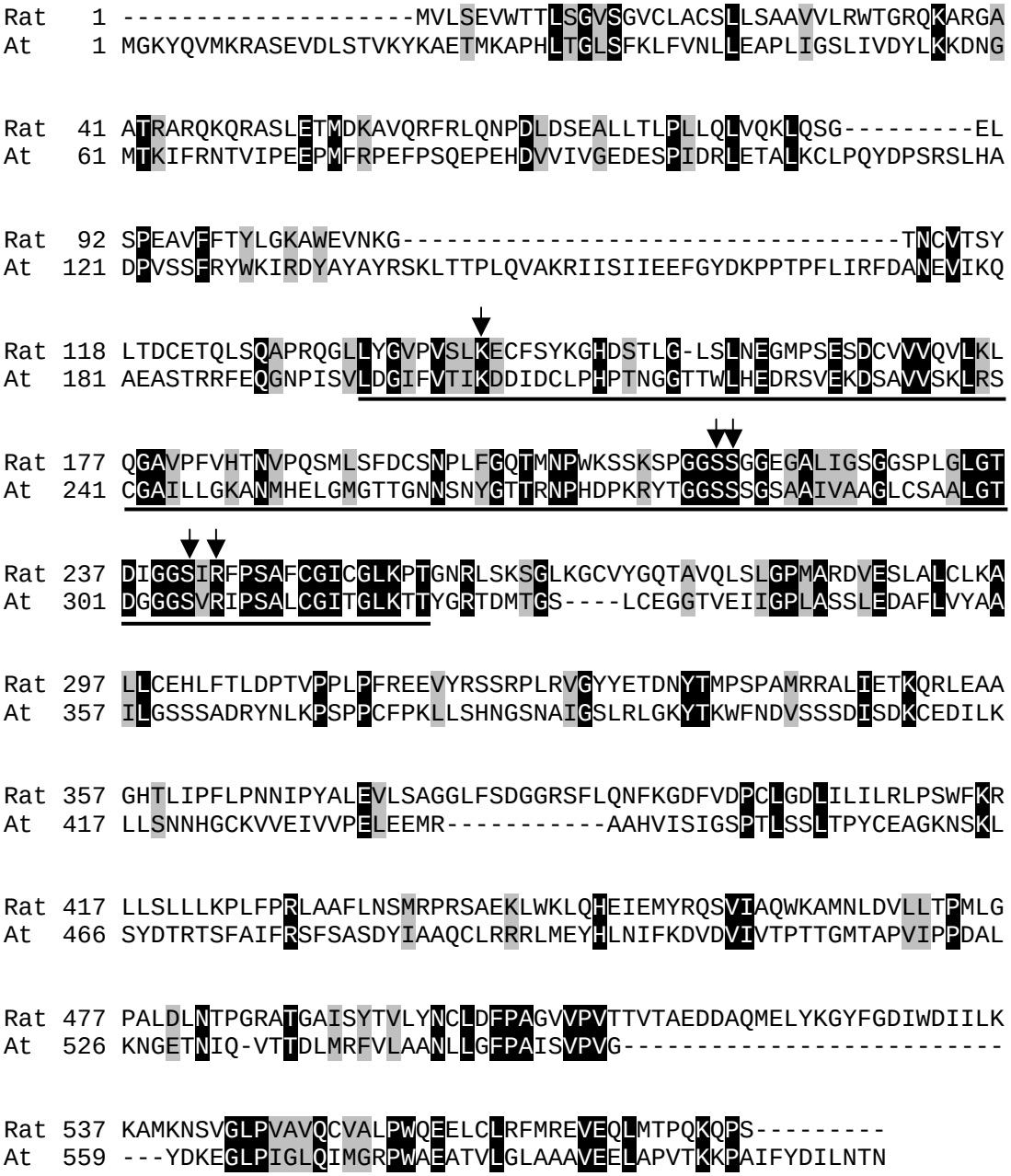
Rat 1 ----------MVLSEVWTTLSGVSGVCLACSLLSAAVVLRWTGRQKARGA
At 1 MGKYQVMKRASEVDLSTVKYKAETMKAPHLTGLSFKLFVNLLEAPLIGSLIVDYLKKDNG
Rat 41 ATRARQKQRASLETMDKAVQRFRLQNPDLDSEALLTLPLLQLVQKLQSG---------EL
At 61 MTKIFRNTVIPEEPMFRPEFPSQEPEHDVVIVGEDESPIDRLETALKCLPQYDPSRSLHA
Rat 92 SPEAVFFTYLGKAWEVNKG----------TNCVTSY
At 121 DPVSSFRYWKIRDYAYAYRSKLTTPLQVAKRIISIIEEFGYDKPPTPFLIRFDANEVIKQ
Rat 118 LTDCETQLSQAPRQGLLYGVPVSLKECFSYKGHDSTLG-LSLNEGMPSESDCVVVQVLKL
At 181 AEASTRRFEQGNPISVLDGIFVTIKDDIDCLPHPTNGGTTWLHEDRSVEKDSAVVSKLRS
Rat 177 QGAVPFVHTNVPQSMLSFDCSNPLFGQTMNPWKSSKSPGGSSGGEGALIGSGGSPLGLGT
At 241 CGAILLGKANMHELGMGTTGNNSNYGTTRNPHDPKRYTGGSSSGSAAIVAAGLCSAALGT
Rat 237 DIGGSIRFPSAFCGICGLKPTGNRLSKSGLKGCVYGQTAVQLSLGPMARDVESLALCLKA
At 301 DGGGSVRIPSALCGITGLKTTYGRTDMTGS----LCEGGTVEIIGPLASSLEDAFLVYAA
Rat 297 LLCEHLFTLDPTVPPLPFREEVYRSSRPLRVGYYETDNYTMPSPAMRRALIETKQRLEAA
At 357 ILGSSSADRYNLKPSPPCFPKLLSHNGSNAIGSLRLGKYTKWFNDVSSSDISDKCEDILK
Rat 357 GHTLIPFLPNNIPYALEVLSAGGLFSDGGRSFLQNFKGDFVDPCLGDLILILRLPSWFKR
At 417 LLSNNHGCKVVEIVVPELEEMR----------AAHVISIGSPTLSSLTPYCEAGKNSKL
Rat 417 LLSLLLKPLFPRLAAFLNSMRPRSAEKLWKLQHEIEMYRQSVIAQWKAMNLDVLLTPMLG
At 466 SYDTRTSFAIFRSFSASDYIAAQCLRRRLMEYHLNIFKDVDVIVTPTTGMTAPVIPPDAL
Rat 477 PALDLNTPGRATGAISYTVLYNCLDFPAGVVPVTTVTAEDDAQMELYKGYFGDIWDIILK
At 526 KNGETNIQ-VTTDLMRFVLAANLLGFPAISVPVG----------
Rat 537 KAMKNSVGLPVAVQCVALPWQEELCLRFMREVEQLMTPQKQPS---------
At 559 ---YDKEGLPIGLQIMGRPWAEATVLGLAAAVEELAPVTKKPAIFYDILNTN

B

```
        215                                                 257
Mouse   GGSSGGEGALIGSGGSPLGLGTDIGGSIRFPSAFCGICGLKPT
Porcine GGSSGGEGALIAAGGSPLGLGTDIGGSIRFPSAFCGICGIKPT
Rat     GGSSGGEGALIGSGGSPLGLGTDIGGSIRFPSAFCGICGLKPT
Human   GGSSGGEGALIGSGGSPLGLGTDIGGSIRFPSSFCGICGLKPT
        279                                                 321
At      GGSSSGSAAIVAAGLCSAALGTDGGGSVRIPSALCGITGLKTT
```

C

```
        CCCCHHHHHHHHHCCCHHHCCCCCCCHHCHHHHHCCCEECCCC
Rat     GGSSGGEGALIGSGGSPLGLGTDIGGSIRFPSAFCGICGLKPT

        CCCCHHHHHHHHHCCHHHCCCCCCCCCCCCHHHHCCCEECCCC
At      GGSSSGSAAIVAAGLCSAALGTDGGGSVRIPSALCGITGLKTT
```

Figure 2. Comparative alignment of *Arabidopsis* NAE amidohydrolase amino acid sequence (GenBank Accession AY308736) with mammalian FAAH. A, Full length alignment of *Arabidopsis* amino acid sequence (GenBank Accession AY308736) with rat FAAH (GenBank Accession U72497). These proteins are members of the amidase signature (AS) sequence-containing superfamily which includes amidase or amidohydrolase (EC 3.5) enzymes involved in the reduction of organic nitrogen compounds and ammonia production (Patricelli and Cravatt, 2000; Chebrou et al., 1996). The AS region is underlined and consists of about 125 amino acids. There is 18.5% identity between the *Arabidopsis* protein and rat FAAH when compared over the entire length of the proteins, whereas there is

37% identity within the AS. Conserved residues essential for rat FAAH activity (Lys142, Ser217, Ser218, Ser241 and Arg243) are indicated with arrowheads. B, Alignment of more conserved AS sequence motif (ref. Ueda et al., 2000) for the enzymes that hydrolyze NAEs; mouse (GenBank # U82536), porcine (GenBank # AB027132), rat (GenBank # U72497), and human (GenBank # U82535) (Giang and Cravatt, 1997). Identical residues within this motif between the plant and animal FAAHs are highlighted in black boxes. Within this motif there is 55-60% identity between the *Arabidopsis* and mammalian FAAH enzymes. C, Secondary structure prediction (PSIPRED, McGuffin et al., 2000; Jones, 1999) of the AS (C, coil; H, helix; E, strand) is depicted above the rat and *Arabidopsis* AS sequence motifs. Residues with similar secondary structure are highlighted in black boxes, illustrating the high degree of similarity within the active site (or AS sequence in NAE amidohydrolase, Ueda et al., 2000). This structural organization has been confirmed for rat FAAH by X-ray crystallography and suggests a functional link between these rat and *Arabidopsis* motif sequences despite limited primary amino acid sequence identity.

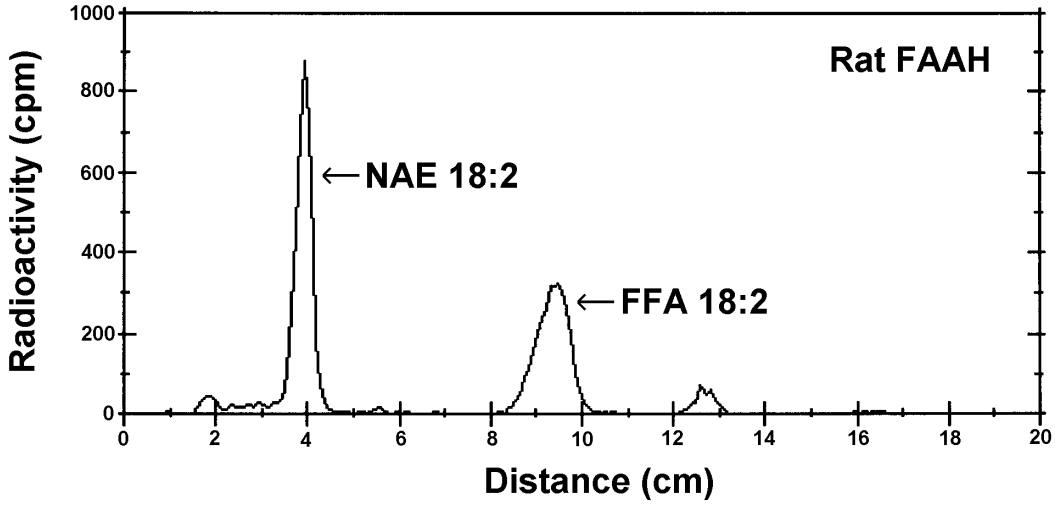
Rat FAAH
Radioactivity (cpm)
1000
800
600
400
200
0
NAE 18:2
FFA 18:2
0
2
4
6
8
10
12
14
16
18
20
Distance (cm)

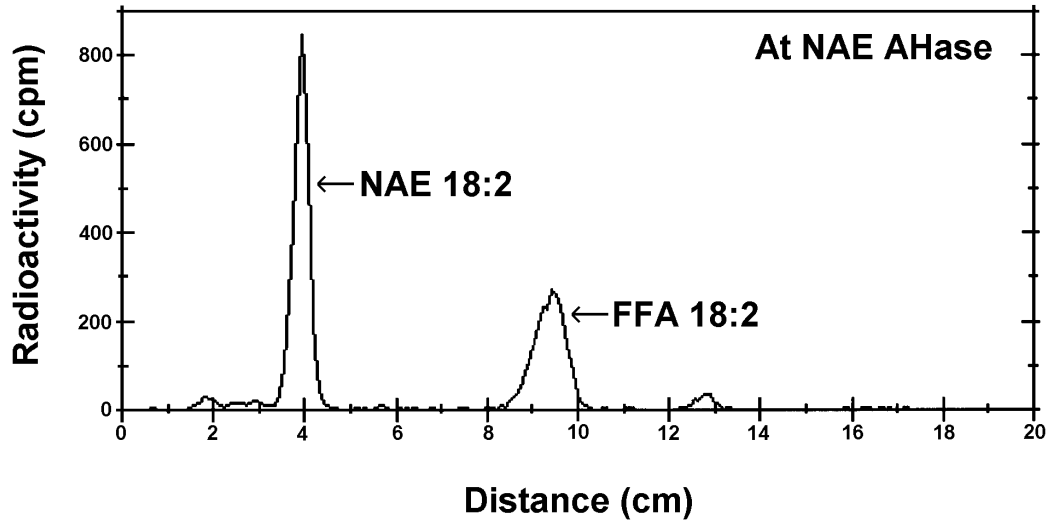
At NAE AHase
Radioactivity (cpm)
800
600
400
200
0
NAE 18:2
FFA 18:2
0
2
4
6
8
10
12
14
16
18
20
Distance (cm)

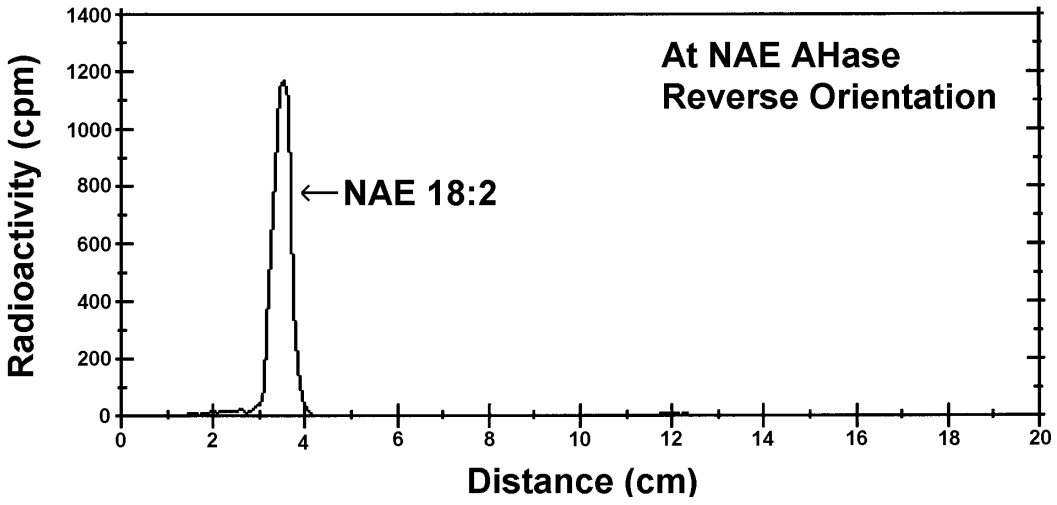

Figure 3. Representative radiochromatograms of NAE amidohydrolase activity assays surveyed in *E. coli* harboring expression plasmids. Lysates from cells expressing recombinant rat FAAH were compared with lysates of cells designed to express the *Arabidopsis* NAE amidohydrolase cDNA in forward (middle panel) or reverse orientation (lower panel) with respect to the lacZ promoter. In all cases cDNAs were in pTrcHis2 expression plasmids and recombinant protein expression was induced by 4 h incubation with 1 mM IPTG. For assays, 100 μM [1-^{14}C]NAE 18:2 (~20,000 dpm) in 50 mM Bis-Tris buffer (pH 9.0) was used. The reactions included 50 μg protein of respective cell lysate and were incubated for 30 min at 30 °C with shaking. Lipids were extracted and separated by TLC. The positions of [1-^{14}C]NAE 18:2 substrate and [1-^{14}C]FFA product are indicated.

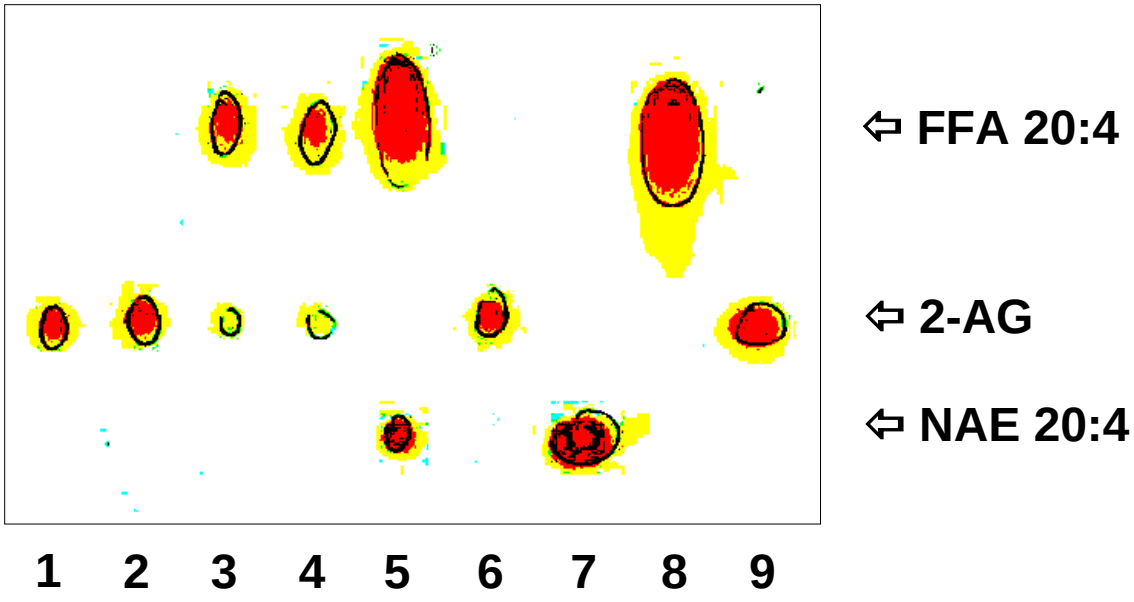

Figure 4. Representative thin layer chromatogram (TLC) of hydrolysis of 2-arachidonoylglycerol (2-AG) by *E. coli* lysate overexpressing NAE amidohydrolase. For the assays, 50 µM 2-AG in 50 mM Bis-Tris buffer (pH 9.0) was used. The reaction included 50 µg protein of respective cell lysate and were incubated for 30 min at 30 °C with shaking as described previously in Fig. 3. (1-2), 2-AG with *E. coli* lysate harboring NAE amidohydrolase cDNA in reverse orientation; (3-4), 2-AG with *E. coli* lysate harboring NAE amidohydrolase cDNA in correct orientation; 5, anandamide (NAE 20:0) with same lysate as in lanes 3 and 4; 6, 2-AG without lysate; (7-9), comigrated standards, NAE 20:4, FFA 20:4 and 2-AG. The positions of substrate and products were identified with comigration of standards.

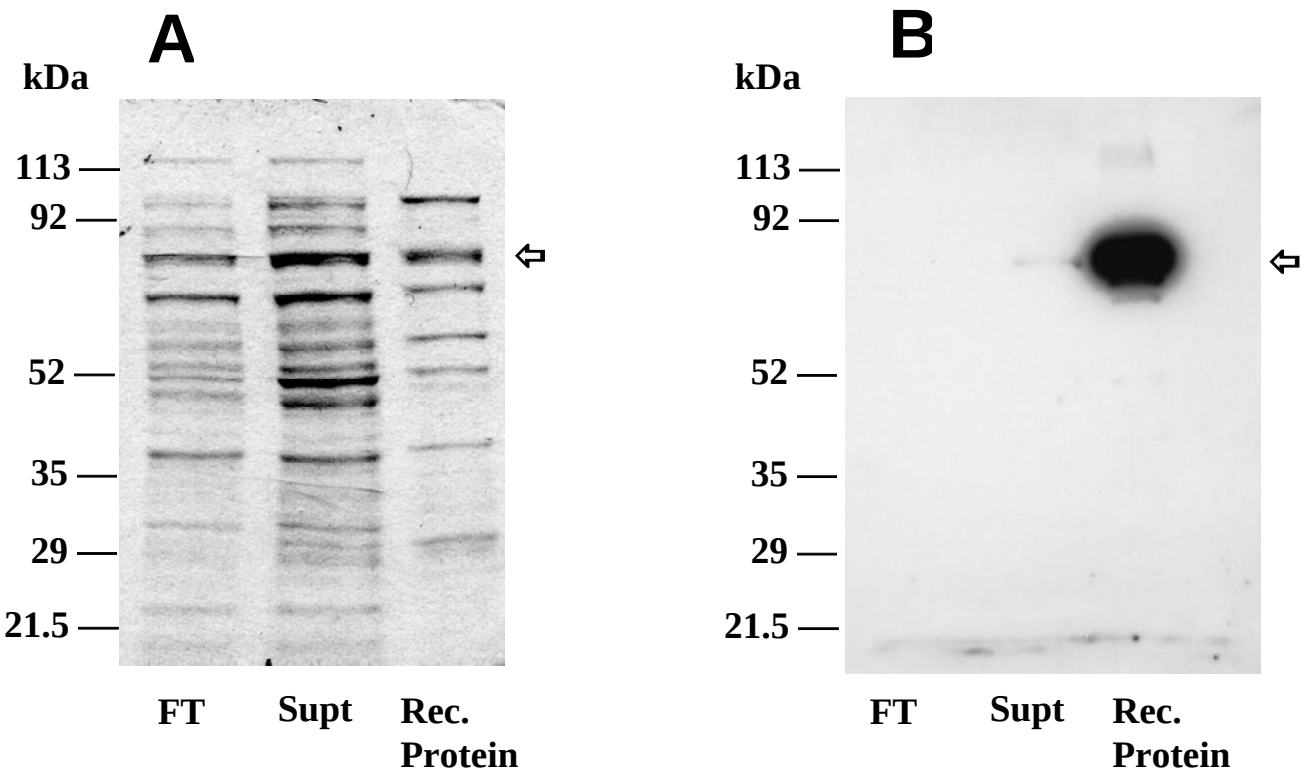
A
kDa
113
92
52
35
29
21.5
FT
Supt
Rec. Protein
B
kDa
113
92
52
35
29
21.5
FT
Supt
Rec. Protein

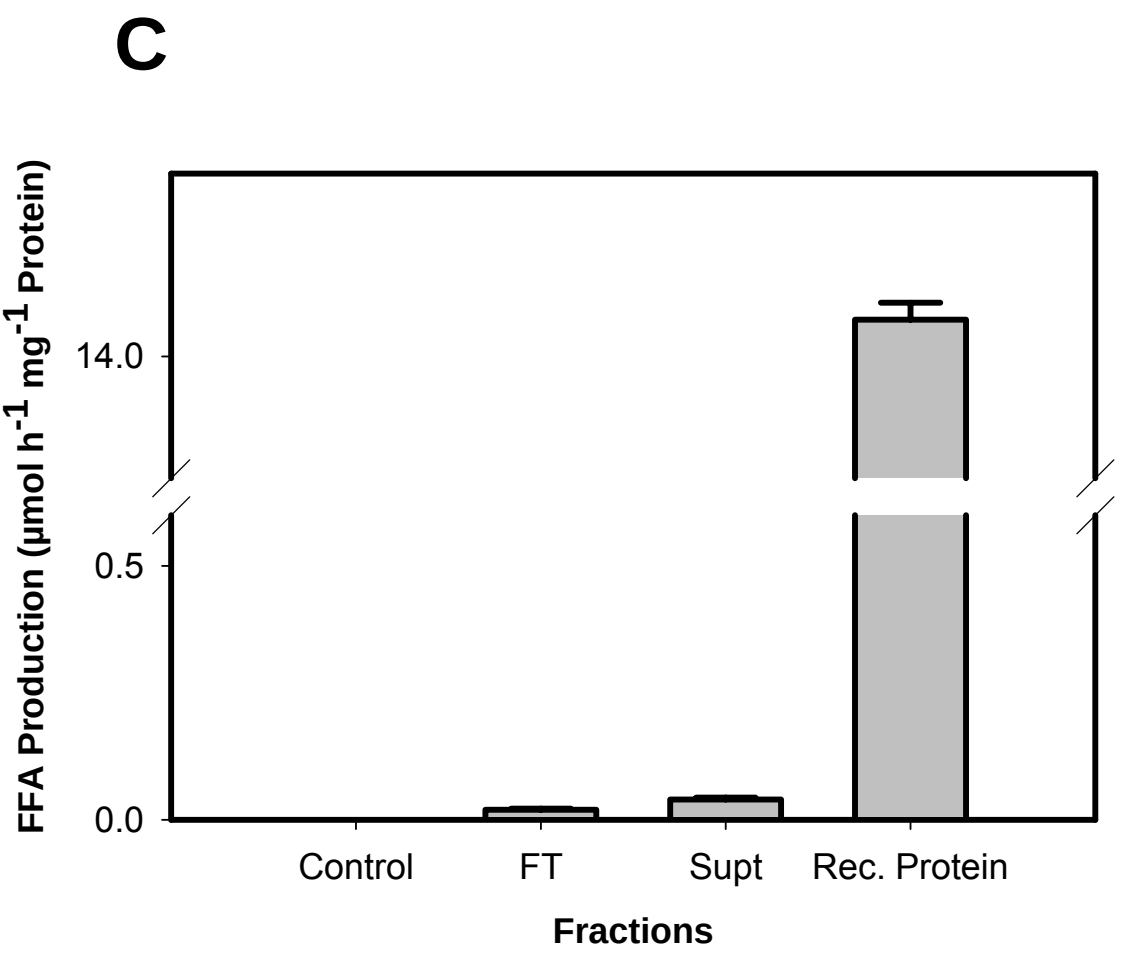

Figure 5. SDS-PAGE, Western blot, and activity assays of recombinant *Arabidopsis* NAE amidohydrolase expressed in *E. coli*. The c-myc-6xHis-tagged recombinant protein expressed in *E. coli* was solubilized in DDM and affinity-purified with Ni^{2+} precharged resin (ProBond, Invitrogen) under "native" conditions. A, Scan of Coomassie blue (R)-stained SDS gel (10 μg of total proteins in each lane except for rec. protein which was 2 μg) of select fractions. B, Western blot analysis of same proteins as in A, probed with anti-c-myc monoclonal antibodies and visualized by indirect chemiluminescence (goat-anti-mouse IgG conjugated to horseradish peroxide). The position of the recombinant

Arabidopsis fusion protein product (predicted to be ~ 70 kDa) is marked with open arrows. Positions of pre-stained standards (not shown) are indicated. FT = flow through and represents proteins not specifically bound to the Ni^{2+} resin (pooled 4 washes). Supt = supernatant and represents total proteins in *E. coli* lysates solubilized in DDM. Rec. protein = recombinant protein fraction affinity purified under "native" conditions. A small but detectable amount of 70 kDa immunoreactive protein was evident in total protein extracts, and as expected this protein was substantially enriched in the affinity-purification. In C, enzymatic assays for NAE 18:2 hydrolysis showed that amidohydrolase activity was enriched coincident with recombinant protein product.

A

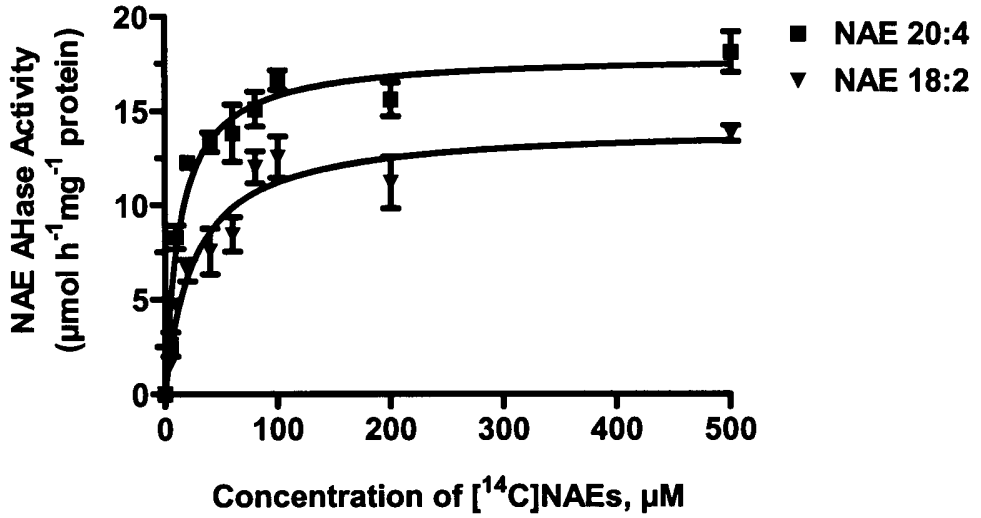
NAE AHase Activity
(μmol h-1mg-1 protein)
20
15
10
5
0
0
100
200
300
400
500
Concentration of [14C]NAEs, μM
NAE 20:4
NAE 18:2

B

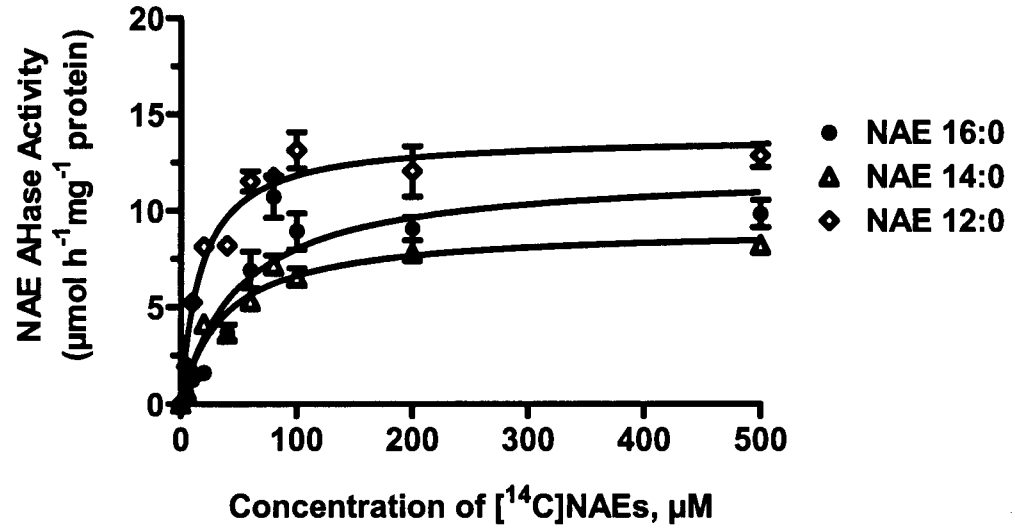
NAE AHase Activity
(μmol h-1mg-1 protein)
20
15
10
5
0
0
100
200
300
400
500
Concentration of [14C]NAEs, μM
NAE 16:0
NAE 14:0
NAE 12:0

Figure 6. Kinetic characterization of affinity-purified recombinant *Arabidopsis* NAE amidohydrolase. Initial velocity measurements were made at increasing concentrations of respective [1-^{14}C]NAE, combined with appropriate amount of non-radiolabeled NAE to give the final substrate concentration indicated. Reactions were initiated by the addition of 1 μg recombinant protein and were carried out in 50 mM Bis-Tris buffer, pH 9.0 in a final volume of 800 μL. Reactions were incubated for 30 minutes with shaking (100 rpm) at 30 °C, and stopped by the addition of 2 mL boiling isopropanol. Lipids were extracted into chloroform, washed, and separated by TLC (Shrestha et al., 2002). Activity was calculated based on the amount of radioactive product formed. Here, data points represent means and standard deviations of triplicate assays, all performed on the same "batch" of purified protein. Plots were generated with Prism software v3.0 (GraphPad Software, San Diego) by fitting the data to the Michaelis-Menten equation. Curve fits yielded correlation coefficients of $r^2 \geq 0.90$ (except for NAE16:0 where $r^2=0.83$), and kinetic parameters summarized in Table I were derived from these plots.

Acknowledgments

This research was supported by a grant from USDA-NRICGP (#2002-35318-12571). I thank Drs. John Ohlrogge and Fred Beisson, Michigan State University, for sharing their catalogue of Arabidopsis lipid genes in advance of its publication. Dr. Cecilia Hillard, Medical College of Wisconsin, with permission of Dr. Benjamin Cravatt, Scripps Research Institute, kindly provided the cloned rat WT-FAAH and △TM-FAAH in pTrcHis2 for our studies.

Literature Cited

Arabidopsis Genomic Initiative (2000) Analysis of the genome sequence of the flowering plant *Arabidopsis thaliana.* Nature 408: 796-815

Becker HD, Min B, Jacobi C, Raczniak G, Pelaschier J, Roy H, Klein S, Kern D, Soll D (2000) The heterotrimeric *Thermus thermophilus* Asp-tRNA(Asn) amidotransferase can also generate Gln-tRNA(Gln). FEBS Lett 476: 140-144

Bisogno T, De Petrocellis L, Di Marzo V (2002) Fatty acid amide hydrolase, an enzyme with many bioactive substrates. Possible therapeutic implications. Current Pharm Design 8: 533-547

Bisogno T, Maurelli S, Melck M, De Petrocellis L, Di Marzo V (1997) Biosynthesis, uptake, and degradation of anandamide and palmitoylethanolamide in leukocytes. J Biol Chem 272: 3315-3323

Blancaflor E, Hou G, Chapman KD (2003) Elevated levels of *N*-lauroylethanolamine, an endogenous constituent of desiccated seeds, disrupt normal root development in *Arabidopsis thaliana* seedlings. Planta 217: 206-217

Boger L, Fecik RA, Patterson JE, Miyauchi H, Patricelli MP, Cravatt BF (2000) Fatty acid amide hydrolase substrate specificity. Bioorg Med Chem Lett 10: 2613-2616

Bracey MH, Hanson MA, Masuda KR, Stevens RC, Cravatt BF (2002) Structural adaptations in a membrane enzyme that terminates endocannabinoid signaling. Science 298: 1793-1796

Bradford MM (1976) A rapid and sensitive method for quantification of microgram quantities of protein utilizing the principle of protein-dye bind. Anal Biochem 72: 248-254

Buckley NE, McCoy KL, Mezey E, Bonner T, Zimmer A, Felder CC, Glass M, Zimmer A (2000) Immunomodulation by cannabinoids is absent in mice deficient for cannabinoid CB2 receptor. Eur J Pharmacol 396: 141-149

Chang TH, Abelson J (1990) Identification of a putative amidase gene in yeast *Saccharomyces cerevisiae*. Nucleic Acids Res 18, 7180-7180

Chapman KD (2000) Emerging physiological roles for *N*-acylphosphatidyl-ethanolamine metabolism in plants: signal transduction and membrane protection. Chem Phys Lipids 108: 221-230

Chapman KD, Tripathy S, Venables BJ, Desouza AD (1998) *N*-Acylethanolamines: formation and molecular composition of a new class of plant lipids. Plant Physiol 116: 1163-1168

Chapman KD, Venables BJ, Markovic R, Blair RW, Bettinger C (1999) *N*-Acylethanolamines in seeds: quantification of molecular species and their degradation upon imbibition. Plant Physiol 120: 1157-1164

Chebrou H, Bigey F, Arnaud A, Galzy P (1996) Study of the amidase signature group. Biochim Biophys Acta 1298: 185-293

Cravatt BF, Giang DK, Mayfield SP, Boger DL, Lerner RA, Gilula NB (1996) Molecular characterization of an enzyme that degrades neuromodulatory fatty-acid amides. Nature 84: 83-87

Cravatt BF, Lichtman AH (2002) The enzymatic inactivation of the fatty acid amide class of signaling lipids. Chem Phys Lipids 121: 135-148

Curnow AW, Hong KW, Yuan R, Kim SI, Martins O, Winkler W, Henkin TM, Soll D (1997) Glu-tRNA^{Gln} amidotransferase: A novel heterotrimeric enzyme required for correct decoding of glutamine codons during translation. Proc Natl Acad Sci USA (1997) 94: 11819-11826

Desarnaud F, Cadas H, Piomelli D (1995) Anandamide amidohydrolase activity in rat brain microsomes. Identification and partial characterization. J Biol Chem 270, 6030-6035.

Deutsch DG, Omeir R, Arreaza G, Salehani D, Prestwich GD, Huang Z, Howlett A (1997) Methyl arachidonyl fluorophosphonate: a potent irreversible inhibitor of anandamide amidase. Biochem Pharmcol 53: 255-260

Di Marzo V, Bisogno T, Sugiura T, Melck D, De Petrocellis L (1998) The endogenous cannabinoid 2-arachidonoylglycerol is inactivated by neuronal- and basophil-like cells: connections with anandamide. Biochem J 331: 15-19

Elbing K, Brent R (2002) Growth in liquid media. *In* Current Protocols in Molecular Biology (Ausubel FM, Brent R, Kingston RE, Moore DD, Seidman JG, Smith JA, Struhl K, eds) Vol 1, pp 1.2.1-1.2.2, John Wiley and Sons, New York

Fowler CJ, Jonsson K-O, Tiger G (2001) Fatty acid amide hydrolase: biochemistry, pharmacology, and therapeutic possibilities for an enzyme hydrolyzing anandamide, 2-arachidonoylglycerol, palmitoylethanolamide, and oleamide. Biochem Pharmacol 62: 517-526

Giang DK, Cravatt BF (1997) Molecular characterization of human and mouse fatty acid amide hydrolases. Proc Natl Acad Sci USA 94: 2238-2242

Goparaju SK, Kurahashi Y, Suzuki H, Ueda N, Yamamoto S (1999) Anandamide amidohydrolase of porcine brain: cDNA cloning, functional expression and site-directed mutagenesis. Biochem Biophys Acta 1441: 77-84

Goparaju SK, Ueda N, Yamaguchi H, Yamamoto S (1998) Anandamide amidohydrolase reacting with 2-arachidonoylglycerol, another cannabinoid receptor ligand. FEBs Lett 422: 69-73

Hansen HS, Moesgaard B, Hansen HH, Petersen G (2000) *N*-Acylethanolamines and precursor phospholipids – relation to cell injury. Chem Phys Lipids 108: 135-150

Hashimoto Y, Nishiyama M, Ikehata O, Horinauchi S, Beppu T (1991) Cloning and characterization of an amidase gene from *Rhodococcus* species N-774 and its expression in *Escherichia coli*. Biochim Biophys Acta 1088: 225-233

Hillard CJ (2000) Biochemistry and pharmacology of the endocannabinoids arachidonylethanolamide and 2-arachidonylglycerol. Prostaglandins & Other Lipid Mediators 61: 3-18

Hillard CJ, Edgemond WS, Campbell WB (1995) Characterization of ligand binding to the cannabinoid receptor of rat brain membranes using a novel method: application to anandamide. J Neurochem 64: 677-683

Jones DT (1999) Protein secondary structure prediction based on position-specific scoring matrices. J Mol Biol 292: 195-202

Katayama K, Ueda N, Katoh I, Yamamoto S (1999) Equilibrium in the hydrolysis and synthesis of cannabimimetic anandamide demonstrated by a purified enzyme. Biochim Biophys Acta 1440: 205-214

Koutek B, Prestwich GD, Howlett AC, Chin SA, Salehani D, Akhavan N, Deutsch DG (1994) Inhibitors of arachidonoyl ethanolamide hydrolysis. J Biol Chem 269: 22937-22940

Krogh A, Larsson B, von Heijne G, Sonnhammer EL (2001) Predicting transmembrane protein topology with a hidden Markov model: application to complete genomes. J Mol Biol 305: 567-580

Lambert DM, Di Marzo V (1999) The palmitoylethanolamide and oleamide enigmas: are these two fatty acid amides cannabimimetic? Current Med Chem 6: 757-773

Lambert DM, Vandevoorde S, Jonsson KO, Fowler CJ (2002) The palmitoylethanolamide family: a new class of anti-inflammatory agents? Current Med Chem 9: 663-674

Mayaux JF, Cerbelaud E, Soubrier F, Faucher D, Petre D (1990) Purification, cloning, and primary structure of an enantiomer-selective amidase from

Brevibacterium sp. strain R312: structural evidence for genetic coupling with nitrile hydratase. J Bacteriol 172: 6764-6773

McGuffin LJ, Bryson K, Jones DT (2000) The PSIPRED protein structure prediction server. Bioinformatics 16: 404-405

McKinney MK, Cravatt BF (2003) Evidence for distinct roles in catalysis for residues of the serine-serine-lysine catalytic triad of fatty acid amide hydrolase. J Biol Chem 276: 37393-37399.

Nakai K, Kanehisa M (1992) A knowledge base for predicting protein localization sites in eukaryotic cells. Genomics 14: 897-911

Omeir RL, Arreaza G, Deutsch DG (1999) Identification of two serine residues involved in catalysis by fatty acid amide hydrolase. Biochem Biophys Res Commun 264: 316-320

Pappan K, Austin-Brown S, Chapman KD, Wang X (1998) Substrate selectivities and lipid modulation of plant phospholipase D alpha, -beta, and -gamma. Arch Biochem Biophys 353: 131-140

Paria BC, Dey SK (2000) Ligand-receptor signaling with endocannabinoids in preimplantation embryo development and implantation. Chem Phys Lipids 108: 211-220

Patricelli MP, Cravatt BF (2000) Clarifying the catalytic roles of conserved residues in the amidase signature family. J Biol Chem 275:19177-19184

Patricelli MP, Lashuel HA, Giang DK, Kelly JW, Cravett BF (1998) Comparative characterization of a wild type and transmembrane domain-deleted fatty

acid amide hydrolase: identification of the transmembrane domain as a site for oligomerization. Biochemistry 37:15177-15187

Patricelli MP, Lovato MA, Cravatt BF (1999) Chemical and mutagenic investigations of fatty acid amide hydrolase: evidence for a family of serine hydrolases with distinct catalytic properties. Biochemistry 38: 9804-9812

Pertwee RG (2001) Cannabinoid receptors and pain. Prog Neurobiol 63:569-611

Pertwee RG, Fernando SR, Griffin G, Abadji V, Makriyannis A (1995) Effect of phenylmethylsulphonyl fluoride on the potency of anandamide as an inhibitor of electrically evoked contractions in two isolated tissue preparations. Eur J Pharmacol 272: 73-78

Sarker KP, Obara S, Nakata M, Kitajima I, Maruyama I (2000) Anandamide induces apoptosis of PC-12 cells: involvement of superoxide and caspase-3. FEBS Lett 472: 39-44

Schmid HH, Berdyshev EV (2002) Cannabinoid receptor-inactive *N*-acylethanolamines and other fatty acid amides: metabolism and function. Prostag Leukotr Essent Fatty Acids 66: 363-376

Schmid HH, Schmid PC, Berdyshev EV (2002) Cell signaling by endocannabinoids and their congeners: questions of selectivity and other challenges. Chem Phys Lipids 121: 111-134

Schmid HHO, Schmid PC, Nataranjan V (1990) *N*-Acylated glycerophospholipids and their derivatives. Prog Lipid Res 29: 1-43

Schmid HHO, Schmid PC, Nataranjan V (1996) The *N*-acylation-phosphodiesterase pathway and cell signaling. Chem Phys Lipids 80:133-142

Schon A, Kannangara CG, Gough S, Soll D (1988) Protein biosynthesis in organelles requires misaminoacylation of tRNA. Nature 331: 187-189

Servant F, Bru C, Carrère S, Courcelle E, Gouzy J, Peyruc D, Kahn D (2002) ProDom: automated clustering of homologous domains. Brief Bioinform 3: 246-251

Shrestha R, Noordermeer MA, Van der Stelt M, Veldink GA, Chapman KD (2002) *N*-Acylethanolamines are metabolized by lipoxygenase and amidohydrolase in compeint pathways during cottonseed imbibition. Plant Physiol 130: 391-401

Sigrist CJ, Cerutti L, Hulo N, Gattiker A, Falquet L, Pagni M, Bairoch A, Bucher P (2002) PROSITE: a documented database using patterns and profiles as motif descriptors. Brief Bioinform 3: 265-274

Sonnhammer EL, von Heijne G, Krogh A (1998) A hidden Markov model for predicting transmembrane helices in protein sequences. Proc Int Conf Intell Syst Mol Biol 6: 175-182

Tiger G, Stentrom A, Fowler CJ (2000) Pharmacological properties of rat brain fatty acid amidohydrolase in different subcellular fractions using palmitoylethanolamide as substrate. Biochem Pharmacol 59: 647-653

Tripathy S, Kleppinger-Sparace K, Dixon RA, Chapman KD (2003) *N*-acylethanolamine signaling in tobacco is mediated by a membrane-associated, high-affinity binding protein. Plant Physiol 131: 1781-1791

Tripathy S, Venables BJ, Chapman KD (1999) *N*-Acylethanolamines in signal transduction of elicitor perception: attenuation of alkalinization response and activation of defense gene expression. Plant Physiol 121: 1299-1308

Tsuchiya K, Fukuyama S, Kanzaki N, Kanagawa K, Negoro S, Okada H (1989) High homology between 6-aminohexanoate-cyclic-dimer hydrolases of Flavobacterium and Pseudomonas strains. J Bacteriol 171: 3187-3191

Ueda N (2002) Endocannabinoid hydrolases. *Prostaglandis & Other Lipid Mediators* 68-69: 521-534

Ueda N, Puffenbarger RA, Yamamoto S, Deutsch DG (2000) The fatty acid amide hydrolase (FAAH). Chem Phys Lipids 108:107-121

Van der Stelt M, Veldhuis WB, Van Haaften GW, Fezza F, Bisogno T, Bar PR, Veldink GA, Vliegenthart JFG, Di Marzo V, Nicolay K (2001) Exogenous anandamide protects rat brain against acute neuronal injury in vivo. J Neurosci 21:8765-8771

Wilson RI, Nicoll RA (2002) Endocannabinoid signaling in the brain. Science 296: 678-682

CHAPTER III

ALTERED *N*-ACYLETHANOLAMINE (NAE) AMIDOHYDROLASE EXPRESSION IN *ARABIDOPSIS THALIANA* ALTERS THE SENSITIVITY OF SEEDLINGS TOWARD EXOGENOUS NAE LIPID MEDIATORS

Abstract

Recently a functional homologue of the mammalian fatty acid amide hydrolase was identified in *Arabidopsis thaliana* that degraded a wide range of *N*-acylethanolamines (NAEs) to their corresponding free fatty acids *in vitro*. Here, two T-DNA insertional mutant lines with disruptions in the *Arabidopsis* NAE amidohydrolase (also designated fatty acid amide hydrolase, AtFAAH) gene (*At5g64440*) were identified (Salk Institute-generated lines, 095108 and 118043). Homozygous mutants lacked detectable FAAH transcripts or enzyme activity and exhibited seed germination, seedling growth and root development phenotypes and. The mutant seedlings were more sensitive than wild-type seedlings to exogenously applied NAE 12:0. For example, NAE dose-dependent reduction in primary root length was measured for seedlings at daily intervals for the first week after planting. The concentration of exogenous NAE 12:0 that effectively reduced the rate of primary root elongation to half of that of untreated seedlings (EC_{50}) was 30 μM for wild type, but was substantially lower for T-DNA mutants (18 or 23 μM for Salk_118043 or Salk_ 095108, respectively). On the other hand, transgenic seedlings overexpressing the NAE amidohydrolase enzyme (as a

GFP fusion protein) showed noticeably greater tolerance than that of the wildtype toward exogenous NAE 12:0. Seeds of over-expressors germinated and grew almost normally at 20 μM exogenous NAE 12:0. Taken together, our results are consistent with a metabolic role *in vivo* for the NAE amidohydrolase gene, *At5g64440*, in the catabolism of NAEs, and continue to suggest that this lipid hydrolytic pathway may be important for normal seed germination and seedling growth.

Abbreviations

BSTFA, bis(trimethylsilyl)trifluoroacetamide

C_T, threshold cycle

DMSO, dimethyl sulfoxide

EC_{50}, half-maximal effective concentration

EDTA, ethylenediamine tetraacetic acid

EGTA, ethylene glycol-bis(β-amino ethylether) tetraacetic acid

ETYA, 5,8,11,14-eicosatetraynoic acid

FAAH, fatty acid amide hydrolase

FFA, free fatty acid

GC-MS, gas chromatography-mass spectrometry

GFP, green fluorescent protein

HPLC, high performance liquid chromatography

LOX, lipoxygenase

NAE, *N*-acylethanolamine

MS, Murashige and Skoog

NAE 16:0, *N*-palmitoylethanolamine

NAE 18:2, *N*-linoleoylethanolamine

NAE 20:4, *N*-arachidonoylethanolamine (anandamide)

NAPE, *N*-acylphosphatidylethanolamine

PLD, phospholipase D

RT-PCR, reverse transcriptase - polymerase chain reaction

smGFP, soluble modified green fluorescent protein

T-DNA, transfer DNA

Introduction

N-Acylethanolamines (NAEs) are lipid mediators in animal systems that function as part of the "endocannabinoid" signaling pathway, and are derived from the hydrolysis of *N*-acylphosphatidylethanolamines (NAPEs), a minor phospholipid constituent of cellular membranes (Schmid et al., 1990; Chapman, 2000). NAEs are produced by the action of phospholipase D (Schmid et al., 1996). There are various NAEs in mammals and regulation of NAE levels in mammalian cells is associated with important physiological processes. For example, anandamide, a type of NAE in mammalian brain tissue, is an endogenous ligand for cannabinoid receptor and modulates neurotransmission. It also acts as an endogenous analgesic (Pertwee, 2001). These physiological processes are regulated by both receptor-dependent and receptor-independent pathways (Berdyshev et al., 2001), but these bioactive molecules terminate their signaling function upon hydrolysis by NAE amidohydrolase also designated fatty acid amide hydrolase (FAAH; Cravatt et al., 2001).

In plants, similar to animals there are different NAE profiles in different tissues, and their levels change rather dramatically in response to environmental stimuli or with a change in developmental stage. In leaves, NAE 12:0 and NAE 14:0 are elevated in response to pathogen elicitors, and appear to function in plant defense signaling (Tripathy et al., 1999). On the other hand, NAE 18:2 and NAE 16:0 are prevalent in desiccated seeds and decrease with seed imbibition

and germination raising the possibility that NAE metabolism is involved in the regulation of seed germination and postgerminative growth (Chapman et al., 1999). NAEs were also found to selectively inhibit the activity pf phospholipase Dα *in vitro* in a chain-length-dependent manner and application of NAEs to epidermal section of tobacco and *Commelina communis* abolished abscisic acid induced stomatal closure (Austin-Brown and Chapman, 2002).

It is likely that the regulation of NAE levels is important for normal plant growth and development and certain stress responses. Understanding the pathways involved in NAE metabolism and the characteristics of enzymes in these pathways are important to unraveling the physiological functions of these lipid metabolites in plants. Moreover manipulation of expression of enzyme(s) responsible for NAE metabolism will help to test ideas about NAE function. Based on the evidence to date, one hypothesis is that NAEs are negative regulators of seed germination and postgerminative growth, and their levels need to be depleted during imbibition for synchronous events associated with cell division and expansion. Overall the results presented here will contribute to our current thinking about the physiology of seed development, germination and seedling growth and will serve as a basis to guide future studies.

Recently, I reported the molecular identification of a functional homologue of the mammalian FAAH in *Arabidopsis thaliana* that converts a wide range of NAEs to their corresponding free fatty acids (and ethanolamine) (Shrestha et al., 2003; Chapter II). Functional homologues of the *Arabidopsis* FAAH (AtFAAH) also were identified in *Oryza sativa* (rice) and *Medicago truncatula* supporting a

common mechanism for the regulation of NAE hydrolysis in diverse plant species (including dicot and monocot species). A recent report by Blancaflor et al. (2003) showed *Arabidopsis* seedling growth and development were altered drastically by elevated levels of exogenous NAE 12:0 indicating a possible role for NAE metabolism in root cell expansion/elongation. However, because exogenous NAEs may act non-specifically, and in these studies NAEs were maintained at levels above the physiological concentrations, a molecular genetic approach was taken to manipulate endogenous NAE levels. I reasoned that by altering expression of the enzyme responsible for NAEs' degradation, NAE amidohydrolase (AtFAAH), this might reveal an endogenous role for NAEs within the physiological context of seed germination and seedling growth. Here, AtFAAH loss-of-gene function was explored by insertional mutagenesis (gene knockouts) and two knockout lines with putative NAE amidohydrolase gene disruptions were identified among the publicly available T-DNA tagged *Arabidopsis* insertional mutant lines (Salk_095108 and Salk_118043; Salk Institute Genomic Analysis Laboratory). M3 seeds of these lines were provided by the Arabidopsis Biological Resource Stock Center, Ohio State University. After careful scrutiny of the zygosity of the mutants and determining precise location of T-DNA insertion, the phenotypes of these lines were examined. Also, for comparison transgenic lines overexpressing AtFAAH (as a GFP fusion protein) were provided by Dr. E. Blancaflor, S.R. Noble Foundation.

My results indicate that mutant seedlings grew slower, and were more sensitive to exogenous NAE 12:0 than wild type. By contrast transgenic

seedlings overexpressing the NAE amidohydrolase grew faster than wild type and showed a greater tolerance to exogenous NAE. Beyond the work reported here, these plants with altered NAE amidohydrolase expression will provide new tools to uncover the significance of NAE metabolism in other aspects of the plant physiology.

Results

NAE Amidohydrolase (AtFAAH) Expression in planta

Expression levels of the FAAH gene, *At5g64440*, were evaluated by quantitative reverse-transcriptase (RT)-PCR for different *Arabidopsis* plant stages and tissues (Fig. 1). Expression was detected in all stages and plant parts, and transcript levels were plotted relative to those in stem (lowest transcript levels) (Fig. 1A). Among the tissues of mature plants, transcript levels were highest in siliques (18 fold higher than those measured in stem). The transcript level in desiccated seeds was 2.5 fold higher than in stem and the level increased to 4 fold in imbibed seeds and 19 fold in seedlings (96 h old). The purity of RT-PCR products was confirmed by melting curve analysis and products were further analyzed by electrophoresis (1% agarose gel, see Fig. 1B).

Arabidopsis *AtFAAH T-DNA Insertional Mutants and Transgenics*

Gene function is commonly explored by altering expression of the gene. Two T-DNA insertional mutants, Salk_095108 and Salk_118043 were identified and seeds of these two lines were provided by the *Arabidopsis* Biological resource of Stock Center, Ohio State University. Seeds of these plants were germinated on kanamycin to identify mutant individuals. Progeny of these selected plants were grown for analyses.

Evaluation of zygosity was carried out by PCR with two gene specific and one T-DNA left border specific primers. Details on primer design are described in

"Materials and Methods". The PCR products were sequenced, to identify the precise locations and orientations of the T-DNA insertions. The nucleotide sequences of the PCR products indicated that the insert in Salk_095108 was in the 17th exon and the insert in Salk_118043 was in the 13th intron. The locations, orientations and nucleotide sequences surrounding the T-DNA insertions in two knockout lines are shown in Fig. 2.

The transgenic *Arabidopsis* plants were developed with ectopic overexpression and antisense suppression of AtFAAH 5g64440, and were generated by the E. Blancaflor lab (S.R. Noble Foundation). The full-length FAAH cDNA was cloned downstream from the CaMV 35S promoter in the sense orientation (Fig. 3A) or in the antisense orientation (Fig. 3B) into the binary vector, pCAMBIA 1390. Sense expression constructs included GFP as an inframe fusion with the 3' end of the FAAH cDNA. The plants were transformed by the floral dip method and the transgenic plants were selected on kanamycin. The progeny were selfed and T3 seeds were germinated and grown for expression analyses.

Altered AtFAAH Expression

As a means to understand FAAH function *in planta*, transgenic and mutant *Arabidopsis* plants were generated and/or identified. The At5g64440 transcript occurrence and relative abundance were evaluated with total RNA extracted from leaves of an overexpressor line (OE), an antisense line (AS) and two knockouts (SK08, Salk_095108; SK43, Salk_118043). Here the transcript levels were

normalized to those of wild type. The overexpressor, as expected, had over 3 fold higher transcript levels than wild type. The antisense line showed closer transcript abundance to the wild type (0.79 fold), whereas SK08 showed no detectable transcript and SK43 showed some RT-PCR product (0.33 fold to wild type) (Fig. 4A). The RT-PCR products were analyzed by agarose gel electrophoresis (Fig. 4B) after confirmation with melting curve analysis. The primers used for quantification of AtFAAH mRNA were designed to amplify a 260 bp of near the 5' end of the mRNA. Both knockout lines were homozygous for T-DNA insertions in the gene, and were presumed unable to form processed full length mRNA. Further RT- PCR analyses for the full length ORF (1821 bp) was carried out and indeed no large transcript occurred in either of knockouts (Fig. 4C) indicating the possibility of truncated RNA species intermediate in SK43 leaves.

These transgenic plants along with knockout mutants were examined for NAE amidohydrolase expression, enzyme activity and sensitivity to exogenous NAE sensitivity and morphological phenotypes. NAE amidohydrolase specific activity in microsomes isolated from wild type (WT), knockouts (Salk_095108 and Salk_118043), and transgenic (OE, overexpressors; AS, antisense expressors) *Arabidopsis* plants were compared (Fig. 5). Enzyme activities were measured with equal amounts (400 μg) of microsomal proteins extracted according to Shrestha et al. (2002) with [1-^{14}C]NAE 12:0 or [1-^{14}C]NAE 18:2 as substrates. Microsomes were isolated from above ground tissues of mature (6-week-old) plants, all grown under the same environmental conditions. The activity profiles

were consistent with patterns of FAAH gene transcript levels in these mutants and transgenic plants such that microsomes isolated from antisense and knockouts had less or no activity compared with those from wild type whereas microsomes isolated from overexpressors had 5 times specific activity compared to specific activity in microsomes isolated from wild type (Fig. 5).

AtFAAH Influences Radicle Root Length

Phenotypic comparisons were made between *Arabidopsis* seedling roots of wild type and knockouts (Fig. 6). A reduction in primary root length in knockouts relative to wild type was observed though there was no substantial delay in seed germination. Generally, the wild type seedlings germinated and grown under identical conditions to mutants showed longer radicle length and larger cotyledon size. (upper panel, Fig. 6). The knockout seedlings generally appeared to be smaller in overall size (middle and lower panels, Fig. 6). The seedling phenotypes between wild type and knockouts were visibly different and measurements of rate of radicle/root elongation confirmed that the rate of primary root elongation was reduced by 15-20% in the knockouts over six days postgerminative growth (Fig. 7) compared to the rate of root elongation in wild type seedlings. The differences in root lengths were statistically significant at $p<0.00001$ at all points (t-test).

Sensitivity of Seedlings to Exogenous NAE12:0

Lengths of the primary roots growing in phyta-agar medium supplemented with various concentrations of NAE 12:0 were measured in daily intervals. Root lengths of wild type seedlings were reduced by increasing concentrations of exogenous NAE12:0 (Fig. 8A) as shown previously (Blancaflor et al., 2003). However, similar experiments with knockout (Salk_0118043 and Salk_095108) seedlings indicated that the reduction in root length by increasing concentrations of NAE 12:0 was more pronounced (Fig. 8B and C) compared to wild type (Fig. 8A). These results indicate that the knockout seedlings are more sensitive to exogenous NAE 12:0 than wild type seedlings which was expected since they had no detectable endogenous FAAH activity. Dose response curves were plotted from the data presented in Fig. 8 (A-C) to illustrate the sensitivity of the wild type and knockouts to the exogenous NAE 12:0 (Fig. 9). The half-maximal effective concentration (EC_{50}) was about 30 μM for wild type seedlings whereas the growth rates of both knockouts were more sensitive to exogenous NAE 12:0 with EC_{50}'s of 18 and 23 μM for Salk_118043 and Salk_095108, respectively.

For comparison, root lengths of 6-day-old seedlings of wild type, knockout (Salk_118043) and overexpressor were plotted against the exogenous NAE 12:0 concentration from 0 μM to 40 μM (Fig. 10). The dose-dependent reduction in primary root length was different for these seedlings and followed their endogenous levels of FAAH enzyme activity. This was most evident at 20 – 30 μM NAE 12:0 where knockout seedlings had significantly shorter roots and

overexpressors had significantly longer roots than wild type. Similar, predictable seedling phenotypes were obvious in older seedlings (14-day-old) as well (Fig. 11). The images clearly showed the effects were specific to NAE12:0 since the growth of seedlings in the same concentration of lauric acid was indistinguishable from those grown in solvent only control (DMSO [0.5% final], control). Here lower concentration of NAE12:0 (20 μM) showed moderate inhibitory growth effects on wild type and antisense whereas the effects were more dramatic in both knockouts causing smaller overall plants. On the other hand, overexpressor seedlings showed more luxuriant growth in NAE12:0 than corresponding controls (FFA 12:0 or DMSO, controls). This indicates that FAAH overexpressor seedlings likely metabolize the exogenous NAE12:0 mitigating the inhibitory effect of NAE 12:0.

NAE Profiles and Quantification

In preliminary experiments, endogenous NAE levels were quantified in *Arabidopsis* seeds and seedlings, and compared between wild type and knockouts in order to examine the association of levels/types with observed physiological/cellular changes. There was approximately 25 percent higher total NAE content in seeds of both knockout lines compared with wild type (Fig. 12A). The profiles of NAE types seemed not much different, except NAE14:0 and NAE 16:0 were found almost three fold higher in knockouts compared to wild type seeds. Those NAEs (NAE14:0 and NAE16:0) did not have effect on seedling phenotypes except NAE 14:0 was reported for signaling molecules in stress

related response. The GC/MS data showed approximately 33 percent higher NAE contents in seedlings of knockouts compared to wild type (Fig. 12B). There were not any substantial changes in minor NAEs except NAE14:0 and NAE16:0 were higher in knockouts seedlings as was the case in desiccated seeds. Additional metabolite measurements in these lines will be required at different stages during seed development, seed germination, and seedling growth (particularly in conjunction with FAAH overexpressing lines) to conclusively connect changes in NAE metabolism, NAE profiles, and plant development.

Discussion

Recent molecular genetic evidence with FAAH knockout mice revealed an increase of NAE levels and the mice were supersensitive to endogenous cannabinoid lipid mediators (Cravatt et al., 2001). This indicated a role for FAAH in the regulation of NAE levels for normal mammalian physiology. The mechanism and regulation of NAE levels in plants is not as clear as in animal systems but it is likely that NAE needs to be formed and degraded in a timely fashion to regulate a number of normal physiological processes. Manipulation of NAE levels in a model plant like *Arabidopsis thaliana* will help to uncover its role in plants. Clearly, one prediction was that the *Arabidopsis* FAAH enzyme would be expressed during seed germination and seedling growth consistent with biochemical and physiological data reported in the earlier two chapters.

Characterization of the enzyme in terms of organ specific distributions and developmental controls help to develop a better understanding of the physiological significance of NAE metabolism in higher plants. The identification and isolation of cDNA encoding for NAE amidohydrolase (AtFAAH) helped to study the tissue (plant parts) specific distribution of the enzyme. The transcript occurrence of the gene was found in all plant parts and stages though levels of transcription varied to the extent. The transcript levels were the highest in seedlings (96 h) and siliques (from 6-week-old plant) indicating more potential metabolic activities in those stages (Fig. 1). These results on expression of the

transcript in tissues support the previous reports on expression of the gene. Expressed sequence tag (EST)-derived sequence data indicates that the *At5g64440* gene is expressed in *Arabidopsis* seeds, seedlings and in mixed libraries (www.plantbiology.msu.edu/lipids/genesurvey/FAAH.htm). Massively parallel signature sequencing (MPSS) database information (http://mpss.udel.edu) indicates that *At5g64440* as marked by a unique sequence in exon 21 (GATCTACAAAATCGACGA) is expressed in approximately 100 ppm (relative to transcript abundance) in *Arabidopsis* leaves, roots, callus and inflorescence tissues. Many earlier biochemical studies on specific activity of the enzyme responsible for hydrolyzing NAEs were most active during first 4 – 8 h of commencing cottonseed imbibition and during the same time NAE contents depleted drastically in cottonseeds and other seeds (Shrestha et al., 2002; Chapman et al., 1999). It was postulated that these NAEs might have a role in the regulation of seed germination based on their rapid deletion during seed imbibition (Chapman, 2000). Here the studies on transcription levels measured at three points of desiccated seeds (0 h), imbibed seeds (4h) and seedlings (96 h) showed the gradual increase of transcript levels (Fig. 1). Based on the transcript levels of the enzyme, the enzymatic activity is predicted to be very high in seedlings even after development of greening cotyledons and seedling roots.

Gene function in a physiological context may be explored by altering gene expression. The plants with up regulation, down regulation or complete knock out the expression were generated and/or identified. The transcript levels for overexpressors were about 3 fold higher than wild type, and antisense had closer

transcript levels to wild type. The antisense approach can induce a range of effects (Weigel and Glazebrook, 2002) and here an only very mild reduction in gene expression was observed. There was no full length transcript occurrence for knockouts indicating the disruption of the single copy gene in the genome. There seemed to be formation of abnormal RNA species in one knockout (Salk_118043) since there was a band in Salk_118043 line when amplification of near 5' end with 260 bp was done (Fig. 4B). When NAE amidohydrolase specific activity was measured in microsomes isolated from wild type, knockouts and transgenics *Arabidopsis* plants utilizing NAE12:0 and NAE18:2 as substrates, the activity profiles were found consistent to the patterns of AtFAAH transcript occurrence and/or abundance in these knockout and transgenic plants. There was no activity in the microsomes isolated from knockout plants supporting the disruption of single copy gene in the genome whereas the specific activity in microsomes isolated from overexpressor plants was above 5 fold higher than that of wild type (Fig. 5). These consistent results of enzymatic activities and transcript levels indicate that there is likely only one FAAH gene in *Arabidopsis* responsible for hydrolysis of NAEs. Also, two knockout lines with no enzymatic activity help to clarify the function of the gene *in planta*. Also, both lines with no transcriptions and no enzymatic activities indicate that phenotypes are not the result of multiple T-DNA inserts. Since T-DNA inserts in the AtFAAH gene were examined in both the lines but examination for multiple inserts were not performed. The enzyme activity was localized almost exclusively to microsomes

and was consistent with the same enzyme studied biochemically in cottonseeds (Shrestha et al., 2002).

From the biochemical evidence of NAE amidohydrolase enzyme activities gathered in cottonseeds, the specific activity was the highest during imbibed seeds and was consistent with depletion of NAEs *in vivo* and this is a period just proceeding or coincident with radicle emergence suggesting that NAE metabolism might act in the regulation of seed germination and postgerminative growth. Furthermore, work reported by Blancaflor et al. (2003) showed that NAE 12:0 selectively inhibited root elongation and increased radicle swelling of root tips, and reduced root hair numbers in *Arabidopsis* seedlings supported a potent lipid mediator role for NAEs in seedling growth.

The altered profiles of extractable AtFAAH enzyme activities in mutant and transgenic plants led to predictable differences in sensitivities of seedlings to exogenous NAE 12:0. The knockout plants did not have FAAH transcripts (full length cDNA) or enzymatic activities, and seedlings of these lines indeed were more sensitive to exogenous NAEs. Even in the absence of exogenous NAEs, seedlings of knockout lines showed 15-20 percent reduction in root elongation compared to wild type measured over 6 days postgerminate growth (Fig. 7), whereas overexpressor seedlings had accelerated root elongation compared to wild type (Fig. 10). These data collectively provide the evidence of NAE metabolism in proper regulation of plant growth and development. Apart from these growth phenotypes AtFAAH altered seedlings had different level of sensitivity to exogenous NAE 12:0. The exogenous NAE 12:0 causes reduction

in root elongation in wild type seedlings however the inhibition is higher in the knockout seedlings. Smaller concentration of NAE 12:0 is required for inhibition of radicle/root development in knockouts whereas higher concentration is required for wild type (Fig. 9). These results clearly indicate that knockout seedlings are more sensitive to exogenous NAE 12:0 than wild type seedlings. While overexpressor seedlings were not affected up to 20 μM and above this concentration there were certain levels of effect, whereas the levels of effect for knockouts were much severe (Fig. 10).

Substantial amounts of NAEs are present in desiccated seeds of varieties of species from different families including oil and non-oil seed (Chapman et al., 1999). NAE amidohydrolase is the enzyme responsible for hydrolytic degradation of all NAE including saturated and unsaturated species (Shrestha et al., 2002). It was presumed that endogenous NAE levels would be higher in these knockout seeds. In order to see if these NAE levels/types associated with any physiological/cellular changes, quantification and molecular species profile of NAEs in seeds and seedlings of wild type and two knockout lines were analyzed. As expected the total contents of NAEs in knockout seeds were higher than those of wild type. The NAE contents may vary during the storage of seeds and thus for comparison the seeds were from the same harvest time and were grown under the same condition. The molecular species of NAEs in the *Arabidopsis* seeds consisted mainly of C18, with most prevalent NAE species being the NAE 18:2 followed by NAE 18:1 and NAE 18:3, and NAE 12:0 and NAE 14:0 species present in lower quantities (Fig. 12A). It is possible that these different NAEs

found abundant and trace amounts may have different roles in physiological context and their levels are determined by formation and degradation in control by some mechanisms or environmental perceptions. For example, the role of NAE12:0 was found responsible for root elongation and also regulation of overall growth of the seedlings while NAE 14:0 seems to have a role of signal perception. Other NAEs may have indirect role for the same system like NAE18:2 competitively inhibit anandamide degradation by the amidohydrolase in animal system (DiTomaso et al, 1996; Maccarrone et al, 1998). Though further studies are necessary, it is tempting to speculate that individual NAE types have certain roles and signifies their amount in physiology. In contrast to the prediction, quantification of NAEs in *Arabidopsis* seedlings (96 h) showed no appreciable decline in NAE contents. This might be due to differences in NAPE/NAE metabolism rates as proposed in a model (Shrestha et al., 2002). Further, prediction that a change in AtFAAH expression would result in NAE contents in knockouts on comparison to wild type was not observed. It may be that the mechanisms operate somewhat differently in cottonseeds than in *Arabidopsis* seeds. More extensive studies are needed before a general mechanism for NAE regulation of seedling growth can be proposed however the development of these genetic resources characterized here will facilitate this long-term goal.

Further experiments may include: (1) a study of the effects of NAEs prevalent in seeds and seedlings particularly those of higher NAE content like NAE 18:2, NAE18:3 and NAE 18:1 on the phenotype of knockout seedlings; (2)

a study to check if another enzyme(s) affects levels of NAEs in the seeds and seedlings of knockouts. To test the latter hypothesis, an enzyme assay could be performed utilizing synthetic NAE as substrate and using enzyme source from homogenate fraction extracted from knockout seedlings. Since lipoxygenase is an alternative pathway for degradation of polyunsaturated NAEs in seeds and seedlings, its role especially in those plants with the NAE amidohydrolase pathway disrupted will help to understand its role. A time course experiment on specific activities of NAE amidohydrolase and lipoxygenase pathways was carried out in cottonseeds fractions (Shrestha et al., 2002). Similar experiments in *Arabidopsis* seeds and seedlings would help correlate the specific activities of NAE amidohydroalse, transcript levels of NAE amidohydrolase and NAE contents in the *Arabidopsis* system.

Materials and Methods

Chemicals

[1-^{14}C] Linoleic acid (53 mCi mmol^{-1} in ethanol) was purchased from PerkinElmer Life Sciences, and [1-^{14}C] lauric acid (53 mCi mmol^{-1} in ethanol) was from Amersham Biosciences. Specific types of NAEs were synthesized from respective radiolabeled FFA as described (Shrestha et al., 2002). The purity of the NAE substrates were >99.5%. Radio specificity activity was calculated from the original [1-^{14}C]-labeled FFA and adjusted accordingly with non-radiolabeled synthetic NAE produced by the same method.

Plant Material

Seeds of *Arabidopsis thaliana* L. Heynh. (Ecotype: Columbia) were surface-sterilized with 10% (v/v) ethanol and 10% bleach solution for 5 min each and were rinsed several times with sterile, deionized water. Individual seeds were planted on 0.8% phyta-agar with 0.5X Murashige and Skoog (MS) media (McCourt and Keith, 1998). For different treatments, a stock solution of 10 mM NAE 12:0 in 67% dimethyl sulfoxide (DMSO) was added prior to sterilization (autoclaving) to appropriate final concentration (usually up to 50 μM NAE 12:0). A similar stock of FFA 12:0 was used as a control specificity, and an equivalent amount of solvent was diluted into media as “solvent-only” control. The Petri dishes were placed at slanted position (approximately 30° from vertical) for better

observation of root growth, and were placed in a growth chamber with a 16 h light, 8 h dark cycle at 22 °C. The seedlings for detail root morphology were grown on 0.8% phyta-agar (Gibco) layered onto 62 mmX48 mm sterile cover slips as described (Blancaflor et al., 2003). Images of the radicle were captured using an SZX12 stereomicroscope (Olympus) equipped with a SPOT RT digital camera (Diagnostic Instruments, Sterling Heights, Michi., USA). Some root measurements and images were made at the Dr. Blancaflor lab, S. R. Noble Foundation, OK.

RNA Extraction

Total RNA was isolated from different organs of the plants, seeds, imbibed seeds (4 h) and seedling (96 h) following protocol of phenol/SDS method for plant RNA extraction (Dunn et al., 1988). In brief, approximately 100 mg fresh weight of each sample was harvested, ground to a fine powder in liquid nitrogen and transferred into an eppendorf tube containing 300 μL extraction buffer (stock: 0.2 M NaOAc, pH 5.5, 1% SDS, 10 mM EDTA), 200 μL phenol reagent (stock: 500 g phenol, 300 mL boiling 25 mM NaCl, 10 g Tris, 0.9 g 8-hydroxyquinoline), and 50 μL chloroform reagent (stock: 240 mL chloroform, 10 mL isoamylalcohol). After vortexing, the homogenate was centrifuged at 10, 000 g_{max} for 5 min at 4 °C. The aqueous phase was transferred to a new eppendorf containing 200 μL phenol reagent and 50 μL chloroform reagent, and repeated vortexing and centrifugation. The aqueous phase was transferred to a new eppendorf containing 250 μL chloroform reagent, vertexed and centrifuged at the same

speed for 10 min. The aqueous phase was precipitated in 2 M LiCl (by adding ¼ volume 10 M LiCl) at 4 °C overnight and then centrifuged at 13,000 g_{max} for 15 min. The pellet containing RNA was resuspended in 50 μL DEPC treated water. The total RNA was re-precipitated by adding 1/10 volume 10 M LiCl and 2.5 volume 100% EtOH at -70 °C for 15 min and then centrifuged at 13,000 g_{max} for 15 min followed by resuspending in 25 μL DEPC treated water. The total RNA samples were stored at -80 °C.

Real Time RT-PCR

Real time RT-PCR was performed in a Smart Cycler II (Cepheid) instrument with a real time one step RNA PCR assay kit (Takara Bio Inc.). The total reaction volume was 25 μL containing 2.5 μL 10 X "real time RNA PCR buffer", 5 μL 25mM $MgCl_2$, 2.5 μL 10 mM dNTP mixture, 0.5 μL "RNase inhibitor" (40 U/μL), 0.5 μL "AMV RTase XL" (5 U/μL), 0.5 μL "TaKaRa Ex Taq HS" (5U/μL), 0.5 μL of 20 μM each of gene specific primers. RNA template was included at 0.9 μg. The SYBR™ Green I Stain concentration was 0.25X. The total volume in the reaction was brought to 25 μL by adding RNase free dH_2O.

The reaction mixtures were subjected to the following RT-PCR condition: 50°C for 30 min, one cycle; 95°C for 4 min, one cycle; 94°C for 30 sec, 63°C for 30 sec, and 72°C for 90 sec for 40 cycles, followed by one cycle of melting curve of 60 °C to 95°C with 0.2 degree/sec. For internal standard, the real time RT-PCR condition was the same except annealing temperature was 60°C. The primers used for quantification of mRNAs of internal standard (ACT8) and the

gene of interest (AtFAAH) were: ACT8 forward (F) 5' - GTTAAGGCTGGATTCGCTGG – 3'; ACT8 reverse 5' – GTTAAGAGGAGCCTCGGTAAG – 3'; AtFAAH – F 5' - CCATCTCAAGAACCGGAGCATG – 3'; and AtFAAH - R 5' – GGTGTTGGAGGCTTGTCATAGC – 3'. The primers were chosen that span one intron of the genomic sequence to avoid false positive results arising from amplification of containing genomic DNA.

For the relative quantification of the AtFAAH gene expression a threshold cycle (C_T) method was employed. A C_T value represents a cycle number at which the fluorescence is first detected significantly above the background. Here, SYBR Green I Stain, a dye was utilized as an indicator of PCR product formation. SYBR dyes intercalate with double stranded DNA. Its fluorescence is undetectable when it is free but once bound to dsDNA, its fluorescence increases considerably. This way, PCR product formation during the cycling is detected as accumulation of double stranded DNA products occur. This dye is easy to use, however there is no specificity in this dye since this dye incorporates with all dsDNA and there is a risk of quantifying non specific PCR products. This problem can be overcome to a great extent by analyzing melting curves and separating products on agarose gels. Conditions were optimized such that only the single peaks of the melting curve of each PCR product were observed and were furthered confirmed by a band of correct size on 1% agarose gel. Amplification efficiencies of AtFAAH and ACT8 (internal standard) were tested using different template concentrations and approximately equal PCR efficiencies were obtained

(100% each). ACT8, a subclass of actin gene family was used as the internal reference (An et al., 1996).

Real Time RT-PCR Calculation

The comparative C_T method was used to relative quantify transcript level of AtFAAH in different plant parts and stages. Here, relative expression levels were calculated by comparing the least expression levels among the parts which in this case calibrator (or control) is stem. The C_T values of both AtFAAH and stem (calibrator) were normalized to ACT8 which was utilized as endogenous housekeeping gene. The gene expression relative in a particular tissue or organ in relative to the calibrator was evaluated using the expression $2^{-\Delta\Delta C_T}$ method (Giulietti et al., 2001; Livak & Schmittgen, 2001),

where $\Delta\Delta C_T = \Delta C_{T(sample)} - \Delta C_{T(reference)}$

Here, $\Delta C_{T(sample)}$ is the C_T value of AtFAAH for any sample normalized to ACT8 (internal standard) and $\Delta C_{T(reference)}$ is the C_T value of calibrator which in this case is stem, normalized to ACT8.

On determination of AtFAAH transcription levels in transgenics and mutants, C_T values of wild type (leaf) was used as calibrator for normalization.

The amplification efficiencies were measured for both RT-PCR products, AtFAAH and ACT8, and were found to be 100% efficient.

Homozygous T-DNA Mutants

Two T-DNA insertional mutants were identified among the publicly available T-DNA-tagged *Arabidopsis* insertional mutant lines (Salk_095108, and Salk_118043; Salk Institute Genomic Analysis Laboratory). M3 seeds of these lines were provided by the Arabidopsis Biological Resource Stock Center, Ohio State University and were germinated on kanamycin to identify mutant seedlings. Progeny from the selected plants were tested by PCR to confirm the insertion in the AtFAAH (At5g64440) gene and to identify homozygous individuals. The precise locations and orientations of the T-DNA inserts were confirmed by DNA sequencing of PCR products amplified with T-DNA and gene specific primers. The primers used were: SK08 LP: 5' – TGACATCTCTGACAAATGCGAAGA – 3'; SK08 RP: 5' – GGAAGCCGAGGAGATTTGCAG – 3'; SK08 LB: 5' – GCGTGGACCGCTTGCTGCAACT – 3'; SK43 LP: 5' – TTGCTTCATCTCTGGAAGATGCC – 3'; SK43 RP: 5' – CCTGAAATACAAGACAAATGTGGGA – 3'; and SK43 LB: 5' – GCGTGGACCGCTTGCTGCAACT – 3'. (SK08, Salk_095108; SK43, Salk_118043). PCR products were subcloned into pTrcHis2 and sequenced by UNT in-house facilities.

Construction of Transgenic Plants

Transgenic plants were generated at the Dr. Blancaflor lab, the Noble Foundation, OK. Overexpressor constructs consisted of AtFAAH fused with smGFP were cloned downstream of the CaMV35S promoter in sense orientation

into pCAMBIA1390. Anti-sense constructs had AtFAAH subcloned into pCAMBIA1390 in anti-sense orientation downstream from CaMV35S promoter. The constructs were introduced into *Arabidopsis* plants via *Agrobacterium* mediated transformation by floral dip methods (Clough and Bent, 1998) and the transgenic seedlings were selected on kanamycin.

Preparation of Microsomes

Cell fractions were prepared by differential centrifugation as described (Shrestha et al., 2002). In brief, whole shoots of 6-week-old *Arabidopsis* plants were chopped on ice in a homogenization medium containing 100 mM potassium-phosphate (pH 7.2), 10 mM KCL, 1 mM EDTA, 1 mM EGTA, and 400 mM sucrose, and tissue pieces were homogenized in a dounce tissue homogenizer. The homogenates were filtered through four layers of cheesecloth and centrifuged at 650 g_{max} (4°C) for 15 min (Sorvall RC 5C Centrifuge, SS 34 rotor, Sorvall, Newton, CT). The 650 g_{max} supernatant was centrifuged at 10,000 g_{max} (4°C) for 30 min in the same rotor. The resulting supernatant was centrifuged at 150,000 g_{max} (4°C) for 60 min in Sorvall 90 model ultracentrifuge (Ti45 rotor, Beckman Coulter, Fullerton, CA). Microsomes were resuspended in the same homogenization medium to a volume of 2 mL. Protein concentration was estimated using bovine serum albumin (BSA) as standard according to Bradford (1976).

In vitro *Enzyme Assay, Lipid Extraction and Analysis*

For enzymatic assays *in vitro*, 10 μL of 100 μM of [1-^{14}C]NAE substrate (20,000 dpm), suspended by sonication in 390 μL of 50 mM Bis-Tris propane buffer (pH 9.0). Reactions were initiated by adding 400 μg microsomal proteins (400 μL cell fraction voume). Reactions were incubated at 30°C for 60 minutes with shaking and the reactions were terminated by adding 2 mL of hot 2-propanol (70°C) to the aqueous reactions and were heated for 30 min at 70°C. Further lipid extraction in chloroform was based on Bligh and Dyer (1959); briefly, 1 mL of chloroform was added to the mixtures, and the lipid was extracted at 4°C overnight. One milliliter of chloroform and 2 mL of KCl (1 M) were added to induce phase separation. The aqueous layer was aspirated and organic layer was washed for two more times with 2 mL 1M KCl and one time with 2 mL deionized water (MilliQ UF plus). The organic layer was dried under nitrogen. The lipid types were separated on TLC (hexane:ethyl acetate:methanol, 60:40:5; v/v/v). Identification of the lipid products was performed by co-migration with known standards and quantification of radiolabeled lipids were performed by radiometric scanning (Biosan system 200 image scanner) as described previously (Shrestha et al., 2002).

NAEs Isolation and Profile Determination

NAE quantification was performed by isotope dilution mass spectrometry for extracts of desiccated seeds and seedlings (96 h). Two hundred milligrams of *Arabidopsis* seeds were crushed in a dounce tissue homogenizer (glass) in the presence of hot 2-propanol (70 °C) to inactivate any endogenous phospholipases

(Chapman et al., 1998). Once the seeds were finely ground, 50 ng each of standard deuterated NAEs (20 µL at 2.5 ng/µL each in chloroform) were added. The lipids were extracted by two phase separation into chloroform, filtered, and subjected to normal phase HPLC (22 X 250 mm Alltech Econosil 10 µm particle size preparative column; 2-propanol gradient in hexane at 4.0ml/min). The lipids fractionated with a linear gradient of 2-propanol in hexane as described (Chapman et al., 1999). A synthetic standard NAE 19:2 was used to monitor NAE retention time. The NAE-enriched HPLC fractions were collected (10:75 to 14:75 min), evaporated to dryness under N_2 gas. The completely dried lipid mixtures were derivatized in bis(trimethylsilyl)trifluoroacetamide (BSTFA) for 30 min at 50°C. The derivatized lipids were dried under N_2, reconstituted in 20 µL of hexane and analyzed by a GC (Hewlett-Packard [HP] 5890 series II) coupled to an MS (Hewlett-Packard [HP] 5970) for determination and quantification of NAEs. The capillary column in the GC was 30 m X 0.25 mm i.d. with a 0.25 µm film thickness; model DB-5.625, J&W Scientific, Folsom CA. The injector temperature was 260 °C and the oven temperature was programmed from 40 °C to 280 °C at 10 °C /min. This MS was equipped with an electron impact source (70 eV) and operated for ultimate sensitivity in the selective ion monitoring (SIM) mode. Standard curves and mass spectra were prepared using injected masses of 0.1-30 ng of synthetic NAE from each species (NAE 12:0, NAE 14:0, NAE 16:0, NAE 16:1$^{cis\Delta9}$, NAE 18:0, NAE 18:1$^{cis\Delta9}$, NAE 18:2$^{cis\Delta9,12}$, NAE 18:3$^{cis\Delta9,12,15}$, NAE 20:4$^{cis\Delta5,8,11,14}$ in the presence of 2.5 ng of each interal standard. Final

quantification of endogenous NAE species was calculated from the ratio of analyte (NAE) response to that of the corresponding internal standard.

A

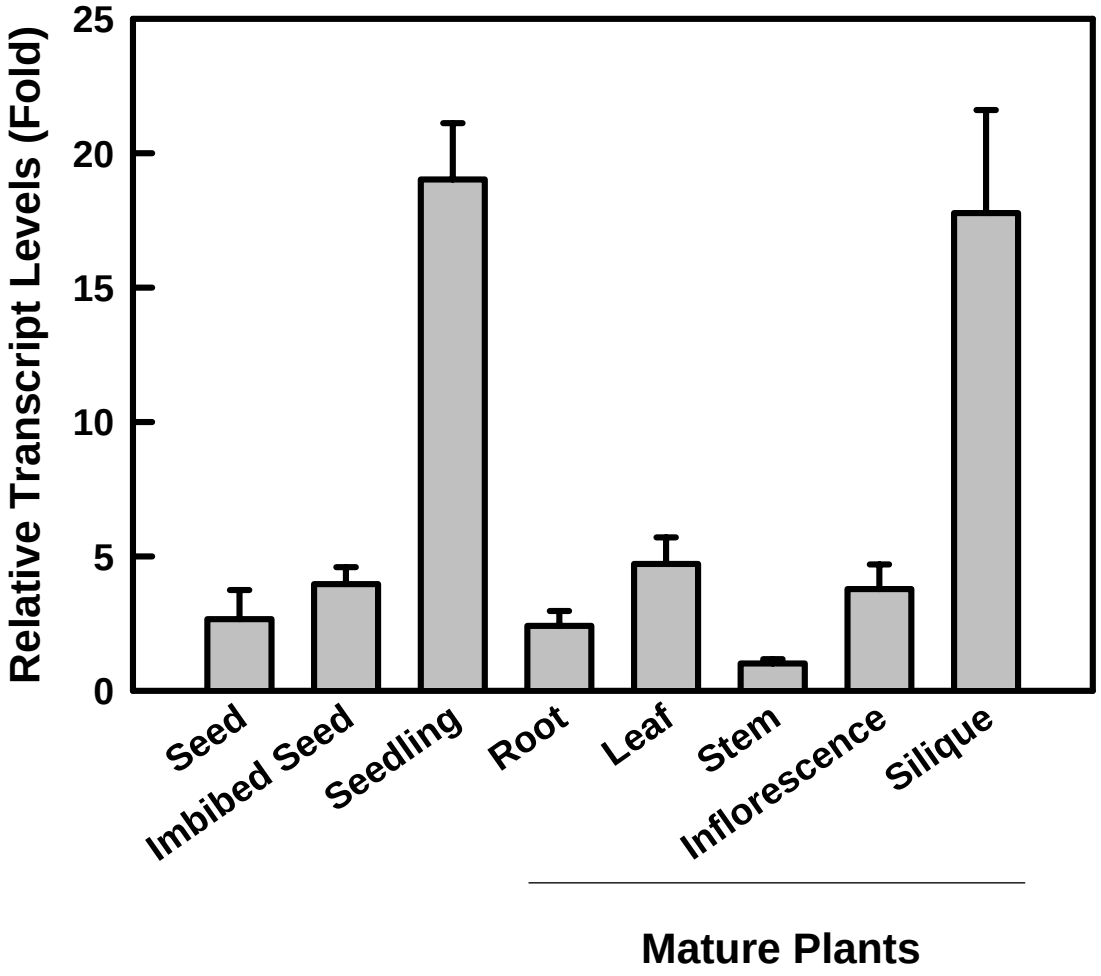
Relative Transcript Levels (Fold)
25
20
15
10
5
0
Seed
Imbibed Seed
Seedling
Root
Leaf
Stem
Inflorescence
Silique
Mature Plants

B

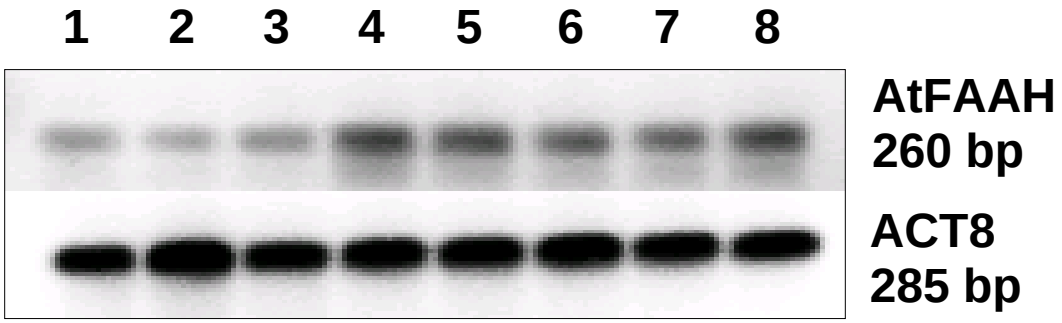
1 2 3 4 5 6 7 8
AtFAAH
260 bp
ACT8
285 bp

Figure 1. *Arabidopsis* FAAH mRNA transcript levels quantified in seeds, seedlings and different organs of mature *Arabidopsis* plants (6-week-old). Relative transcript levels were measured by quantitative real time PCR. ACT8 (a subclass of actin gene family) was used to normalize AtFAAH expression levels and were plotted relative to transcript levels in stems. The relative expression data were calculated following the $2^{-\Delta\Delta C}{}_T$ method as described (Livak and Schmittgen, 2001) (A). Data points represent means $\pm$ SD of triplicates of an experiment. Details of the method are described in "Materials and Methods". The purity of the specific PCR products were confirmed by melting curve analysis and also by right size single bands on electrophoresis with 1% agarose after completion of RT-PCR (B). The results showed an expression in all plant tissues however expression levels were different with highest levels quantified in seedlings (96 h) and siliques of six-week-old plants. 1, seeds; 2, imbibed seeds (4 h); 3, seedlings (96 h); 4, root; 5, leaf; 6, inflorescence; 7, stem; and 8, siliques.

Salk_095108

A

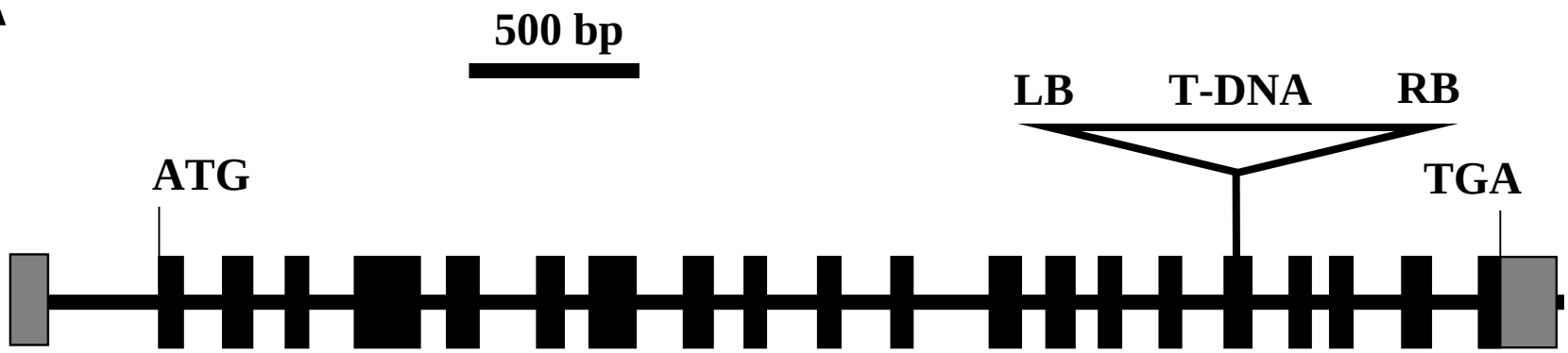

B

*TGACATCTCTGACAAATGCGAAGA*CATCCTTAAGCTCCT
ATCAAACAATCACGGTTGCAAAGTAATCTGAACATTTCA
GTACTTCTCTCTCAATCTACGGATACAATGTTTCAGCTA
CAATCTCTCTCTATTGTTTTCATTTCAGGTGGTGGAGAT
AGTGGTTCCTGAACTGGAAGAGATGCGTGCAGCCCATGT
TATTTCGATTGGGTCTCCAACACTGTCTTCTCTTACTCC
CTACTGTGAAGCTGGGTATGTCTCTAGCTCTATCATCTA
TGAACCAAATTAGAACTTTGGTTTAAGAACTCCCACATT
TGTCTTGTATTTCAGGAAAAATTCAAAACTAAGTTATGA
CACTCGTACCAGCTTTGCAATTTTCCGTTCATTCTCTGC
TTCAGACTATATCGCTGCTCAATGTCTTAGGTAAGCGGC
AATAGAATAATGCACTGTATGCGCAGCTTTCACTTTTGC
TTCTAAAGTCACAAGAGTAAACCAATATTGATAGAATTT
TTGTTGCAGGCGAAGATTGATGGAGTATCACTTGA**CGCT**
TAGACAACTTAATAACACATTGCGGACGTTTTTAATGTA
CTGGGGTGGTTTTTCTTTTCACCAGTGAGACGGGCAACA
GCTGATTGCCCTTCACCGCCTGGCCCTGAGAG*AGTTGCA*
GCAAGCGGTCCACGC

C

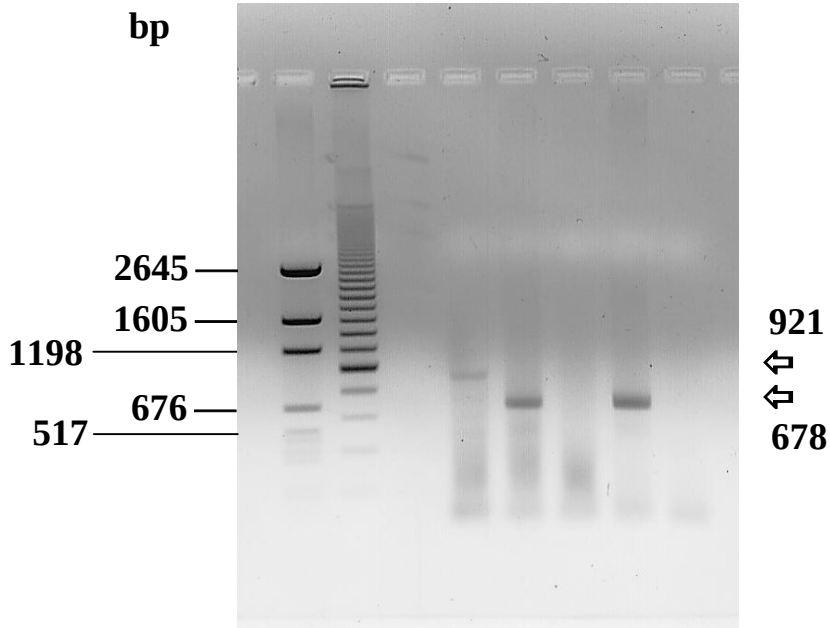

Salk_118043

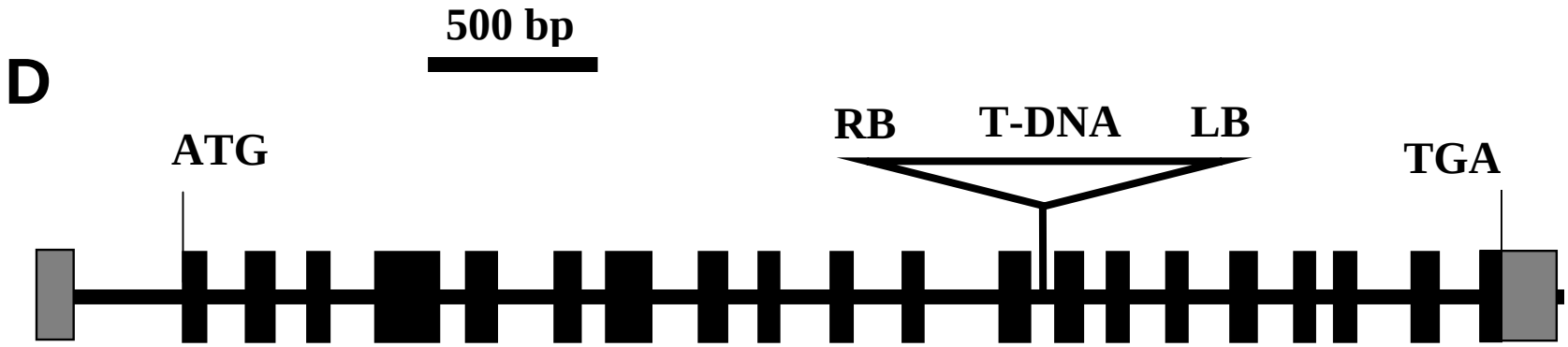

E

GCGTGGACCGCTTGCTGCAACTCTCTCAGGGCCAGGCGG
TGAAGGGCAATCAGCTGTTGCCCGTCTCACTGGTGAAAA
GAAAAACCACCCCAGTACATTAAAAACGTCCGCAATGTG
TTATTAAGTTGTCTAAGCGTCAATTTGTTTACACCACAA
TATATCCTGAGTTGGGATTTGTTATATCAGTGGCATATT
TAGTGCCTTGTTTTTATCCATGCAGTGGTTTAATGATGT
CAGTTCAAGTGACATCTCTGACAAATGCGAAGACATCCT
TAAGCTCCTATCAAACAATCACGGTTGCAAAGTAATCTG
AACATTTCAGTACTTCTCTCTCAATCTACGGATACAATG
TTTCAGCTACAATCTCTCTCTATTGTTTTCATTTCAGGT
GGTGGAGATAGTGGTTCCTGAACTGGAAGAGATGCGTGC
AGCCCATGTTATTTCGATTGGGTCTCCAACACTGTCTTC
TCTTACTCCCTACTGTGAAGCTGGGTATGTCTCTAGCTC
TATCATCTATGAACCAAATTAGAACTTTGGTTTAAGAAC
TCCCACATTTGTCTTGTATTTCAGG

F

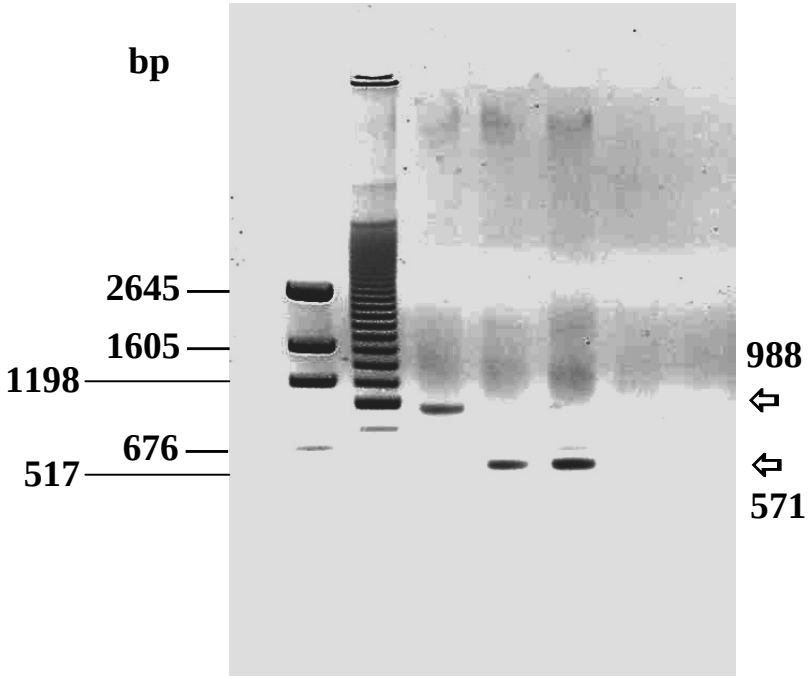

Figure 2. Isolation of T-DNA insertional mutants. (A) and (D) Scheme of the *Arabidopsis* NAE amidohydrolase (AtFAAH) gene with the organization of exon (boxes) and introns (lines) presented. The locations and orientation of the T-DNA insertion are shown. T-DNA insertion in Salk_118043 is in the 13th intron (A) and the T-DNA insertion in Salk_095108is in the 17th exon (D).

(B) and (E) Nucleotide sequences of PCR fragments amplified with T-DNA and gene specific primers. Bold type represents T-DNA sequence, underlined type represents genomic sequence and italic type (both bold and underlined) represents primers used to amplify the T-DNA insertion from genomic cDNA. The orientation of T-DNA insertion is opposite in two knockout lines; left end of T-DNA, left border (LB) is attached to 5' in Salk_118043 (B) and LB is attached to 3' end in Salk_095108 (E).

(C) and (F) DNA gel analysis of At5G64440 in mutants (Salk_095108, and Salk_118043) lines to confirm the zygosity of individuals. Wild type was used as control. The PCR products were amplified using three primers; one left end of T-DNA specific, LB and two gene specific primers. The primers used were designed in such a way that wild type bands were about 900 bp; knockout bands were above 410 but smaller than 900 by using http://signal.salk.edu/tdnaprimers.html. Homozygous would get one band while heterozygous would get both bands. Here, single bands were obtained indicating homozygous mutant plants. The size of mutant band was 571 for Salk_118043 (C) and 678 bp for Salk_095108 (F). The sizes of wild type were 988 bp and 921

bp in Salk_118043 and Salk_095108, respectively. DNA extraction and PCR was done using REDExtract-N-Amp Plant PCR kit (Invitrogen).

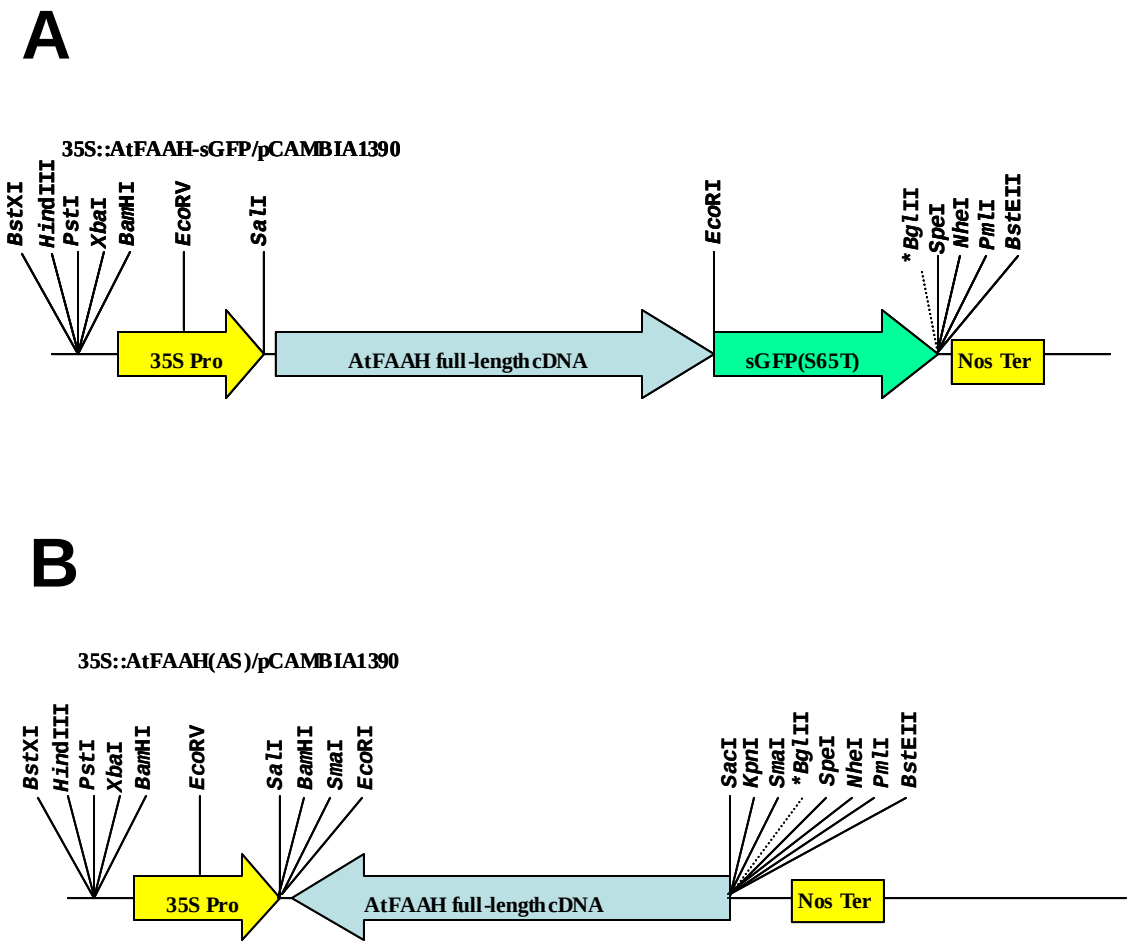

Figure 3. Expression construct used in transformation experiments (constructed at the Blancaflor lab, the S.R. Nobel Foundation, OK). (A) sense-expression construct includes the full-length AtFAAH cDNA fused to a cDNA encoding the soluble modified GFP (smGFP) fluorescent protein sequence at 3' end of AtFAAH cDNA inserted in sense orientation downstream of cauliflower mosaic virus (CaMV) 35S promoter. (B) Anti-sense expression construct includes the same cDNA encoding for NAE amidohydrolase (without fusion to smGFP

encoding cDNA) sequence inserted in anti-sense orientation downstream from the CaMV 35S promoter.

A

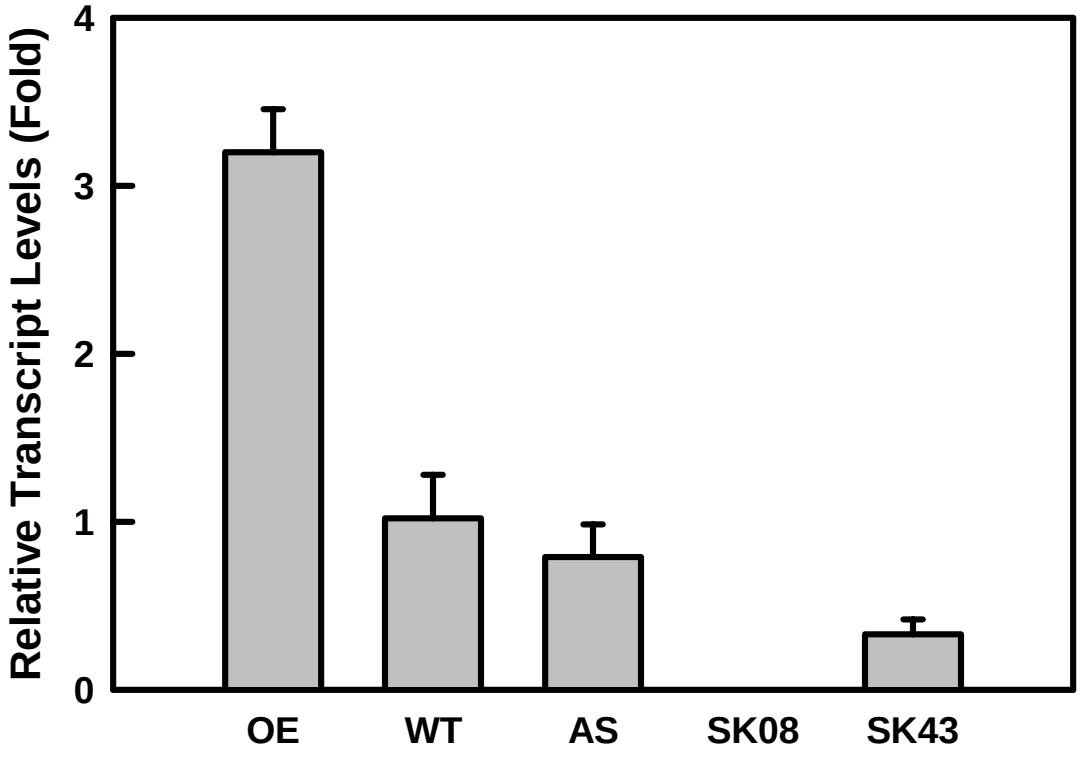
Relative Transcript Levels (Fold)
4
3
2
1
0
OE
WT
AS
SK08
SK43

B

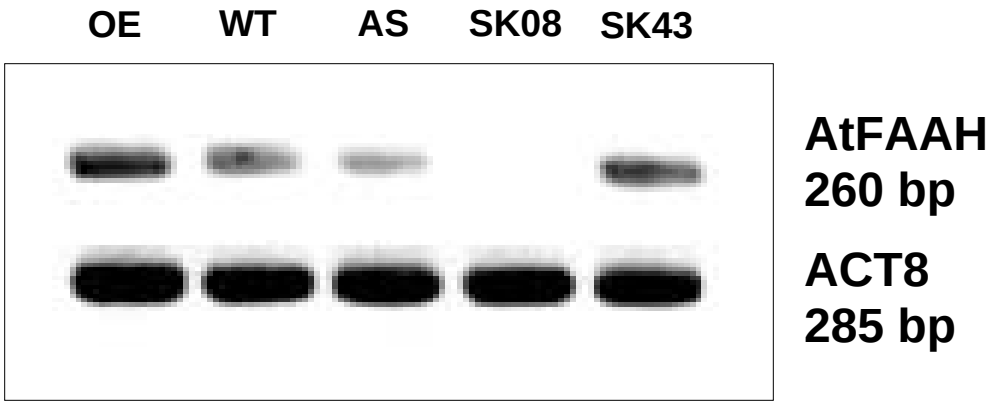
OE
WT
AS
SK08
SK43
AtFAAH
260 bp
ACT8
285 bp

C

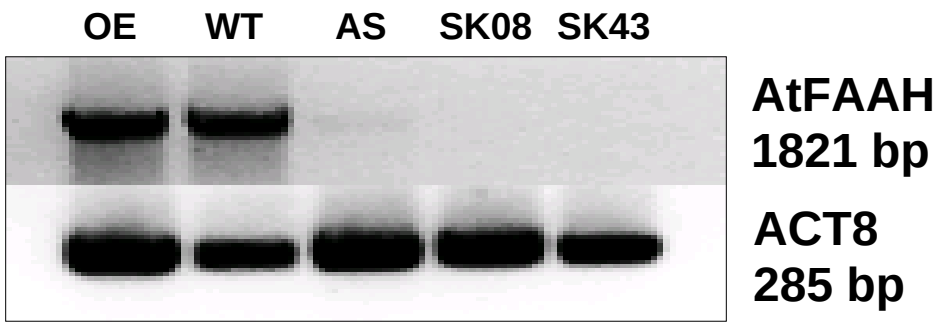

Figure 4. Comparison of *Arabidopsis* FAAH transcript occurrence and levels in transgenic, wild type and knockouts. The transcript levels were measured as described in “Materials and Methods”. For relative quantification in transgenics and knockouts, transcript levels in wild type (leaf) were used as a calibrator (A). Data points represent means ± SD of triplicates of an experiment. The purity of specific PCR products was confirmed by melting curve analysis and was further confirmed by right size single bands on electrophoresis gel (B). The transcript occurrence using RT-PCR of full length cDNA of AtFAAH was described (C). Transcription occurrence was found in all except knockouts. Knockout SK43 with T-DNA insertion in the intron showed some transcription though there was no full length transcript indicates the possibility of abnormal RNA species. OE, overexpressor; WT, wild type; AS, antisense; SK08, Salk_095108; SK43, Salk_118043.

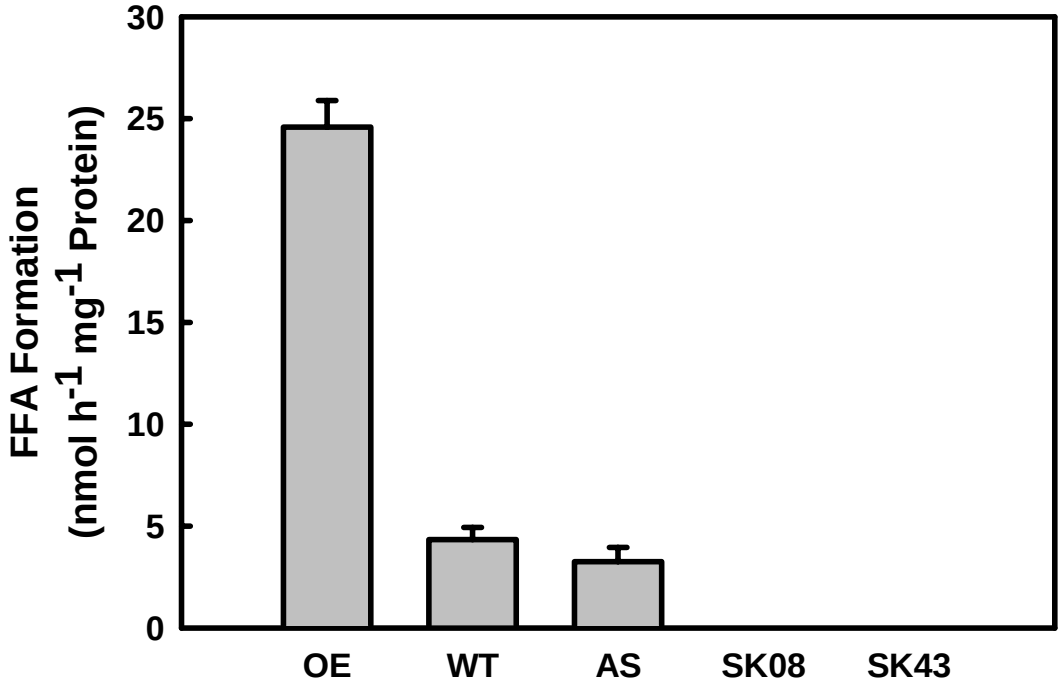

Figure 5. Altered FAAH activity in microsomes of transgenics and knockouts. The amount of free fatty acid formation was determined by incubating synthetic NAE 12:0 with 150,000 g_{max} (60 min) microsomes from 10,000 g_{max} (30 min) supernatant of shoots (6-week-old). The specific enzymatic activity in microsomes isolated from AtFAAH overexpressor plants was approximately five times higher than those from wild type. The AtFAAH fused to soluble modified GFP expressed heterologously in *E. coli* was capable of hydrolyzing NAEs (data not shown), indicating that the higher specific activity was due to the overexpressed GFP fused AtFAAH protein. Real time RT-PCR and fluorescent microscopy study confirmed the presence of introduced GFP fusion AtFAAH was stably transformed. There was nearly same amount of specific activity in the microsomes from antisense plants indicating only a mild effect. There was no

activity in the microsomes of both the knockouts. The bars represent the mean ± SD of 3 replicates, one experiment. A similar result was observed when NAE 18:2 was utilized as a substrate. OE, overexpressor; WT, wild type; AS, antisense; SK08, Salk_095108; SK43, Salk_118043.

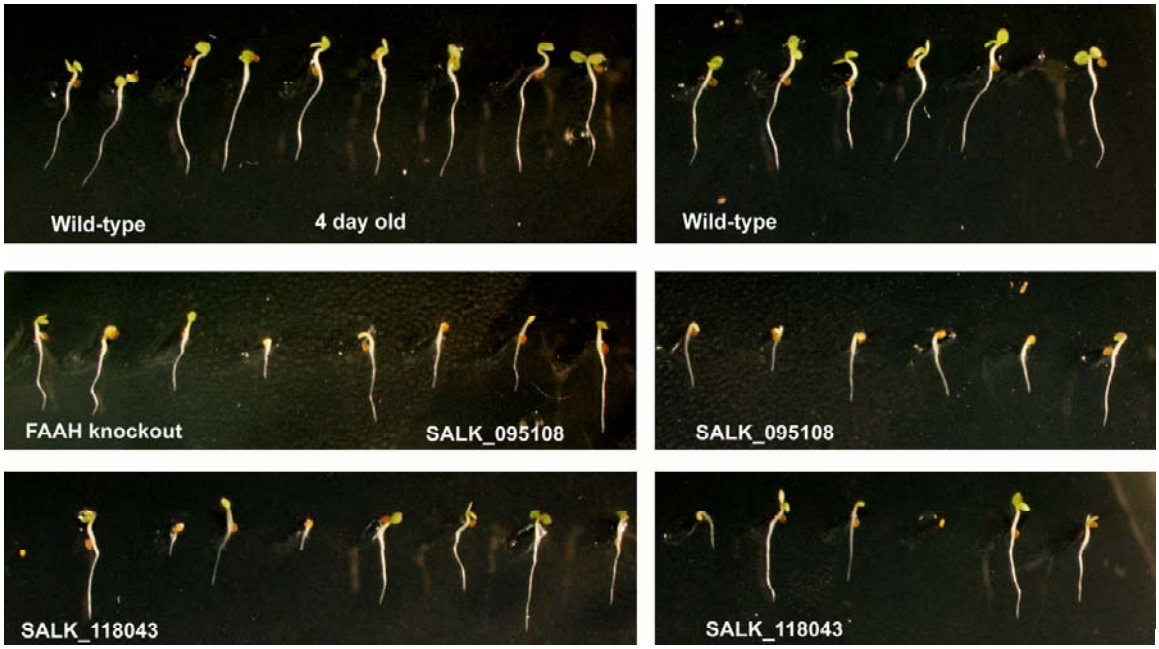

Figure 6. General morphological phenotypes of 4-day-old *Arabidopsis thaliana* seedlings. Wild type seedlings grew better - long radicle root length, cotyledons were developed (upper panel). T-DNA knockout seedlings with insertional of T-DNA in exon disrupting the gene responsible for AtFAAH production, were affected in radicle root length elongation and cotyledons were not as developed (middle panel) as in wild type. They generally appeared to be wild type plants treated with lower concentration of exogenous NAE 12:0 described by Blancaflor et al. (2003). T-DNA knockouts plants with T-DNA insertion in intron of At5g64440 (lower panel). The seedlings' phenotypes are similar between the two knockouts.

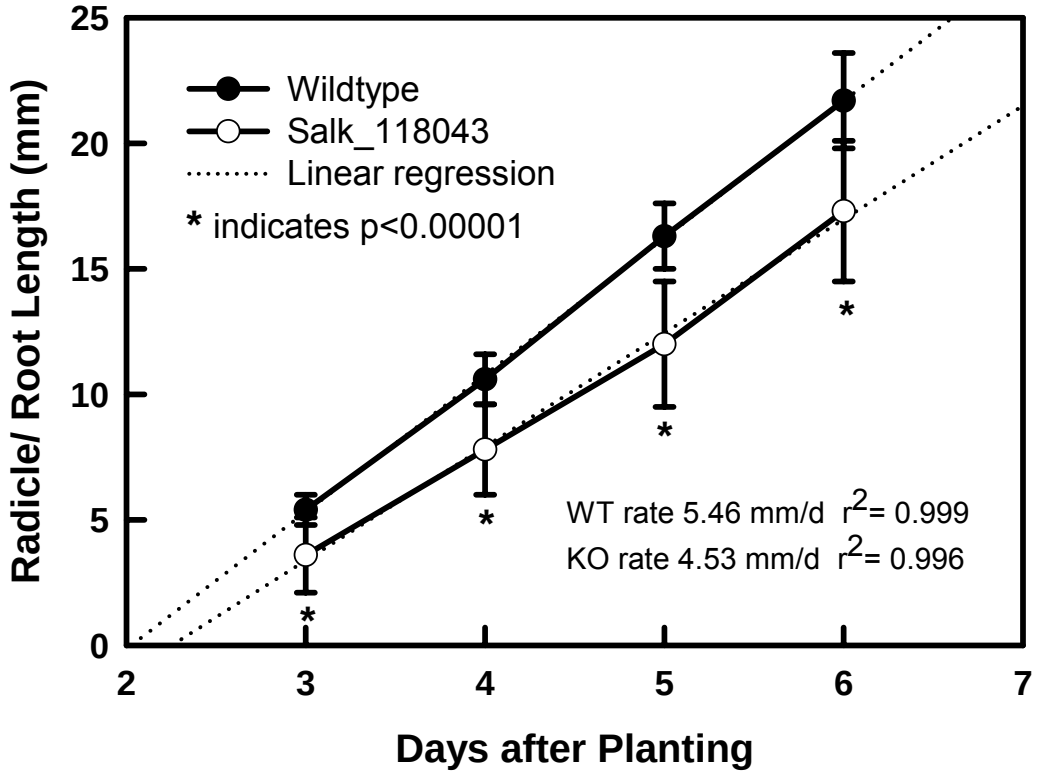

Figure 7. Measurements of radicle root lengths of wild type (WT) and knockouts (KOs). Seeds of wild type and knockouts were planted in plain phyta-agar medium and root length were measured everyday after germination. The primary root length and rate of elongation of WT was higher than knockouts in all the considered points with statistical significance $p<0.00001$ (student's t-test). Only one knockout (Salk_118043) was shown in the graph since the elongation of radicle root length was statistically not different when two knockouts (Salk_118043 and Salk_095108) were compared. The data points are means standard deviation from 20 or more seedlings and one representative of a typical experiment.

A

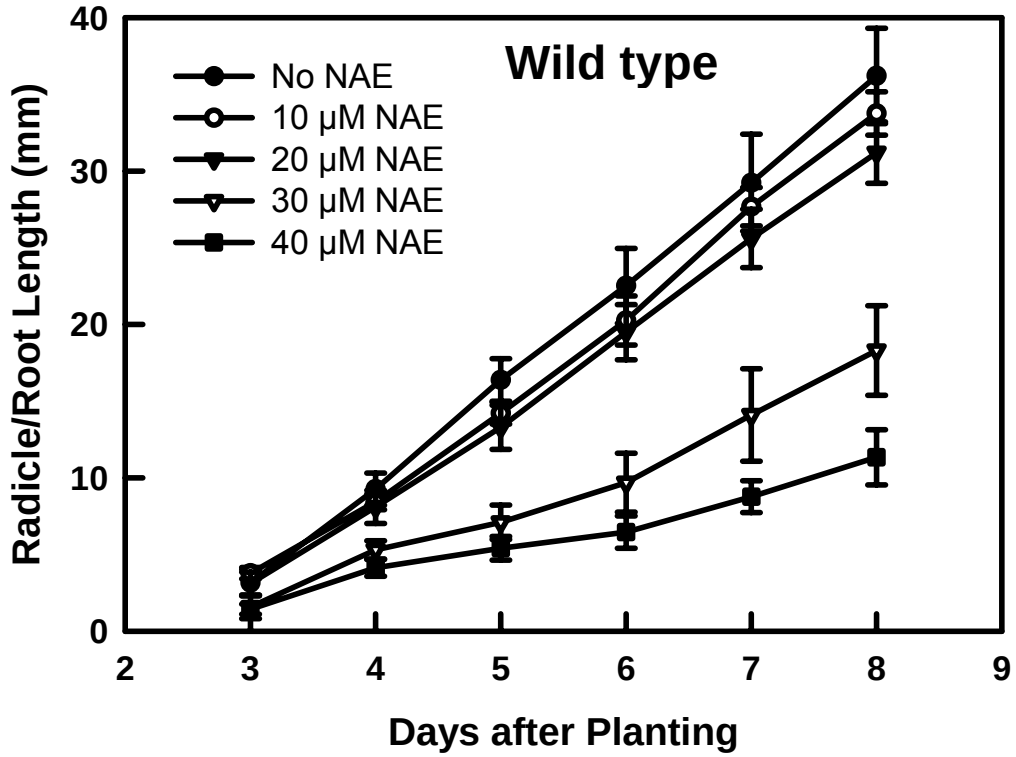
Wild type
No NAE
10 μM NAE
20 μM NAE
30 μM NAE
40 μM NAE
Radicle/Root Length (mm)
Days after Planting
0
10
20
30
40
2
3
4
5
6
7
8
9

B

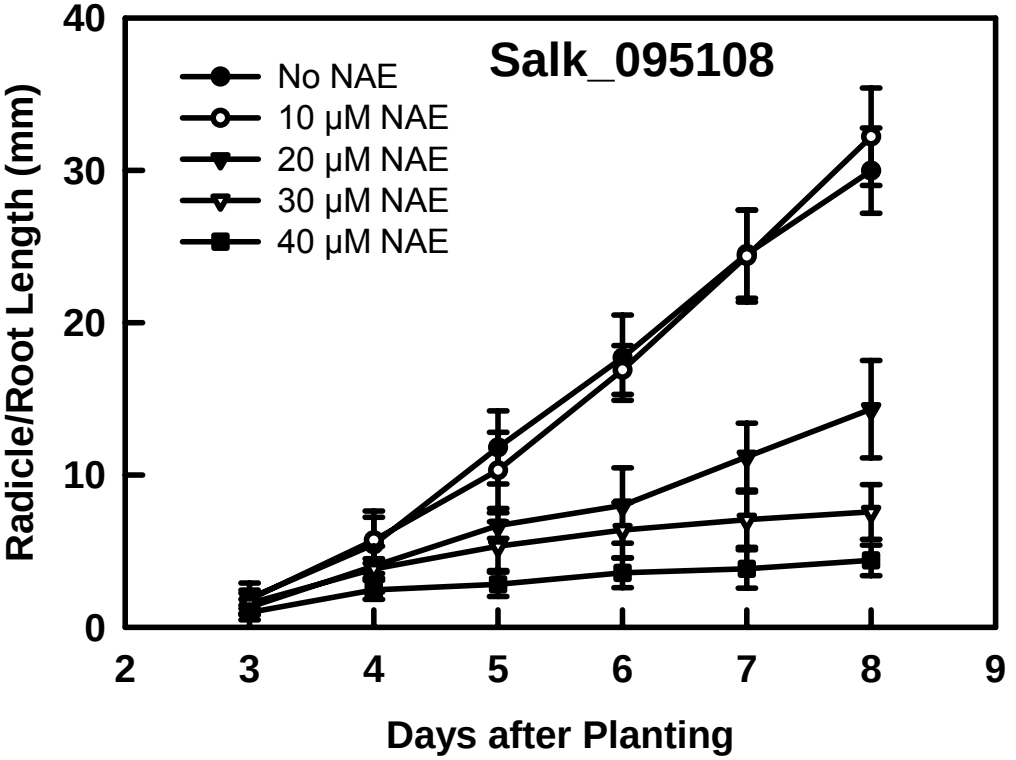
Salk_095108
No NAE
10 μM NAE
20 μM NAE
30 μM NAE
40 μM NAE
Radicle/Root Length (mm)
Days after Planting
0
10
20
30
40
2
3
4
5
6
7
8
9

C

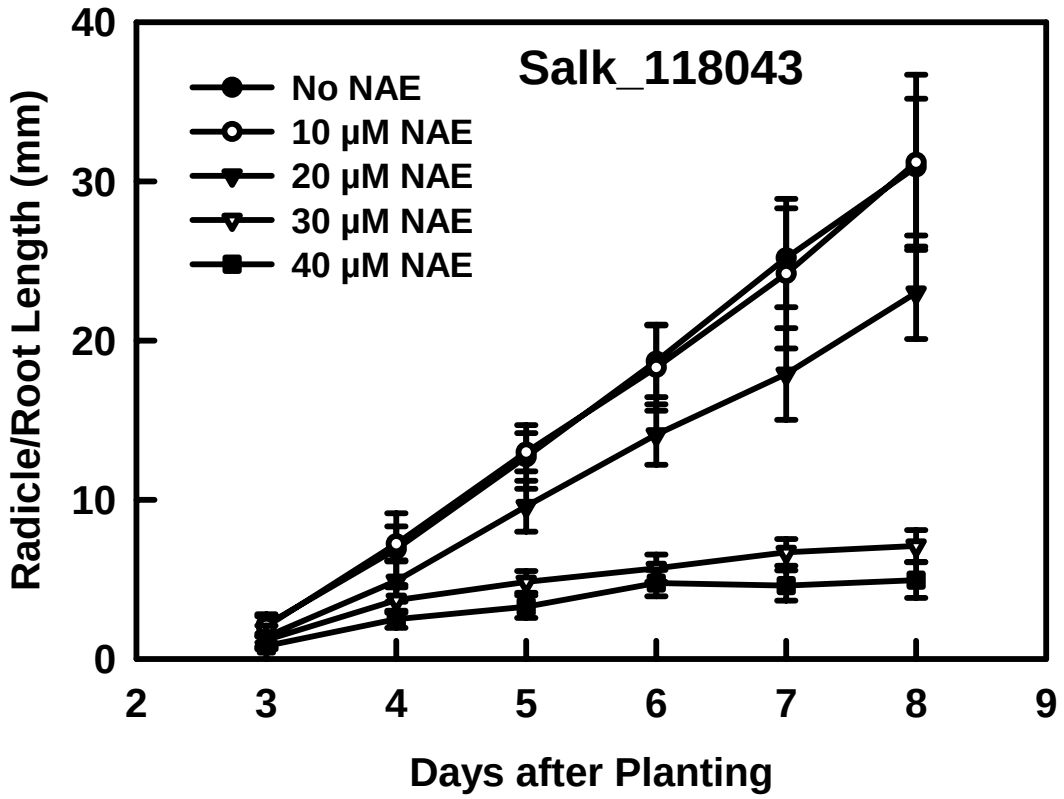

Figure 8. (A - C) Measurement of radicle root length elongation in different concentration of NAE 12:0. Seeds of *Arabidopsis* were planted on phyta-agar medium with different concentration of NAE 12:0 and lengths were measured everyday after germination from 3rd day to eight days. The effect of exogenous NAE, particularly higher representation after 30 µM was prominent both in wild types and knockouts, indicating that knockout plants were sensitive to exogenous NAE than wild type. Data points are means from 20 or more individuals and one representation of a typical experiment.

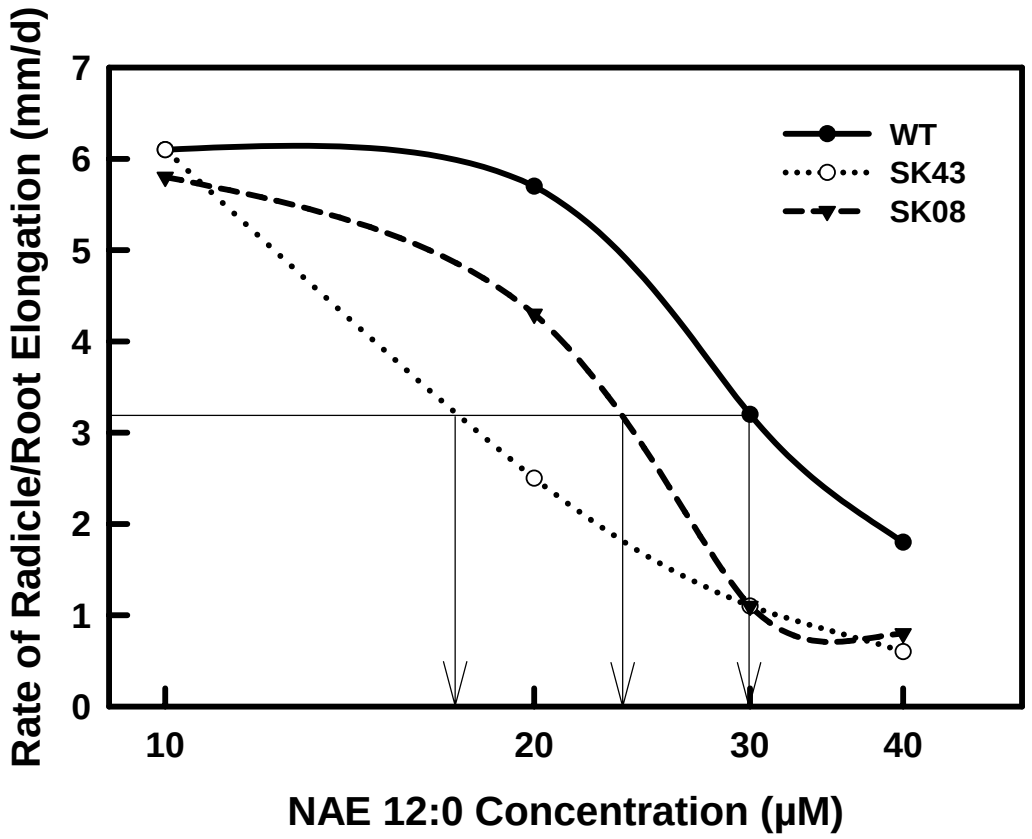

Figure 9. Dose response curve comparison was made among wild type (WT) and knockouts (SK08, Salk_095108; SK43, Salk_118043). The data of Figure 8 (A - C) were replotted here to compare the sensitivity of the plants to exogenous NAE 12:0. Rate of root elongation was plotted against NAE12:0 concentrations. The EC_{50} for knockouts were much lower than for the wild type indicating that the inhibition effect of exogenous NAE 12:0 is higher in knockouts than wild type.

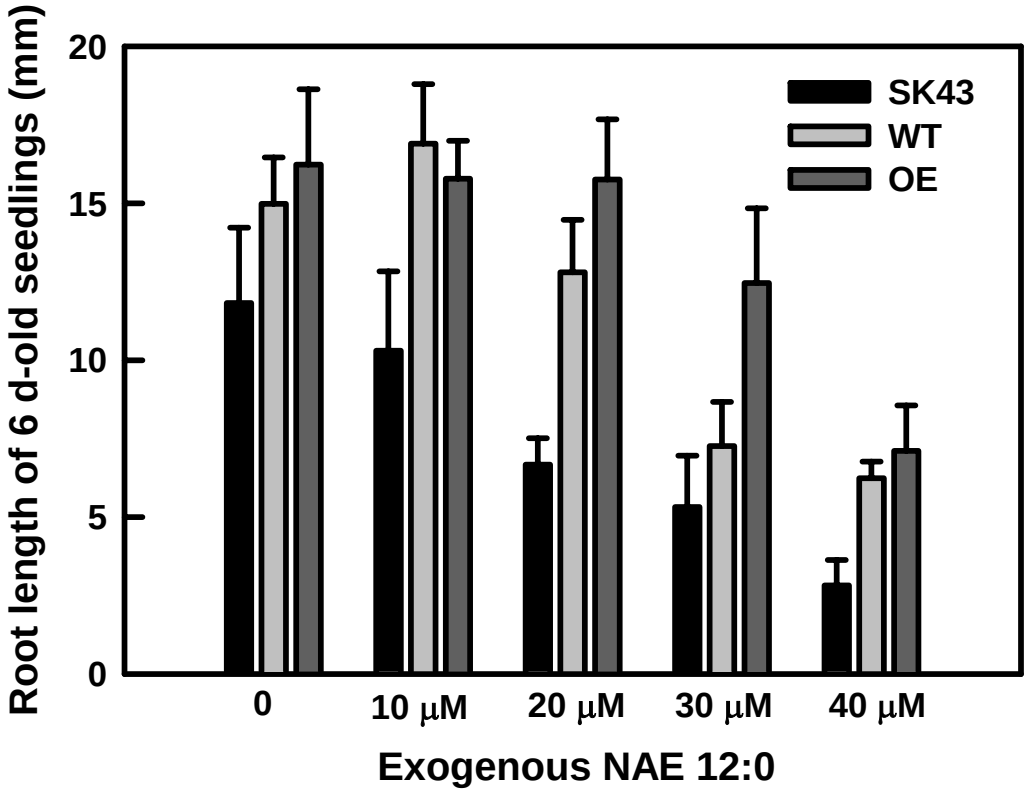

Figure 10. Measurements of root lengths of knockouts (SK43, Salk_118043), wild type (WT) and overexpressor (OE) seedlings inhibited by NAE 12:0 6-days after planting. Seedlings were germinated and grown under identical conditions and values represent the means ± SD of 20 seedlings at each treatment. Generally, there was dose-dependent inhibition in root length elongation of knockout and wild type and overexpressor, although the degree of inhibition was different.

Wild type

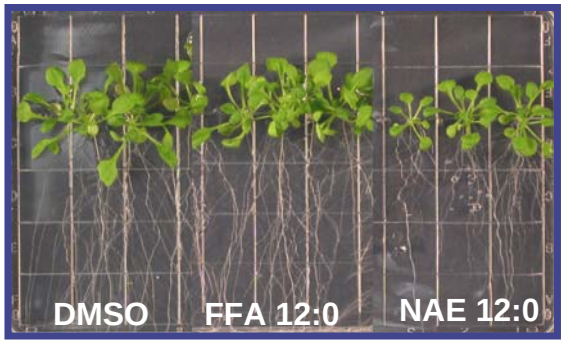

Antisense

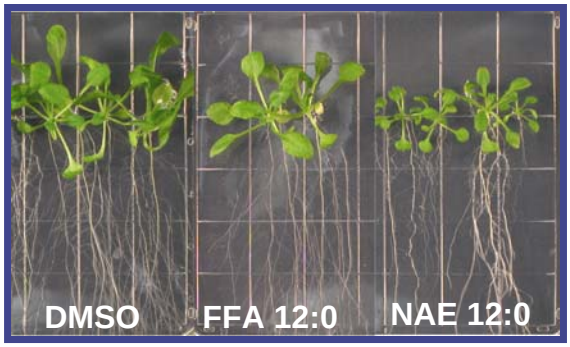

Salk_118043

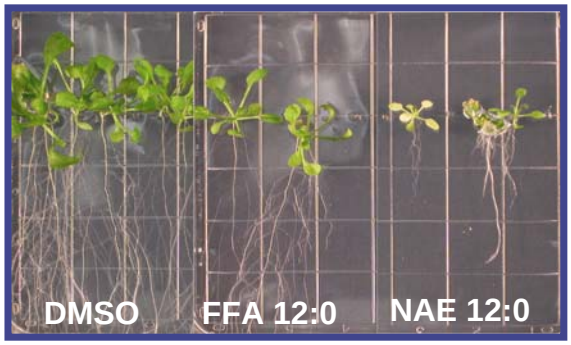

Salk_095108

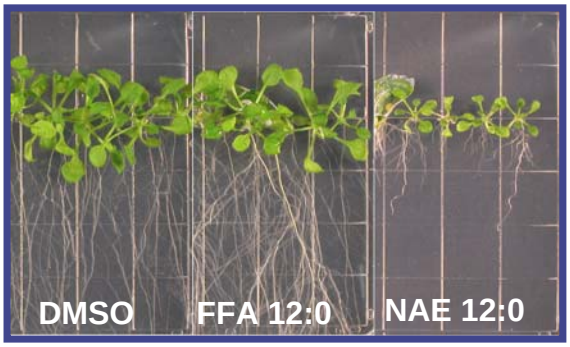

Ovevexpress

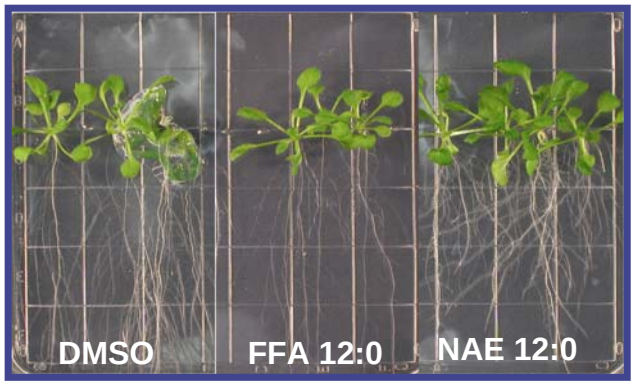

Figure 11. General morphological effect of NAE 12:0 (20 μM) on wild type, knockouts, antisense and overexpressor *Arabidopsis* seedlings is shown. There was moderate effect of NAE 12:0 on wild type seedlings. The effects were more sever to the knockout seedlings, both Salk_118043 and Salk_095108. The effect for antisense seedlings was not much different than wild type whereas there was no effect for overexpressor seedlings both in terms of root and cotyledonary developments.

A

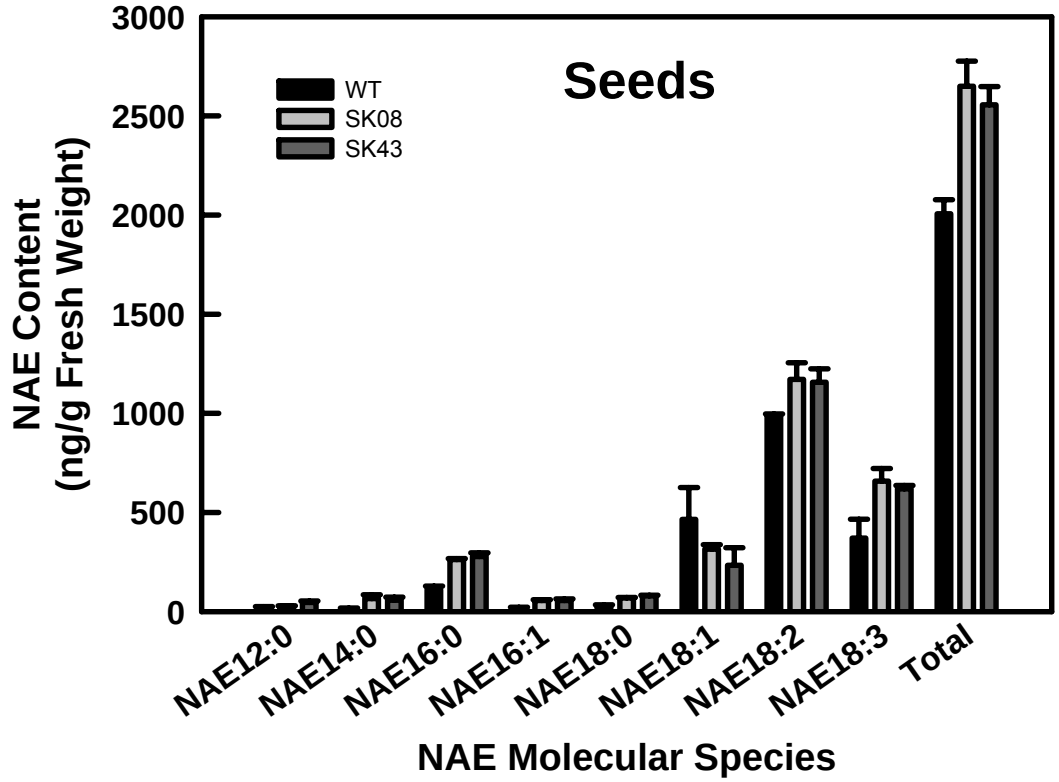
Seeds
WT
SK08
SK43
NAE Content
(ng/g Fresh Weight)
3000
2500
2000
1500
1000
500
0
NAE12:0
NAE14:0
NAE16:0
NAE16:1
NAE18:0
NAE18:1
NAE18:2
NAE18:3
Total
NAE Molecular Species

B

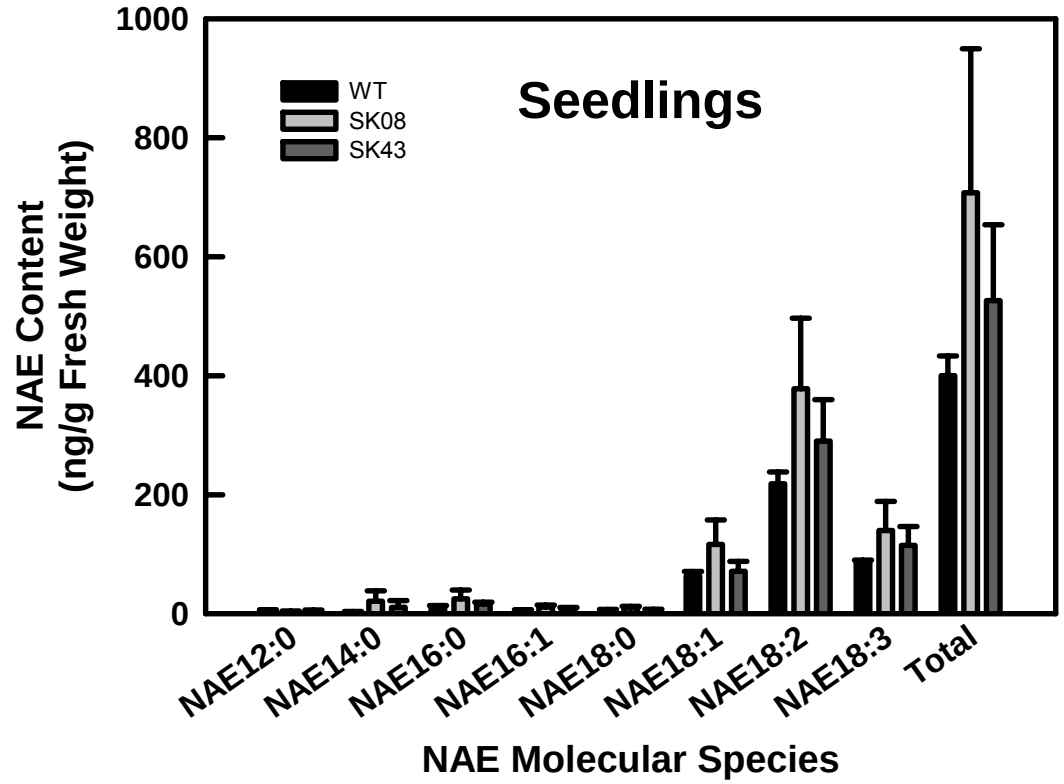
Seedlings
WT
SK08
SK43
NAE Content
(ng/g Fresh Weight)
1000
800
600
400
200
0
NAE12:0
NAE14:0
NAE16:0
NAE16:1
NAE18:0
NAE18:1
NAE18:2
NAE18:3
Total
NAE Molecular Species

Figure 12. Quantification of NAEs in seeds and seedlings by isotope-dilution mass spectrometry. (A) Quantification of NAEs in desiccated *Arabidopsis* seeds. Detected and quantified molecular species of NAEs and total NAE summed from the individual type in wild type (WT), Salk_095108 (SK08) and Salk_118043 (SK43), respectively. (B) Quantification of NAEs in *Arabidopsis* seedlings (96 h). Detected and quantified molecular species of NAEs and total in wild type, SK08 and SK43, respectively. Bars represent the means $\pm$ SD of three independent extractions and fractionations.

Acknowledgments

I would like to thank Dr. Blancaflor's lab, Samuel Roberts Noble Foundations, OK for generating transgenic *Arabidopsis* plants, and making some seedling root measurements. I thank Dr. Barney Venables, University of North Texas for helpful advice regarding NAE quantification.

Literature Cited

An Y-Q, McDowell JM, Huang S, McKinney EC, Chambliss S, Meaghe RB (1996) Strong, constitutive expression of the *Arabidopsis* ACT2/ACT8 actin subclass in vegetative tissues. Plant J 10: 107-121

Austin-Brown S, Chapman KD (2002) Inhibition of phospholipase Dα by N-acylethanolamines. Plant Physiol 129: 1892-1898

Berdyshev EV, Schmid PC, Krebsbach RJ, Hillard CJ, Huang C, Chen N, Dong Z, Schmid HH (2001) Cannabinoid-receptor-independent cell signaling by *N*-Acylethanolamines. Biochem J 360: 67-75

Blancaflor E, Hou G, Chapman KD (2003) Elevated levels of *N*-lauroylethanolamine, an endogenous constituent of desiccated seeds, disrupt normal root development in *Arabidopsis thaliana* seedlings. Planta 217: 206-217

Bligh EG, Dyer WG (1959) A rapid method of total lipid extraction and purification. Can J Biochem Physiol 37: 911-917

Bradford MM (1976) A rapid and sensitive method for quantification of microgram quantities of protein utilizing the principle of protein-dye bind. Anal Biochem 72: 248-254

Chapman KD (2000) Emerging physiological roles for *N*-acylphosphatidylethanolamine metabolism in plants: signal transduction and membrane protection. Chem Phys Lipids 108: 221-230

Chapman KD, Tripathy S, Venables BJ, Desouza AD (1998) *N*-Acylethanolamines: formation and molecular composition of a new class of plant lipids. Plant Physiol 116:1163-1168

Chapman KD, Venables BJ, Markovic R, Blair RW, Bettinger C (1999) *N*-Acylethanolamines in seeds: quantification of molecular species and their degradation upon imbibition. Plant Physiol 120: 1157-1164

Clough SJ, Bent A (1998) Floral dip: A simplified method for *Agrobacterium*-mediated transformation of *Arabidopsis thaliana.* Plant J 16: 735-743

Cravatt BF, Demarest K, Patricelli MP, Bracey MH, Giang DK, Martin BR, Lichtman AH (2001) Supersensitivity to anandamide and enhanced endogenous cannabinoid signaling in mice lacking fatty acid amide hydrolase. Proc Natl Acad Sci 98:9371-9376

Dunn K, Dickstein R, Feinbaum R, Burnett BK, Peterman TK, Thoidis G, Goodman HM, Ausubel FM (1988) Developmental regulation of nodule-specific genes in alfalfa root nodules. Mol Plant Microbe Interact 2: 66-74

DiTomaso E, Beltramo M, Piomelli D (1996) Brain cannabinoids in chocolate. Nature (Lond) 382: 677-678

Giulietti A, Overbergh L, Valckx D, Decallonne B, Bouillon R, Mathieu C (2001) An overview of real-time quantitative PCR: applications to quantify cytokine gene expression. Methods 25:386-401

Livak KJ, Schmittgen TD (2001). Analysis of relative gene expression data using real-time quantitative PCR and the $2\text{-}2^{-\Delta\Delta C_T}$ method. Methods 25: 402-408

Maccarrone M, Van der Stelt M, Rossi A, Veldink GA, Vliegenthart JFG, Agro AF (1998) Anandamide hydrolysis by human cells in culture and brain. J Biol Chem 273: 32332-32339

McCourt P, Keith K (1998) Sterile techniques in *Arabidopsis.* In: *Arabidopsis* protocols (Eds Martenz-Zapater JM, Salinas J) Humana Press Inc., NJ 07512. 82: 13-17

Pertwee RG (2001) Cannabinoid receptors and pain. Prog Neurobiol 63:569-611

Schmid HHO, Schmid PC, Nataranjan V (1990) *N*-Acylated glycerophospho-lipids and their derivatives. Prog Lipid Res 29: 1-43

Schmid HHO, Schmid PC, Nataranjan V (1996) The *N*-acylation-phosphodiesterase pathway and cell signaling. Chem Phys Lipids 80:133-142

Shrestha R, Dixon RA, Chapman KD (2003) Molecular identification of a functional homologue of the mammalian fatty acid amide hydrolase in *Arabidopsis thaliana*. J Mol Biol 278: 34990-34997

Shrestha R, Noordermeer MA, Van der Stelt M, Veldink GA, Chapman KD (2002) *N*-Acylethanolamines are metabolized by lipoxygenase and amidohydrolase in competing pathways during cottonseed imbibition. Plant Physiol 130: 391-401

Tripathy S, Venables BJ, Chapman KD (1999) *N*-Acylethanolamines in signal transduction of elicitor perception: attenuation of alkalinization response and activation of defense gene expression. Plant Physiol 121: 1299-1308

Weigel D, Glazebrook J, ed (2002) *Arabidopsis* – A laboratory manual. Cold Spring Harbor Laboratory Press, New York.

SUMMARY AND SIGNIFICANCE

There are various NAEs in mammals and regulation of NAE levels in mammalian cells is associated with important physiological processes. For example, anandamide, a type of NAE in mammalian brain tissue, is an endogenous ligand for cannabinoid receptor and modulates neurotransmission. It also acts as an endogenous analgesic (Pertwee, 2001). Oleamide, a primary amide induces sleep in animals (Cravatt et al., 1995). These physiological processes are regulated by both receptor-dependent and receptor-independent pathways (Berdyshev et al., 2001). These bioactive molecules terminate their signaling function upon hydrolysis by fatty acid amide hydrolase (FAAH).

In plants, NAE profiles are different in different tissues, and NAE levels change rather dramatically in response to environmental stimuli or with a change in developmental stage. In leaves NAE 12:0 and NAE 14:0 are produced and appear to function in plant defense signaling (Tripathy et al., 1999), whereas NAE 18:2 and NAE 16:0 are prevalent in desiccated seeds and decrease with seed imbibition (Chapman et al., 1999). Regulation of NAE levels likely is important for normal growth and development and responses of plants to stresses. Understanding the pathways involved in NAE metabolism and the characteristics of enzymes in these pathways will be important to unraveling the physiological functions of these lipid metabolites in plants. Moreover manipulation of expression of NAE metabolism enzymes will help to test ideas

about NAE function. One hypothesis is that in plants, NAEs are negative regulators of seed germination and their levels need to be depleted during imbibition for synchronous events associated with cell division and expansion.

The two abundant NAEs in desiccated seeds, *N*-palmitoylethanolamine (NAE 16:0) and *N*-linoleoylethanolamine (NAE 18:2), were used as representatives of NAEs to evaluate their metabolic fate in imbibing seeds and subcellular localization of those enzymes responsible for catabolism of these substrates. The results suggested that endogenous NAEs in desiccated seeds were metabolized by two pathways – one producing free fatty acids (FFAs) and other likely producing NAE-derived oxylipins. The presumed enzyme responsible for NAE-oxylipin formation was distributed both in membrane and cytosol-enriched fractions, whereas the enzyme responsible for FFA formation was localized almost exclusively to membranes. The concentration dependent effect of two mammalian LOX inhibitors (eicosatetraynoic acid and nordihydroguaiaretic acid) indicated the involvement of lipoxygenase (LOX) on oxylipin formation. GC/MS analysis identified the putative NAE oxylipins as α-ketols of 13-hydroperoxy NAE (12-oxo-13-hydroxy-*N*-(9Z)-octadecenoylethanolamine) demonstrating that NAE 18:2 was metabolized by 13-LOX (and 13-AOS) in extracts of imbibed cottonseeds raising the possibility that a new class of oxylipins may be involved in seed germination. Phenylmethylsulfonyl fluoride, a serine protease inhibitor inhibited the production of FFA from NAE 18:2 and NAE 16:0 in concentration dependent manner suggesting the involvement of an amidohydrolase. By contrast there was only little inhibition by arachidonyl

trifluoromethyl ketone (ATMK), a potent anandamide analog mammalian inhibitor. The difference in sensitivity to ATMK may indicate a different property of cottonseed NAE amidohydrolase or may simply be a reflection of the lack of arachidonyl fatty acid derivatives in higher plant tissues.

The LOX activity in cytosol-enriched fraction was highest at 8 h after commencing imbibition and the activity remained at this level throughout the first 24 h of postgerminative growth. These results indicate that metabolism of NAEs is most active during seed imbibition, just prior to and during seed germination (12-18 h after commencing imbibition), and well before the period of lipid mobilization (24-48 h after commencing inhibition; Chapman and Sprinkle, 1996) for postgerminative seedling growth. Radiotracer experiments with imbibing seeds showed consistent results with those obtained *in vitro*. The results of these biochemical studies indicated that there are two pathways capable of metabolizing NAEs in seeds - a LOX-mediated pathway selective for unsaturated NAEs and a NAE amidohydrolase activity, which utilizes both saturated and unsaturated NAEs, and forms the basis for work described in chapters 2 and 3.

My efforts in chapter two were to identify and isolate plant DNA sequences that encode for NAE amidohydrolase responsible for hydrolyzing NAEs (both saturated and unsaturated) into respective FFAs and ethanolamine. In animal systems, fatty acid amide hydrolase (FAAH, E.C. 3.5.1.4), a member of the amidase signature (AS) family, acts on NAEs to produce FFA and ethanolamine, terminating NAE signaling function. Mammalian FAAH enzymes have a conserved stretch of approximately 130 amino acids (Patricelli and Cravatt,

2000) containing a Ser/Ser/Lys catalytic triad. Taking these conserved residues in the amidase signature consensus sequence into consideration, several plant orthologs were identified computationally. Candidate plant orthologs of mammalian FAAH were identified through searches of *Arabidopsis thaliana*, *Medicago truncatula* and cotton DNA databases assembled at TIGR.org. The reason for choosing cotton is because much of the research work done in this lab has been on physiological and biochemical information of NAPE metabolism in seeds and seedlings of this plant species. The reasons for choosing the other two plant species in addition to cotton are because of extensive genomic resources available to date. The *Arabidopsis* genome provides information on full-length predicted proteins. This species is ideal for testing FAAH due to simplicity in transformation and availability of various mutant lines.

The enzyme responsible for NAE hydrolysis in mammals has been identified at the molecular level, and although an analogous enzyme activity was identified in microsomes of imbibed cottonseeds, no molecular information was available for this enzyme in plants. Here in chapter two, the identification, the heterologous expression (in *E. coli*) and the biochemical characterization of an *Arabidopsis thaliana* FAAH homologue were reported. The cDNA was predicted to encode 607 amino acids with 18.5 percent identity of the putative amino acid sequence with rat FAAH over the entire length. However, the residues (Lys-142, Ser-217, Ser-218, Ser-241 and Arg-243) determined to be important for FAAH catalysis were conserved in this protein sequence. It has a single transmembrane domain near the *N*-terminus similar to that of the rat FAAH

protein. The cDNA was expressed in *E. coli* as an epitope/His-tagged fusion protein and the expressed protein indeed hydrolyzed a range of NAEs to their respective FFAs (and ethanolamine). Kinetic parameters for the recombinant *Arabidopsis* protein were consistent with those properties of the rat FAAH supporting identification of this *Arabidopsis* FAAH as a mammalian FAAH homologue. Also, the recombinant protein was consistent with the enzyme characterized previously in plants (Chapter I) based on kinetic parameters and inhibitor studies. Collectively these data now provide support at the molecular level for a conserved mechanism between plants and animals for the metabolism of NAEs.

After molecular identification of a functional homologue of the mammalian FAAH from *Arabidopsis thaliana*, the tissue-specific distribution and developmental appearance of the enzyme were determined. The expression of the transcript was found in all the plant parts, seeds and seedlings with varied levels. The expression levels were the least in stem whereas the highest in siliques and seedlings. Manipulation of the FAAH gene expression in *Arabidopsis thaliana* would help to begin to assess the physiological role of this metabolic pathway in seed germination was another objective in this report (Objective 3). Recent molecular genetic evidence with FAAH knockout mice revealed an increase of NAE levels and the mice were supersensitive to endogenous cannabinoid lipid mediators (Cravatt et al., 2001) indicating a role for FAAH in the regulation of NAE levels for normal physiology. The mechanism and regulation of NAE levels in plants is not as clear as in animal systems but it

is likely that NAE needs to be formed and degraded in a timely fashion to regulate a number of normal physiological processes. Gene function was explored by insertional mutagenesis (gene knockout) and a putative knockouts were identified among the publicly available T-DNA tagged *Arabidopsis* insertional mutant lines. M3 seeds of two lines were geminated on kanamycin to identify mutant seedlings. Progeny from selected plants were tested by PCR to confirm the insertion in At5g64440 gene, and identified homozygous individuals. In addition to the knockouts, transgenic plants were also tested for the role of the gene. In order to confirm the role the expression of the gene *in planta*, microsomes were isolated from wild type, knockouts and transgenic plants were subjected to enzymatic activity utilizing NAE 12:0 and NAE 18:2 as substrates. The activity profiles were consistent with the pattern of FAAH expression in these mutants and transgenic plants such that microsomes isolated from knockouts had no activities whereas those from overexpressors had several fold higher activity than those of wild type. Homozygous mutants exhibited seed germination, seedling growth and root development phenotypes. The measurements of root elongation showed the rate reduction in knockouts by 15-20% compared to wild type. While the cotyledon size was lager in the overexpressor seedlings than those of wild type. The phenotypes were more dramatic in the presence of exogenous NAE 12:0. The mutant seedlings were more sensitive to exogenously applied NAE 12:0 than wild type and overexpressor. For example, NAE dose-dependent reduction in primary root length was measured for seedlings. The concentration of exogenous NAE 12:0

that effectively reduced the rate of primary root elongation to half of that of untreated seedlings (EC_{50}) was substantially lower for T-DNA mutants. On the other hand, transgenic seedlings overexpressing the NAE amidohydrolase enzyme showed noticeably greater tolerance than that of the wild-type toward exogenous NAE 12:0. Besides the root elongation, the mutant seedlings were devoid of root hairs. However, overexpressors were more tolerant to the exogenous NAE 12:0. Taken together, these results are consistent with a metabolic role *in vivo* for the NAE amidohydrolase gene, *At5g64440*, in the catabolism of NAEs, and suggest that this lipid hydrolytic pathway may be important for normal seed germination and seedling growth.

NAE profiles and contents showed no appreciable difference among wild type and mutants in seeds and seedlings. There was approximately 25 percent higher total NAE content in knockout seeds than those of wild type and NAE 14:0 and NAE 16:0 were almost three fold higher in seeds of knockouts. There was approximately 33 percent higher NAE contents in knockout seedlings on comparison to those of wild type and NAE 14:0 and NAE 16:0 were higher in knockouts as was the case in seeds. Further research needs to be done to confirm the depletion of NAEs during germination and growth, and also to reconcile NAE profiles and contents with activities of the enzyme encoded by the FAAH gene. In any case identification of Arabidopsis FAAH and development of plants with altered expression of this single gene will provide the tools necessary to understand NAE function in higher plants.

The significance of this research may be summarized as the identification of metabolic fate of NAEs during seed germination, the molecular identification of functional homologues of the mammalian fatty acid amide hydrolase in plants for the first time, and the preliminary analysis of the functional role of this enzyme in *Arabidopsis thaliana*. There continue to be many unanswered questions in this area; however, it is hoped that the research results described here will serve as a basis to guide future studies.

COMPREHENSIVE LIST OF REFERENCES

An Y-Q, McDowell JM, Huang S, McKinney EC, Chambliss S, Meaghe RB (1996) Strong, constitutive expression of the *Arabidopsis* ACT2/ACT8 actin subclass in vegetative tissues. Plant J 10: 107-121

Arabidopsis Genomic Initiative (2000) Analysis of the genome sequence of the flowering plant *Arabidopsis thaliana.* Nature 408: 796-815

Austin-Brown S, Chapman KD (2002) Inhibition of phospholipase Dα by N-acylethanolamines. Plant Physiol 129: 1892-1898

Becker HD, Min B, Jacobi C, Raczniak G, Pelaschier J, Roy H, Klein S, Kern D, Soll D (2000) The heterotrimeric *Thermus thermophilus* Asp-tRNA(Asn) amidotransferase can also generate Gln-tRNA(Gln). FEBS Lett 476: 140-144

Ben-Shabat S, Fride E, Sheskin T, Tamiri T, Rhee M-H, Vogel Z, Bisogno T, De Petrocellis L, Di Marzo V, Mechoulam R (1998) An entourage effect: inactivate endogenous fatty acid glycerol esters enhance 2-arachidonoyl-glycerol cannabinoid activity. Eur J Pharmacol 353: 23

Berdyshev EV, Schmid PC, Krebsbach RJ, Hillard CJ, Huang C, Chen N, Dong Z, Schmid HH (2001) Cannabinoid-receptor-independent cell signaling by *N*-Acylethanolamines. Biochem J 360: 67-75

Bisogno T, De Petrocellis L, Di Marzo V (2002) Fatty acid amide hydrolase, an enzyme with many bioactive substrates. Possible therapeutic implications. Current Pharm Design 8: 533-547

Bisogno T, Maurelli S, Melck M, De Petrocellis L, Di Marzo V (1997) Biosynthesis, uptake, and degradation of anandamide and palmitoylethanolamide in leukocytes. J Biol Chem 272: 3315-3323

Blancaflor E, Hou G, Chapman KD (2003) Elevated levels of *N*-lauroylethanolamine, an endogenous constituent of desiccated seeds, disrupt normal root development in *Arabidopsis thaliana* seedlings. Planta 217: 206-217

Bligh EG, Dyer WG (1959) A rapid method of total lipid extraction and purification. Can J Biochem Physiol 37: 911-917

Boger DL, Fecik RA, Patterson JE, Miyauchi H, Patricelli MP, Cravatt BF (2000) Fatty acid amide hydrolase substrate specificity. Bioorg Med Chem Lett 10: 2613-2616

Bracey MH, Hanson MA, Masuda KR, Stevens RC, Cravatt BF (2002) Structural adaptations in a membrane enzyme that terminates endocannabinoid signaling. Science 298: 1793-1796

Bradford MM (1976) A rapid and sensitive method for quantification of microgram quantities of protein utilizing the principle of protein-dye bind. Anal Biochem 72: 248-254

Buckley NE, McCoy KL, Mezey E, Bonner T, Zimmer A, Felder CC, Glass M, Zimmer A (2000) Immunomodulation by cannabinoids is absent in mice deficient for cannabinoid CB2 receptor. Eur J Pharmacol 396: 141-149

Chang TH, Abelson J (1990) Identification of a putative amidase gene in yeast *Saccharomyces cerevisiae*. Nucleic Acids Res 18, 7180-7180

Chapman KD (2000) Emerging physiological roles for *N*-acylphosphatidyl-ethanolamine metabolism in plants: signal transduction and membrane protection. Chem Phys Lipids 108: 221-230

Chapman KD (2004) Occurrence, metabolism, and prospective functions of *N*-acylethanolamines in plants. Prog Lipid Res (In press)

Chapman KD, Moore TS, Jr (1993) *N*-Acylphosphatidylethanolamine synthesis in plants: occurrence, molecular composition, and phospholipid origin. Arch Biochem Biophys 301: 21-33

Chapman KD, Sprinkle WB (1996) Developmental, tissue-specific and environmental factors regulate the biosynthesis of *N*-Acylphosphatidylethanolamine in cotton (*Gossypium hirsutum* L.). Plant Physiol 149: 277-284

Chapman KD, Trelease RN (1991a) Acquisition of membrane lipids by differentiating glyoxysomes: role of lipid bodies. J Cell Biol 115: 995-1007

Chapman KD, Trelease RN (1991b) Intracellular localization of phosphotidylcholine and phosphotidylethanolamine synthesis in cotyledons of cotton seedlings. Plant Physiol 95: 69-76

Chapman KD, Tripathy S, Venables BJ, Desouza AD (1998) *N*-Acylethanolamines: formation and molecular composition of a new class of plant lipids. Plant Physiol 116:1163-1168

Chapman KD, Venables BJ, Markovic R, Blair RW, Bettinger C (1999) *N*-Acylethanolamines in seeds: quantification of molecular species and their degradation upon imbibition. Plant Physiol 120: 1157-1164

Chebrou H, Bigey F, Arnaud A, Galzy P (1996) Study of the amidase signature group. Biochim Biophys Acta 1298: 185-293

Clough SJ, Bent A (1998) Floral dip: A simplified method for *Agrobacterium*-mediated transformation of *Arabidopsis thaliana.* Plant J 16: 735-743

Cravatt BF, Demarest K, Patricelli MP, Bracey MH, Giang DK, Martin BR, Lichtman AH (2001) Supersensitivity to anandamide and enhanced endogenous cannabinoid signaling in mice lacking fatty acid amide hydrolase. Proc Natl Acad Sci 98:9371-9376

Cravatt BF, Giang DK, Mayfield SP, Boger DL, Lerner RA, Gilula NB (1996) Molecular characterization of an enzyme that degrades neuromodulatory fatty-acid amides. Nature 84: 83-87

Cravatt BF, Lichtman AH (2002) The enzymatic inactivation of the fatty acid amide class of signaling lipids. Chem Phys Lipids 121: 135-148

Cravatt BF, Prosper-Garcia O, Siuzdak G, Gilula NB, Henriksen SJ, Boger DL, Lerner RA (1995) Chemical characterization of a family of brain lipids that induce sleep. Science 268: 1506-1509

Curnow AW, Hong KW, Yuan R, Kim SI, Martins O, Winkler W, Henkin TM, Soll D (1997) Glu-tRNA^{Gln} amidotransferase: A novel heterotrimeric enzyme required for correct decoding of glutamine codons during translation. Proc Natl Acad Sci USA (1997) 94: 11819-11826

Desarnaud F, Cadas H, Piomelli D (1995) Anandamide amidohydrolase activity in rat brain microsomes. Identification and partial characterization. J Biol Chem 270, 6030-6035.

Deutsch DG, Omeir R, Arreaza G, Salehani D, Prestwich GD, Huang Z, Howlett A (1997) Methyl arachidonyl fluorophosphonate: a potent irreversible inhibitor of anandamide amidase. Biochem Pharmcol 53: 255-260

Di Marzo V, Bisogno T, Sugiura T, Melck D, De Petrocellis L (1998) The endogenous cannabinoid 2-arachidonoylglycerol is inactivated by neuronal- and basophil-like cells: connections with anandamide. Biochem J 331: 15-19

DiTomaso E, Beltramo M, Piomelli D (1996) Brain cannabinoids in chocolate. Nature (Lond) 382: 677-678

Dunn K, Dickstein R, Feinbaum R, Burnett BK, Peterman TK, Thoidis G, Goodman HM, Ausubel FM (1988) Developmental regulation of nodule-specific genes in alfalfa root nodules. Mol Plant Microbe Interact 2: 66-74

Elbing K, Brent R (2002) Growth in liquid media. *In* Current Protocols in Molecular Biology (Ausubel FM, Brent R, Kingston RE, Moore DD, Seidman JG, Smith JA, Struhl K, eds) Vol 1, pp 1.2.1-1.2.2, John Wiley and Sons, New York

Feussner I, Kuhn H, Wasternack C (2001) Lipoxygenase-dependent degradation of storage lipids. Trends Plant Sci 6: 268-273

Fowler CJ, Jonsson K-O, Tiger G (2001) Fatty acid amide hydrolase: biochemistry, pharmacology, and therapeutic possibilities for an enzyme hydrolyzing anandamide, 2-arachidonoylglycerol, palmitoylethanolamide, and oleamide. Biochem Pharmacol 62: 517-526

Giang DK, Cravatt BF (1997) Molecular characterization of human and mouse fatty acid amide hydrolases. Proc Natl Acad Sci USA 94: 2238-2242

Giulietti A, Overbergh L, Valckx D, Decallonne B, Bouillon R, Mathieu C (2001) An overview of real-time quantitative PCR: applications to quantify cytokine gene expression. Methods 25:386-401

Goparaju SK, Kurahashi Y, Suzuki H, Ueda N, Yamamoto S (1999) Anandamide amidohydrolase of porcine brain: cDNA cloning, functional expression and site-directed mutagenesis. Biochem Biophys Acta 1441: 77-84

Goparaju SK, Ueda N, Yamaguchi H, Yamamoto S (1998) Anandamide amidohydrolase reacting with 2-arachidonoylglycerol, another cannabinoid receptor ligand. FEBs Lett 422: 69-73

Grullich C, Duvoisin RM, Wiedmann M, Leyen K (2001) Inhibition of 15-lipoxygenase leads to delayed organelle degradation in the reticulocyte. FEBS Lett 489: 51-54

Hansen HS, Moesgaard B, Hansen HH, Petersen G (2000) *N*-Acylethanolamines and precursor phospholipids – relation to cell injury. Chem Phys Lipids 108: 135-150

Hashimoto Y, Nishiyama M, Ikehata O, Horinauchi S, Beppu T (1991) Cloning and characterization of an amidase gene from *Rhodococcus* species *N*-774 and its expression in *Escherichia coli*. Biochim Biophys Acta 1088: 225-233

Hillard CJ (2000) Biochemistry and pharmacology of the endocannabinoids arachidonylethanolamide and 2-arachidonylglycerol. Prostaglandins & Other Lipid Mediators 61: 3-18

Hillard CJ, Edgemond WS, Campbell WB (1995) Characterization of ligand binding to the cannabinoid receptor of rat brain membranes using a novel method: application to anandamide. J Neurochem 64: 677-683

Jones DT (1999) Protein secondary structure prediction based on position-specific scoring matrices. J Mol Biol 292: 195-202

Katayama K, Ueda N, Katoh I, Yamamoto S (1999) Equilibrium in the hydrolysis and synthesis of cannabimimetic anandamide demonstrated by a purified enzyme. Biochim Biophys Acta 1440: 205-214

Koutek B, Prestwich GD, Howlett AC, Chin SA, Salehani D, Akhavan N, Deutsch DG (1994) Inhibitors of arachidonoyl ethanolamide hydrolysis. J Biol Chem 269: 22937-22940

Kozak KR, Crews BC, Morrow JD, Wang L-H, Ma YH, Weinander R, Jakobsson P-J, Marnett LJ (2002) Metabolism of the endocannabinoids, 2-arachidonylglycerol and anandamide, into prostaglandin, thromboxane, and prostacyclin glycerol esters and ethanolamides. J Biol Chem 277: 44877-44885

Krogh A, Larsson B, von Heijne G, Sonnhammer EL (2001) Predicting transmembrane protein topology with a hidden Markov model: application to complete genomes. J Mol Biol 305: 567-580

Kuehl FF, Jacob TA, Ganley OH, Ormond RE, Meisinger MAP (1957) The identification of *N*-(2-hydroxyethaly)-palmitamide as a naturally occurring anti-inflammatory agent. J Am Chem Soc 79: 5577-5578

Kulkarni AP, Sajan M (1999) Lipoxygenase – another pathway for glutathione conjugation of xenobiotics: A study with human term placental lipoxygenase and ethacrynic acid. Arch Biochem Biophys 371: 220-227

Lambert DM, Di Marzo V (1999) The palmitoylethanolamide and oleamide enigmas: are these two fatty acid amides cannabimimetic? Current Med Chem 6: 757-773

Lambert DM, Vandevoorde S, Jonsson KO, Fowler CJ (2002) The palmitoylethanolamide family: a new class of anti-inflammatory agents? Current Med Chem 9: 663-674

Livak KJ, Schmittgen TD (2001). Analysis of relative gene expression data using real-time quantitative PCR and the $2\text{-}2^{-\Delta\Delta C}{}_{T}$ method. Methods 25: 402-408

Maccarrone M, Van der Stelt M, Rossi A, Veldink GA, Vliegenthart JFG, Agro AF (1998) Anandamide hydrolysis by human cells in culture and brain. J Biol Chem 273: 32332-32339

Mayaux JF, Cerbelaud E, Soubrier F, Faucher D, Petre D (1990) Purification, cloning, and primary structure of an enantiomer-selective amidase from *Brevibacterium* sp. strain R312: structural evidence for genetic coupling with nitrile hydratase. J Bacteriol 172: 6764-6773

McCourt P, Keith K (1998) Sterile techniques in *Arabidopsis.* In *Arabidopsis* protocols (Eds Martenz-Zapater JM, Salinas J) Humana Press Inc., NJ 07512. 82: 13-17

McGuffin LJ, Bryson K, Jones DT (2000) The PSIPRED protein structure prediction server. Bioinformatics 16: 404-405

McKinney MK, Cravatt BF (2003) Evidence for distinct roles in catalysis for residues of the serine-serine-lysine catalytic triad of fatty acid amide hydrolase. J Biol Chem 276: 37393-37399.

Nakai K, Kanehisa M (1992) A knowledge base for predicting protein localization sites in eukaryotic cells. Genomics 14: 897-911

Omeir RL, Arreaza G, Deutsch DG (1999) Identification of two serine residues involved in catalysis by fatty acid amide hydrolase. Biochem Biophys Res Commun 264: 316-320

Pappan K, Austin-Brown S, Chapman KD, Wang X (1998) Substrate selectivities and lipid modulation of plant phospholipase D alpha, -beta, and -gamma. Arch Biochem Biophys 353: 131-140

Paria BC, Dey SK (2000) Ligand-receptor signaling with endocannabinoids in preimplantation embryo development and implantation. Chem Phys Lipids 108: 211-220

Patricelli MP, Cravatt BF (2000) Clarifying the catalytic roles of conserved residues in the amidase signature family. J Biol Chem 275:19177-19184

Patricelli MP, Lashuel HA, Giang DK, Kelly JW, Cravett BF (1998) Comparative characterization of a wild type and transmembrane domain-deleted fatty

acid amide hydrolase: identification of the transmembrane domain as a site for oligomerization. Biochemistry 37:15177-15187

Patricelli MP, Lovato MA, Cravatt BF (1999) Chemical and mutagenic investigations of fatty acid amide hydrolase: evidence for a family of serine hydrolases with distinct catalytic properties. Biochemistry 38: 9804-9812

Pertwee RG (2001) Cannabinoid receptors and pain. Prog Neurobiol 63:569-611

Pertwee RG, Fernando SR, Griffin G, Abadji V, Makriyannis A (1995) Effect of phenylmethylsulphonyl fluoride on the potency of anandamide as an inhibitor of electrically evoked contractions in two isolated tissue preparations. Eur J Pharmacol 272: 73-78

Rawyler AJ, Braendle RA (2001) *N*-Acylphosphatidylethanolamine accumulation in potato cells upon energy shortage caused by anoxia or respiratory inhibitors. Plant Physiol 127: 240-251

Sandoval JA, Huang Z-H, Garrett DC, Gage DA and Chapman KD (1995) *N*-Acylphosphatidylethanolamine in dry and imbibing cotton (*Gossypium hirsutum* L.) seeds: amounts, molecular species and enzymatic synthesis. Plant Physiol 109: 269-275

Sarker KP, Obara S, Nakata M, Kitajima I, Maruyama I (2000) Anandamide induces apoptosis of PC-12 cells: involvement of superoxide and caspase-3. FEBS Lett 472: 39-44

Schmid HH, Berdyshev EV (2002) Cannabinoid receptor-inactive *N*-acylethanolamines and other fatty acid amides: metabolism and function. Prostag Leukotr Essent Fatty Acids 66: 363-376

Schmid HH, Schmid PC, Berdyshev EV (2002) Cell signaling by endocannabinoids and their congeners: questions of selectivity and other challenges. Chem Phys Lipids 121: 111-134

Schmid HHO (2000) Pathways and mechanisms of *N*-acylethanolamine biosynthesis: can anandamide be generated selectively? Chem Phys Lipids 108: 71-87

Schmid HHO, Schmid PC, Nataranjan V (1990) *N*-Acylated glycerophospho-lipids and their derivatives. Prog Lipid Res 29: 1-43

Schmid HHO, Schmid PC, Nataranjan V (1996) The *N*-acylation-phosphodiesterase pathway and cell signaling. Chem Phys Lipids 80:133-142

Schmid PC, Zuzrte-Augustin ML, Schmid HHO (1985) Properties of rat liver N-acylethanolamine amidohydrolase. J Biol Chem 260: 14145-14149

Schon A, Kannangara CG, Gough S, Soll D (1988) Protein biosynthesis in organelles requires misaminoacylation of tRNA. Nature 331: 187-189

Servant F, Bru C, Carrère S, Courcelle E, Gouzy J, Peyruc D, Kahn D (2002) ProDom: automated clustering of homologous domains. Brief Bioinform 3: 246-251

Shrestha R, Dixon RA, Chapman KD (2003) Molecular identification of a functional homologue of the mammalian fatty acid amide hydrolase in *Arabidopsis thaliana*. J Mol Biol 278: 34990-34997

Shrestha R, Noordermeer MA, Van der Stelt M, Veldink GA, Chapman KD (2002) *N*-Acylethanolamines are metabolized by lipoxygenase and amidohydrolase in competing pathways during cottonseed imbibition. Plant Physiol 130: 391-401

Sigrist CJ, Cerutti L, Hulo N, Gattiker A, Falquet L, Pagni M, Bairoch A, Bucher P (2002) PROSITE: a documented database using patterns and profiles as motif descriptors. Brief Bioinform 3: 265-274

Sonnhammer EL, von Heijne G, Krogh A (1998) A hidden Markov model for predicting transmembrane helices in protein sequences. Proc Int Conf Intell Syst Mol Biol 6: 175-182

Tiger G, Stentrom A, Fowler CJ (2000) Pharmacological properties of rat brain fatty acid amidohydrolase in different subcellular fractions using palmitoylethanolamide as substrate. Biochem Pharmacol 59: 647-653

Tripathy S, Kleppinger-Sparace K, Dixon RA, Chapman KD (2003) *N*-acylethanolamine signaling in tobacco is mediated by a membrane-associated, high-affinity binding protein. Plant Physiol 131: 1781-1791

Tripathy S, Venables BJ, Chapman KD (1999) *N*-Acylethanolamines in signal transduction of elicitor perception: attenuation of alkalinization response and activation of defense gene expression. Plant Physiol 121: 1299-1308

Tsuchiya K, Fukuyama S, Kanzaki N, Kanagawa K, Negoro S, Okada H (1989) High homology between 6-aminohexanoate-cyclic-dimer hydrolases of Flavobacterium and Pseudomonas strains. J Bacteriol 171: 3187-3191

Ueda N (2002) Endocannabinoid hydrolases. *Prostaglandis & Other Lipid Mediators* 68-69: 521-534

Ueda N, Kurahashi Y, Yamamoto S, Tokunaga T (1995) Parital purification and characterization of the porcine brain enzyme hydrolyzing and synthesizing anandamide. J Biol Chem 270: 23823-23827

Ueda N, Puffenbarger RA, Yamamoto S, Deutsch DG (2000) The fatty acid amide hydrolase (FAAH). Chem Phys Lipids 108:107-121

Ueda N, Yamanaka K, Yamamoto S (2001) Purification and characterization of an acid amidase selective for *N*-palmitoylethanolamine, a putative endogenous anti-inflammatory substance. J Biol Chem 276(38): 35552-35557

Van der Stelt M, Nieuwenhuizen WF, Veldink GA, Vliegenthart JFG (1997) Dioxygenation of *N*-linoleoyl amides by soybean lipoxygenase-1. FEBS Lett 411: 287-290

Van der Stelt M, Noordermeer MA, Kiss T, Van Zadelhoff G, Merghart B, Veldink GA, Vliegenthart JFG (2000) Formation of a new class of oxylipins from *N*-acyl(ethanol)amines by the lipoxygenase pathway. Eur J Biochem 267: 2000-2007

Van der Stelt M, Veldhuis WB, Van Haaften GW, Fezza F, Bisogno T, Bar PR, Veldink GA, Vliegenthart JFG, Di Marzo V, Nicolay K (2001) Exogenous

anandamide protects rat brain against acute neuronal injury in vivo. J Neurosci 21:8765-8771

Van Zadelhoff G, Veldink GA, Vliegenthart JFG (1998) With anandamide as substrate Plant 5-lipoxygenases behave like 11-lipoxygenase. Biochem Biophy Res Comm 248: 33-38

Weigel D, Glazebrook J, ed (2002) *Arabidopsis* – A laboratory manual. Cold Spring Harbor Laboratory Press, New York.

Wiley JL, Dewey MA, Jefferson RG, Winckler RL, Bridgen DT, Willoughby KA, Martin BR (2000) Influence of phenylmethylsulfonyl fluoride on anandamide brain levels and pharmacological effects. Life Sci 67: 1573-1583

Wilson RI, Nicoll RA (2002) Endocannabinoid signaling in the brain. Science 296: 678-682